THE UNIVERSITY
of EDINBURGH

Transcriptional and Functional Consequences of Neuron-Astrocyte Interactions

Zoeb Jiwaji

MA BM BCh MRCP FRCA

A thesis submitted for the degree of
Doctor of Philosophy

2019

Supervisors
Giles Hardingham
Siddharthan Chandran

College of Medicine and Veterinary Medicine
University of Edinburgh, United Kingdom

Declaration

I declare that this thesis has been composed solely by myself and that it has not been submitted, in whole or in part, in any previous application for a degree. Except where stated otherwise by reference or acknowledgment, the work presented is entirely my own.

Parts of this work have been published in Hasel et al., 2017.

Acknowledgements

I owe thanks and gratitude to a large number of people for their help, mentorship and guidance during the preparation of this work. In particular:

- My supervisors Giles Hardingham and Siddharthan Chandran.
- All members of the Hardingham and Chandran labs.
- The Wellcome Trust and the Edinburgh Clinical Academic Tract scheme for funding my fellowship.

Finally, I would like to thank my wonderful wife Lisa for all her love and support, right from the very beginning, through everything.

Lay Summary

Star-shaped cells called astrocytes are a common cell type in the brain. They have a number of roles that are important for the health of surrounding nerve-cells (called neurons). However, the factors that control astrocyte functions are poorly understood.

In this thesis, I describe studies that set out to understand the signals that control astrocyte functions and properties, both in healthy brains and during dementia. First, I investigated how neurons communicate with astrocytes. I found that when neurons are more active, they changed levels of important genes in astrocytes. This in turn increased the ability of astrocytes to provide fuel to more active neurons – thus ensuring energy supply met energy demand in the healthy brain. Using mice kept in light versus darkness, and measuring the levels of astrocyte genes in the area of the brain receiving input from the eyes, I showed that the changes in astrocyte gene levels seen in response to active neurons also occurred in live animals.

Next, I describe studies that set out to understand how astrocytes are affected during dementia. I used a mouse with a mutation associated with early-onset dementia in human patients and investigated how this changed levels of genes in astrocytes. I found that during dementia, astrocytes changed their properties in ways that are both harmful and protective to neurons. By boosting one of these key protective functions (the ability of astrocytes to clear damaging

molecules called “free-radicals”), I found that dementia-associated damage could be slowed down.

Therefore, the studies in this thesis contribute towards our understanding of what controls astrocyte functions in health, and demonstrate that enhancing certain properties of these cells may help protect brains during dementia.

Abstract

Astrocytes play a large number of roles essential for CNS health and are important mediators in CNS disease, demonstrating both neuroprotective and neurotoxic phenotypes. Non-cell autonomous interactions between neurons and astrocytes have been implicated in regulating astrocyte function and phenotype, but the scope and mechanisms of how neuronal signals control astrocytes are poorly understood.

The data presented in this thesis describe how neuron-astrocyte interactions influence astrocyte transcriptional pathways to control homeostatic and neuroprotective functions in health and disease. First, I show that healthy astrocytes are modulated by a physiological signal: neuronal synaptic activity. Using an *in vitro* astrocyte-neuron co-culture model, I describe how synaptic activity alters astrocyte transcription via CREB-dependent signalling to boost the astrocyte-neuron lactate shuttle pathway – an important pathway for energy provision in the CNS.

Second, by exposing astrocyte-specific EGFP-ribosome reporter mice to a light-stimulus paradigm, I demonstrate that altered synaptic activity influences astrocyte transcription in a more complex *in vivo* model. I further describe how activity-dependent neuronal and astrocyte transcriptional pathways are altered upwards or downwards when neuronal activity is suppressed during anaesthesia or when neuronal activity is enhanced with transcranial electrical stimulation.

Finally, I explore the consequences of neurodegenerative disease on astrocyte transcription and phenotype. Using a transgenic mouse model of frontotemporal dementia (FTD), I describe how neuronal tauopathy drives upregulation of both neurotoxic and neuroprotective astrocyte transcriptional signatures. One key signature found was upregulation of the cyto-protective transcription factor Nrf2 pathway, and I demonstrate that boosting Nrf2 in reactive astrocytes confers neuroprotection in our model of human tauopathy.

Collectively, these investigations add to our growing understanding of how astrocyte transcription and function are altered both by physiological signals and during neurodegeneration, and highlight the astrocyte Nrf2 pathway as a putative target for therapeutic benefit in neurodegenerative disease.

Contents

Abbreviations

ACSF	Artificial cerebrospinal fluid
AD	Alzheimer's disease
AMPA	a-Amino-3-hydroxy-5-methyl-4-isoxazolepropionic acid hydrobromide
ANLS	Astrocyte-neuron lactate shuttle
ANOVA	Analysis of variance
APOE	Apolipoprotein E
AR-C	AR-C155858
ATP	Adenosine 5-triphosphate
BCA	Bicinchoninic acid
BiC	Bicuculline
cAMP	cyclic adenosine monophosphate
CFP	Cyan fluorescent protein
Cilos	Cilostazol
CREB	cAMP Response Element Binding Protein
Cx	Cortex
Cyto-B	Cytochalasin B
DAPI	4',6–diamidino–2–phenylindole
DIV	Day in vitro
DTT	Dithiothreitol
Forsk	Forskolin
FRET	Förster resonance energy transfer
FTD	Frontotemporal dementia
GABA	g-Aminobutyric acid
GFP	Green fluorescent protein
GPCR	G-protein coupled receptor
HEPES	4-(2-Hydroxyethyl)piperazine-1-ethanesulfonic acid,
IBMX	3-isobutyl-1-methylxanthine
IPS	Induced pluripotent stemcell
KEAP-1	Kelch-like erythroid cell-derived protein with cap 'n' collar (CNC) homology associated protein 1
NMDA	N-Methyl-D-aspartic acid
NRF2	Nuclear Factor Erythroid 2-related factor 2
NTES	Non-invasive transcranial electrical stimulation
QPCR	Quantitative polymerase chain reaction
SC	Spinal cord
SDS	Sodium dodecyl sulfate
TRAP	Translating Ribosome Affinity Purification
TTX	Tetrodotoxin
YFP	Yellow fluorescent protein

Chapter 1

Introduction

1.1. Astrocyte functions during normal physiology

Astrocytes are a common cell-type in the CNS (von Bartheld, Bahney and Herculano-Houzel, 2016). The concept that they provide mere passive structural support has become superseded by emerging research identifying a number of active astrocyte functions essential for CNS physiology in health and disease. Known astrocyte roles are outlined in Table 1-1.

In this introduction, I expand upon specific astrocyte anatomical and functional adaptations of particular relevance to this thesis. I next discuss how these functions are modulated by intracellular and extracellular signals. Finally, I introduce how astrocyte function and phenotype change following injury and disease, and the roles that astrocytes play in neurodegenerative conditions such as dementia.

Table 1-1 Astrocyte Functions

Category	*Function*	*Description*
Neuronal health and synaptic transmission	Synapse formation	Release of prosynaptic molecules and function as part of the tripartite synapse (expanded below)
	Synapse elimination	Mediate synapse elimination through MEGF10 and MERTK pathways (Chung *et al.*, 2013).
	Neuronal growth	Secretion of neurotrophic growth factors (BDNF, NGF, GDNF) (Houlgatte *et al.*, 1989).
	Secretion of extracellular matrix (ECM).	Express a range of proteoglycans essential for CNS extracellular matrix formation and neuronal adhesion molecules (N-cadherin, laminin and neural cell adhesion molecule (NCAM) during development, in health and following injury (Wiese, Karus and Faissner, 2012).
CNS physiology	K^+ balance	Elevated K^+ following synaptic transmission is cleared by astrocytes; redistributed through astrocyte gap junctions and returned at sites of low K^+ concentration via astrocyte Kir4.1 channels (Hertz and Chen, 2016).
	Brain metabolism	Produce lactate for neuronal metabolic function (expanded below).
	CNS glycogen storage	Astrocytes are the predominant glycogen store in the CNS, and astrocyte glycogen is essential in protecting the brain from hypoglycaemia (Brown and Ransom, 2007).

Category	*Function*	*Description*
CNS Physiology (Cont)	Thyroid hormone activation	Uptake inactive T4 hormone from the blood and convert to active T3 (Morte and Bernal, 2014). Activated thyroid hormone is essential for myelination and brain development.
	Cholesterol synthesis	Astrocytes have a key role in producing cholesterol. This is secreted and delivered to neurons as a complex with apolipoprotein (apo) E and required for neuronal membrane formation and synapse function (Mauch *et al.*, 2001).
	Glymphatic flow	Astrocyte pulsatile motion is coupled with water-egress through vascular-bound Aqp4 channels required for pumping and clearing CNS waste through the glympathic system – the CNS equivalent of the lymphatic network (Iliff *et al.*, 2012).
	Circadian rhythm	Astrocyte regulation of extracellular glutamate modulates the oscillatory patterns of neurons in the suprachiasmic nucleus to regulate night-time activity of the mammalian circadian clock (Brancaccio *et al.*, 2017).
Neuroprotective functions	Antioxidant function	Provide antioxidant support to nearby neurons (expanded below).

Category	*Function*	*Description*
	Glutamate uptake	Essential for CNS glutamate uptake and clearance (expanded below).
	Ammonia clearance	Detoxify ammonia by converting it into glutamine and astrocyte dysfunction has been implicated in hepatic encephalopathy (Rao *et al.*, 2005).
Blood brain barrier and vasculature interactions	CNS water homeostasis	Express aquaporin water channels on their basal membrane which are essential for maintain CNS water homeostasis (Potokar, Jorgačevski and Zorec, 2016).
	Vasomodulation and neurovascular coupling	Astrocytes contact the vasculature, and hypothesised to be responsible for reactive hyperaemia – the process where blood flow in local parts of the brain is coupled to activity (expanded below).
	Regulation of blood brain barrier permeability	Astrocyte end-feet are one constituent of the BBB, and astrocyte transporter expression and end-feet anatomy can modulate BBB permeability (expanded below).

Category	*Function*	*Description*
Inflammatory Functions	Formation of glial scar	Following injury, astrocytes become reactive and proliferate, forming a glial scar to contain inflammatory processes. The neuroprotective vs neurotoxic effects of scar formation are described below.
	Inflammatory cytokine production and complement activation.	Secrete both proinflammatory and antinflammatory cytokines and chemokines, including Il-1, IL-6, TNF-Alpha and and IFN-gamma (Lau and Yu, 2001). Secrete complement factors C1q and C3, which activates complement and postulated to mediate synapse loss in dementia (Perry and Holmes, 2014).

1.1.1. Anatomical distribution and heterogeneity

The anatomical distribution of astrocytes in the CNS is highly organised. They tile the entire CNS in a non-overlapping and contiguous manner. Their perivascular end-feet contact cerebral blood vessels directly (Mathiisen *et al.*, 2010), and they extend peripheral processes to make contact with neurons at synapses, dendrites, axons and somata (Weber and Barros, 2015). Thus they act as the interface between neurons and the cerebral vasculature **(Figure 1.1)**.

Soon after their discovery by Rudolf Virchow (Virchow, 1858), it became clear that astrocytes represent a heterogeneous population. For over a hundred years they have been classified as two main subtypes based on morphology and location: grey matter (protoplasmic) astrocytes and white matter (fibrous) astrocytes (Cajal, 1909; Miller and Raff, 1984). In addition, it is also recognised that that there are specialized astroglia, such as Bergmann glia in the cerebellum or Müller cells of the retina (Farmer and Murai, 2017).

With the advent of transcriptomics, it is emerging that astrocytes demonstrate even greater diversity. Recent studies have described regional (Itoh *et al.*, 2018) and cortical layer-specific (Bayraktar *et al.*, 2018; Lanjakornsiripan *et al.*, 2018) heterogeneity in astrocyte populations. Additionally, astrocytes demonstrate heterogeneity in their phenotypic response to injury or disease. This is discussed in more detail in section 1.3.

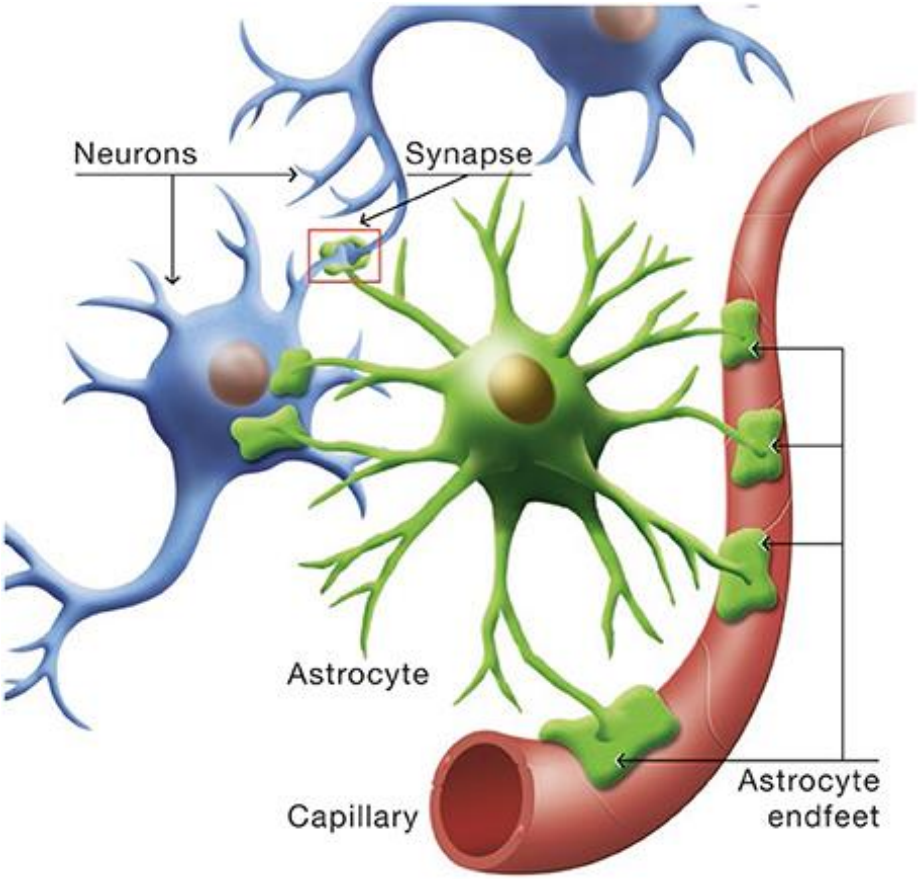

Figure 1.1 - Cytoarchitectural relationship of astrocytes within the neuro-glia-vascular unit (from Demetrius, Magistretti and Pellerin, 2015)**.** Astrocytes tile the vasculature and communicate with neuronal bodies and synapses, acting as an interface between the blood stream and the nervous system.

1.1.2. Astrocyte roles in CNS signalling

1.1.2.1. *Synapse modulation*

Astrocytes play important roles in synapse formation and maintenance, both during CNS development and in adulthood. The importance of astrocytes in promoting synaptogenesis was first demonstrated by the observation that rodent neurons cultured in isolation have very few synapses. The addition of astrocytes leads to an increase in both synapse number and strength (Pfrieger and Barres, 1997). An individual astrocyte covers an area that contains (and hence could make contact with) as many as 10^5 synapses in the mouse cortex (Bushong *et al.*, 2002). Their close proximity with the pre-synaptic and post-synaptic clefts has led to the development of the "Tripartite" synapse hypothesis **(Figure 1.2)**. This postulates that astrocytes play a critical role in influencing and shaping synapse formation and strength (Allen and Eroglu, 2017).

Astrocytes strengthen synapses through multiple contact and secreted signals. Key astrocyte factors identified to enhance synapse number and transmission include thrombospondins (Christopherson *et al.*, 2005); secreted protein acidic and rich in cysteine-like 1 (SPARCL1) (Kucukdereli *et al.*, 2011); glypicans 4 and 6 (Allen *et al.*, 2012); cholesterols (Mauch *et al.*, 2001); and cytokines including TNF-α and TGF-β (Diniz *et al.*, 2012).

Astrocyte ensheathment of synapses has been shown to be a dynamic process influenced by numerous factors, including neuronal activity (Bernardinelli *et al.*, 2014), and glia have been shown to regulate the formation of multiple synapse

types, including cholinergic, GABAergic and glumatergic synapses (Cao and Ko, 2007, Elmariah *et al.*, 2005, Ullian *et al.*, 2001).

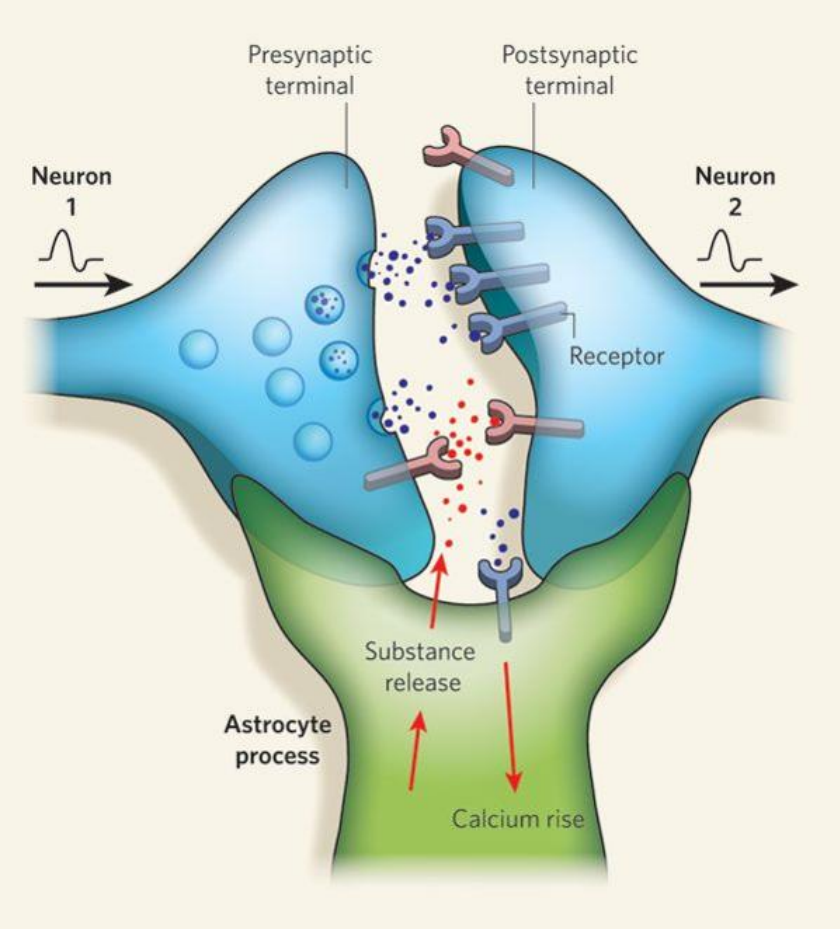

Figure 1.2 - The tripartite synapse (adapted from Allen and Barres, 2009). Astrocytes ensheath synapses and are hypothesised to respond to neuronal signals and to secrete factors that modulate synapse strength and transmission.

As well as positive roles in promoting synapse formation, astrocytes have been implicated in synapse elimination. This is both via direct means (e.g. phagocytosis) (Chung *et al.*, 2013) and by indirect means involving microglia and complement activation (Bialas and Stevens, 2013). Synapse elimination is an important process involved in both normal physiology for circuit remodelling and in disease-induced synapse loss.

1.1.2.2. *Gliotransmission*

Astrocytes have been postulated to release gliotransmitters: neuroactive substances that have been implicated in modulating synaptic activity. This is discussed in further detail in section 1.2, together with mechanisms by which neurons may direct astrocyte signalling.

1.1.3. Functions for CNS homeostasis:

1.1.3.1. *Glutamate uptake*

Glutamate is the main excitatory neurotransmitter in the CNS. It acts primarily on N-methyl-D-aspartate (NMDA) and α-amino-3-hydroxy-5-methyl-4-isoxazolepropionic acid (AMPA) receptors, and has important roles in learning, memory and motor function. However, excess glutamate can lead to excitotoxicity and neuronal death (Dong, Wang and Qin, 2009).

Astrocytes are the main uptakers of glutamate in the CNS (Anderson and Swanson, 2000). They express high-affinity glutamate transporters (EEAT1 and EEAT2) which are coupled to transmembrane sodium flux. High expression of glutamine synthetase inside the astrocyte converts glutamate into glutamine. This maintains a gradient for continued glutamate uptake, with glutamine being recycled back to neurons for reconversion into glutamate. This glutamate-glutamine cycle is essential for maintaining normal synaptic function, and critical following injury in removing excess glutamate from the CNS.

1.1.3.2. *Neurovascular coupling*

As described above, astrocyte end-feet line the vasculature and along with endothelium and pericytes, constitute the blood brain barrier. The blood brain barrier is characterised by a specialised network of tight-junctions which limits movement of hydrophilic substances between the bloodstream and the CNS (Cabezas *et al.*, 2014). This both protects the brain from toxic substances and allows tight control of the CNS physiological environment. Astrocytes express a large number of specialised transporters (for example, the glucose transporter GLUT1 and aquaporins) which actively transfer substances across the BBB to regulate metabolic homeostasis and water balance in the CNS (Nagelhus and Ottersen, 2013).

Astrocytes may regulate blood flow into the CNS and acts as an important cell-type in determining the phenomenon of reactive hyperaemia (Nippert, Biesecker and Newman, 2018). Reactive hyperaemia is the process by which

blood supply to the brain is coupled to energy demand. Increased neuronal activity leads to localised vasodilation of regulating arterioles and capillaries, increasing local blood flow. The effects of astrocyte stimulation on blood-vessel dynamics is complex and incompletely understood. Experiments have shown that calcium transients in astrocytes can induce both vasodilation and vasoconstriction (Mulligan and MacVicar, 2004), with differing signalling pathways postulated to act between capillaries and arterioles (Mishra *et al.*, 2016). Signalling messengers that have been implicated include glutamate induced release of astrocyte vasoactive substances such as nitric oxide, arachidonic acid, prostaglandins and 20-hydroxyeicosatetraenoic acid (20-HETE) which have both direct and indirect effects on vascular smooth-muscle (Howarth, 2014). Astrocyte-endothelial interactions are also important for controlling BBB permeability (Abbott, 2002).

1.1.3.3. *Metabolism*

Astrocytes have been implicated in playing a key role in CNS metabolic homeostasis. The CNS has high energy requirements. Whilst comprising only 2% of total body mass, the brain utilises approximately 20% of total oxygen and 25% of total glucose consumed by the body (Bélanger, Allaman and Magistretti, 2011). Most of this energy fuels synaptic activity rather than action potentials and energy requirements can increase significantly due to excitotoxicity during times of injury and disease (Attwell and Laughlin, 2001).

Whilst sources of energy provision for neurons were classically considered to be from oxidation of glucose or ketone bodies taken up directly by neurons, the astrocyte-neuron lactate shuttle (ANLS) hypothesis (Magistretti *et al.*, 1999; Bélanger, Allaman and Magistretti, 2011) postulates that that astrocyte-derived metabolic precursors (lactate and pyruvate) may serve as the predominant fuel source for neuronal oxidative phosphorylation **(Figure 1.3)**.

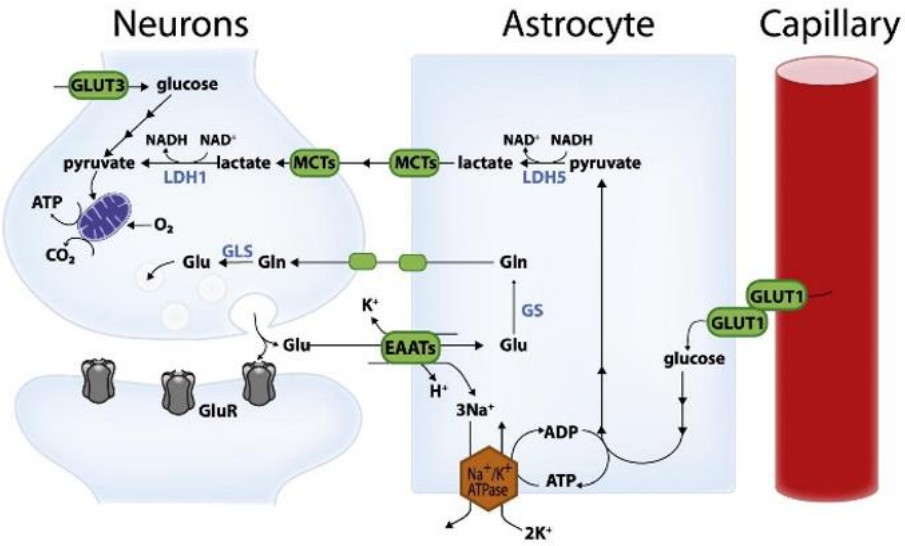

Figure 1.3 - The Astrocyte-Neurone Lactate Shuttle (adapted from Bélanger, Allaman and Magistretti, 2011)**.** Astrocytes take up glucose from the bloodstream for conversion into lactate via glycolysis. Lactate is then exported to neurons where it is utilised to generate ATP via the citric-acid cycle and oxidative phosphorylation. Lactate production is hypothesised to be acutely coupled to glutamate uptake. Changes in Na/K+ gradients across the astrocytes due to glutamate uptake require increased ATP to power membrane Na/K pumps. ATP production is provided by increased glycolytic flux, which generates lactate for export to neighbouring neurons.

Astrocytes are suited morphologically and phenotypically to the role of providing CNS metabolic support. Their anatomical position adjacent to, and wrapped around, the cerebral vasculature allows uptake of metabolic substances directly from the bloodstream. High concentrations of the high capacity glucose transporter GLUT1 on their endfeet act as the predominant route for glucose entry into the CNS (Chuquet *et al.*, 2010; Zimmer *et al.*, 2017).

Astrocytes also have several biochemical adaptations for high glycolytic rates and lactate export. Pyruvate dehydrogenase (an essential enzyme for allowing entry of pyruvate into the Krebs cycle) is kept at reduced levels in astrocytes by phosphorylation (Itoh *et al.*, 2003), and astrocytes have low levels of the aspartate-glutamate complex aralar (Ramos *et al.*, 2003). This means that conversion of pyruvate to lactate is the preferred pathway for regenerating NAD cofactor in astrocytes, hence promoting this pathway and lactate formation. Finally, astrocytes have high levels of the enzyme 6-phosphofructose-2-kinase-fructose-2,6- bisphosphatase-3 (Pfkfb3), a key activator of phosphofructokinase, the rate-limiting step of glycolysis. Pfkfb3 is continuously degraded in neurons and therefore levels are virtually absent – resulting in a lower glycolytic rate in neurons (Herrero-Mendez *et al.*, 2009).

The importance of the ANLS in CNS function is illustrated by gene-interference experiments in drosophila, where silencing of glial glucose transporters or glial glycolysis genes cause neuronal death, whilst silencing of neuronal glycolytic genes result in no abnormal phenotype (Volkenhoff *et al.*, 2015). Inhibition of

astrocyte-specific lactate exporters lead to memory impairment and loss of LTP in rodents, which is rescued by lactate infusion but not by glucose (Suzuki *et al.*, 2011). In this study, inhibition of neuronal lactate importers also leads to memory impairment but this cannot be rescued by lactate, suggesting the requirement for lactate transfer from astrocytes to neurons. And lactate has been suggested to have other neurotrophic and memory-promoting effects independent of its role as an energy substrate, for example by signalling through hydroxycarboxylic acid (HCA) receptors (DiNuzzo, 2016).

Therefore, the above studies demonstrate that the ANLS is an important pathway for neuronal and CNS homeostatic function. However, the manner in which this pathway is regulated, and specifically the manner in which neuronal activity influences astrocyte capacity to provide metabolic CNS support was unknown, and understanding this was an important aim for the studies in this thesis.

1.1.4. Neuroprotective functions:

In addition to roles in normal physiology, astrocytes have a number of important neuroprotective roles.

1.1.4.1. *Antioxidant protection*

Neurons are especially vulnerable to oxidative stress (Dringen, Gutterer and Hirrlinger, 2000). Their high metabolic requirements result in the generation of high levels of reactive oxygen species (ROS). This is coupled with an increased vulnerability to oxidative damage given their poor regenerative potential and requirement to function for an entire lifetime. Therefore the CNS requires significant and robust antioxidant pathways.

Paradoxically, neurons have low intrinsic antioxidant capacity, exhibiting low levels of key antioxidant molecules such as glutathione peroxidase, catalase and superoxide dismutases (Bell and Giles E Hardingham, 2011). This is achieved by epigenetic suppression of the antioxidant master transcription factor NF-E2-related factor 2 (Nrf2) in neurons and is believed to be due to the essential requirement for redox signalling for neuronal development (Bell *et al.*, 2015). Therefore, neurons rely on neighbouring astrocytes, which express high levels of Nrf2, for antioxidant protection. Nrf2 activation in astrocytes leads to an enhanced capacity for astrocytes for generating glutathione precursors (e.g. cysteinylglycine), which can be transported to neurons and used to generate glutathione (a key antioxidant) in an activity-dependent manner.

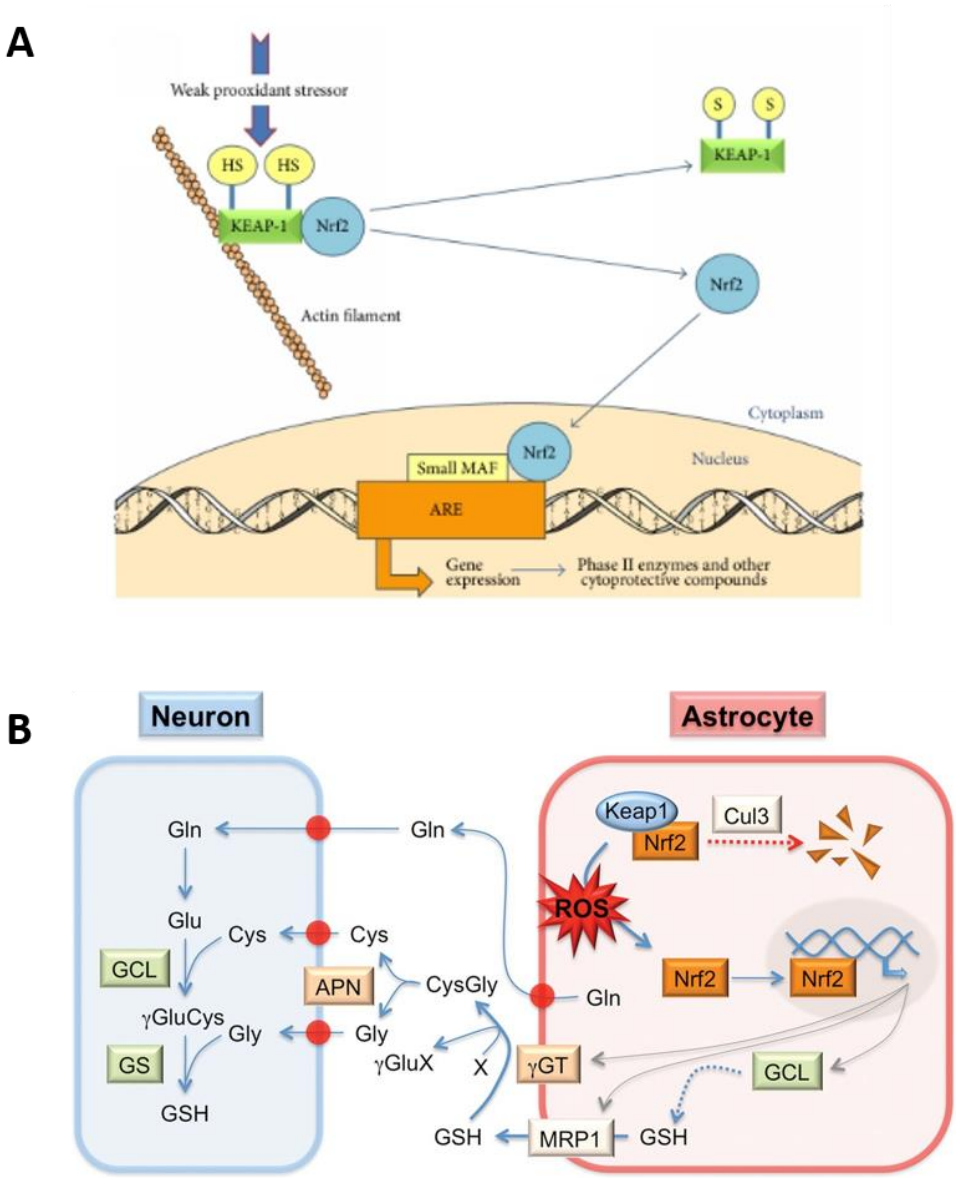

Figure 1.4 - The transcription factor Nrf2 is activated in response to antioxidant stress in astrocytes. A. (Adapted from: Houghton, Fassett and Coombes, 2016). An altered cellular redox environment leads to oxidation of a critical cysteine residue on the Nrf2 inhibitor KEAP-1 causing its dissociation from Nrf2. This allows Nrf2 translocation into the nucleus, where it activates a battery of antioxidant genes. **B.** (Adapted from Fernandez-Fernandez *et al.*, 2012.) Nrf2 activation in astrocytes leads to the synthesis of glutathione precursors which are supplied to neurons to provide antioxidant support.

The levels of key antioxidant pathways are dynamically regulated within the cell to ensure that antioxidant capacity matches changing levels in ROS production. Nrf2 nuclear levels are kept low by being bound to its negative regulator Kelch-like erythroid cell-derived protein with cap 'n' collar homology associated protein 1 (Keap1) (Kansanen *et al.*, 2013) **(Figure 1.4)**. This association targets Nrf2 ubiquitination for proteosomal degradation. Changes in the cellular redox environment leads to modification of the cysteine residues on Keap1. This leads to dissociation of Keap1 from Nrf2, allowing its translocation in the nucleus. Here it binds to antioxidant response elements (ARE) leading to the activation of a large number of antioxidant genes as summarised in **Table 2**.

Evidence for the importance of astrocytic vs neuronal Nrf2 can be demonstrated by knock-out experiments. Nrf2-deficient neurons do not demonstrate increased vulnerability, and pharmacological activation of Nrf2 in neurons does not increase levels of Nrf2 target genes. However activation of Nrf2-mediated transcription in astrocytes is able to confer neuroprotection via a mechanism that involves release of astrocytic glutathione (Bell *et al.*, 2011).

Section summary

Astrocytes play an expanding number of roles essential for CNS homeostasis and neuroprotection. In this thesis, I aim to investigate how specific signals can regulate these functions to alter CNS homeostatic pathways and examine how key astrocyte functions and phenotype might be altered in disease.

Table 1-2 Nrf2 target genes and key antioxidant pathways in the CNS

Nrf2 Target Gene(s)	*Function*
Haemoxygenase (Hmox-1)	Generates the antioxidants carbon monoxide and bilirubin from haemoglobin.
Superoxide dismutases (Sod)	Converts superoxide (O_2^-) into molecular oxygen or hydrogen peroxide (H_2O_2), for subsequent breakdown by catalase.
Catalase (Cat)	Catalyses the conversion of H2O2 into water and oxygen.
Glutathione pathway enzymes.	Upregulation of genes needed for the production, use and recycling of glutathione, including glutatmylcysteine ligase (Gclc), glutathione reductase, glutathione-s-transferase(GST) and glutathione synthetase. Glutathione reduces peroxides and ROS directly or by acting as an electron donor for glutathione peroxidases.
NAD(P)H: quinone acceptor oxidoreductase (NQO1)	Couples NADPH to oxidise free-radical quinones into hydroxyquinones.
Thioredoxin (Trx), sulfiredoxins (Srxn) and Peroxiredoxin (Prx) pathway enzymes	A family of proteins that remove peroxides. Trx donates electrons to oxidised proteins such as Prx, reducing their disulfide bonds. This allows Prx to remove H_2O_2. Following a severe oxidative insult, the cysteine residues on Prx can be oxidised to sulfinic or sulfonic acid. These cysteines can be reduced by Srxn (ATP-dependent reductases), hence recharging Prx.

1.2. Signals that control astrocyte function and phenotype

Given the large number of important astrocyte functions outlined above, emerging data that astrocytes are controlled by a number of internal and external signals is not surprising. Whilst a complete description of all signalling pathways implicated to influence astrocytes is beyond the scope of this introduction, in this section I will expand further on specific key signalling pathways and those of relevance to the studies described in this thesis.

1.2.1. Intracellular signals

1.2.1.1. *Astrocyte calcium signalling*

The principle intracellular signalling molecule that has been studied in astrocytes is calcium. The observation that extracellular glutamate leads to intracellular calcium fluctuations in astrocytes was the first indication that astrocytes could dynamically respond to their extracellular environment and were more than passive support cells in the CNS (Cornell-Bell *et al.*, 1990).

Astrocytes demonstrate a complex pattern of calcium fluctuations, both at rest and in response to neuronal activity. Calcium fluctuations can be restricted to microdomains (called calcium 'sparkles' or 'bursts') or propagate throughout the cell as calcium waves (Khakh and McCarthy, 2015; Bindocci *et al.*, 2017). Astrocytes are connected to each other via gap junctions, allowing calcium wave

propagation to neighbouring non-stimulated astrocytes. It has been suggested that astrocyte calcium waves can be integrated, processed and transmitted – forming a secondary CNS communications network augmenting neuronal networks in the CNS (Scemes and Giaume, 2006). However, the exact consequences and implications of astrocyte calcium activity on astrocyte function has not yet been fully understood.

The upstream activators and downstream effectors of astrocyte calcium signals are summarised in **Figure 1.5**.

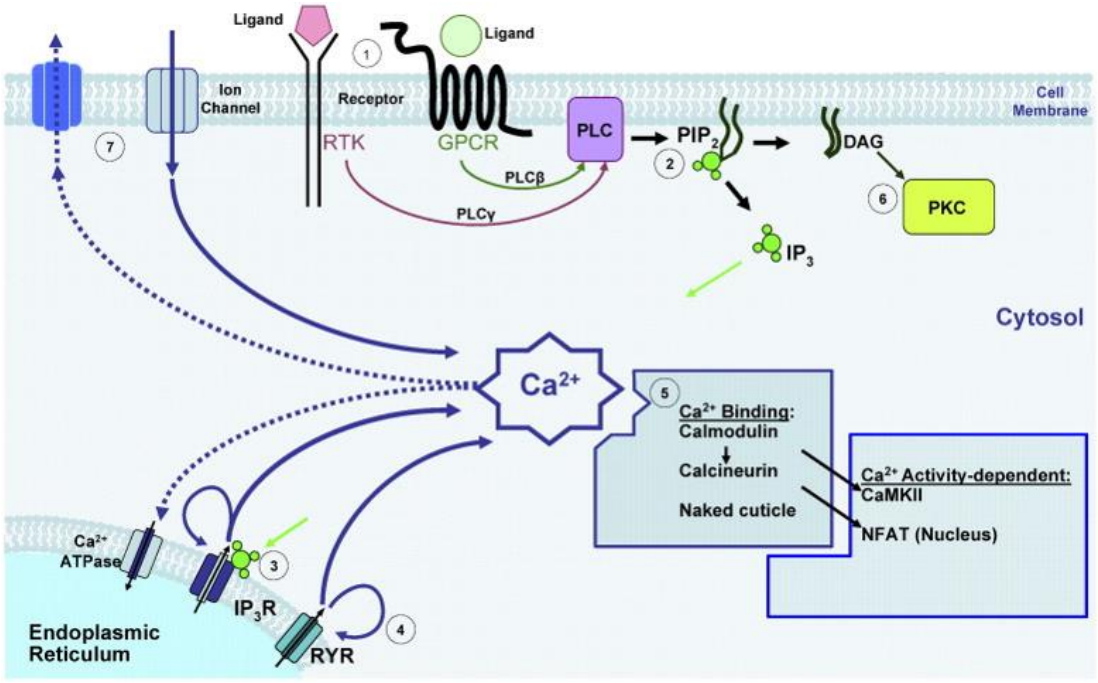

Figure 1.5 - Upstream and downstream pathways involved in astrocyte calcium signalling (Adapted from Slusarski and Pelegri, 2007). **(1)** Binding of agonists induces activation of g-protein coupled receptors (GPCR) and receptor tyrosine kinases (RTK). **(2)** Activation of phospholipase C leads to hydrolysis of PIP2 giving rise to IP3 and DAG. **(3)** IP3 binds to receptors on the ER and triggers Ca^{2+} release from intracellular stores. **(4)** Signalling can cascade by calcium-induced calcium release with Ca^{2+} binding to ryanodine receptors (RyR). **(5)** Intracellular Ca^{2+} activates Ca^{2+} binding proteins **(6)** Alternative pathways activates other kinases (e.g. PKC). **(7)** Signalling is controlled by Ca^{2+} extrusion via plasmalemmal pumps and Na+/Ca^{2+} exchange as well as by uptake into intracellular stores,

1.2.1.2. *G-protein coupled receptors*

Signal transduction in neurons typically occurs via ionotropic receptors such as the NMDA and AMPA channels. These alter cellular current and ion flow through the cell membrane, leading to activation of voltage-dependent channels and inducing signal propagation via action-potentials. Astrocytes do not typically express voltage-dependent channels and are considered to be electrically unexcitable. Instead they utilise a number of metabotropic receptors for cellular signalling (Bradley and Challiss, 2012), which respond to signalling substances including glutamate (acting via mGlu3 and mGlu5 receptors), noradrenaline, VIP, adenosine and ATP (Bradley and Challiss, 2012; Orr *et al.*, 2015).

These ligands bind to G-protein receptors (GPRs) which in turn drive a number of downstream signalling pathways. GPRs can be categorised into Gq, Gs and Gi subtypes. Gq receptors couple to protein kinase C (PKC) to induce activation of phospholipase C, leading to the production of inositol 1,4,5-trisphosphate (IP3). This binds specific receptors in the endoplasmic reticulum causing Ca^{2+} release. This calcium release then propagates throughout the cell and is modulated by both positive and negative control mechanisms. Gs and Gi receptors couple to adenylate-cylase (either activating or inhibiting the enzyme) leading to increased production of the second messenger cAMP, and activation of protein-kinase A. This can then phosphorylate and activate transcription factors as detailed below.

1.2.1.3. *Role of the CREB transcription factor in astrocytes*

Initiation of the above second messenger cascades ultimately leads to downstream activation of numerous transcription factors. The full discussion of all astrocyte transcription factors is beyond the scope of this introduction, but I will consider the role of one key CNS transcription factor here - c-AMP responsive element binding protein (CREB).

CREB is part of a family of transcription factors, termed the basic leucine zipper domain family, which includes other similar factors such as Activating Transcription Factor 1 (ATF1) and cAMP Responsive Element Modulator (CREM) (Lonze and Ginty, 2002). CREB family transcription factors can be activated by multiple pathways. Classical CREB activation occurs via G-coupled receptors that induce cAMP- PKA signalling, allow the nuclear localisation of PKA and phosphorylation of CREB at Ser 133 (Shaywitz and Greenberg, 1999). CREB can also be activated by Ca^{2+}, both by PKC signalling and by activation of calmodulin dependent kinases (CamKs), as well as through growth factor signalling pathways (**Figure 1.6**).

These pathways converge to induce phosphorylation of CREB which allows it to dimerise and bind to DNA at cAMP regulatory element (CRE) regulatory sites. CRE is classically described as an 8 nucleotide palindromic sequence (TGACGTCA), but this has been expanded by later works to include sequence variations (Craig et al. 2001). Binding of CREB to CRE sites induces the expression of a large number of genes that modulate cellular function.

Further complexity of control arises from CREB exhibiting multiple splice variants which demonstrate different properties. Some of these variants (for example one isoform produced by an alternative intronic promoter, inducible cAMP response element repressor (ICER)), act as a transcriptional repressor (Jaworski *et al.*, 2018).

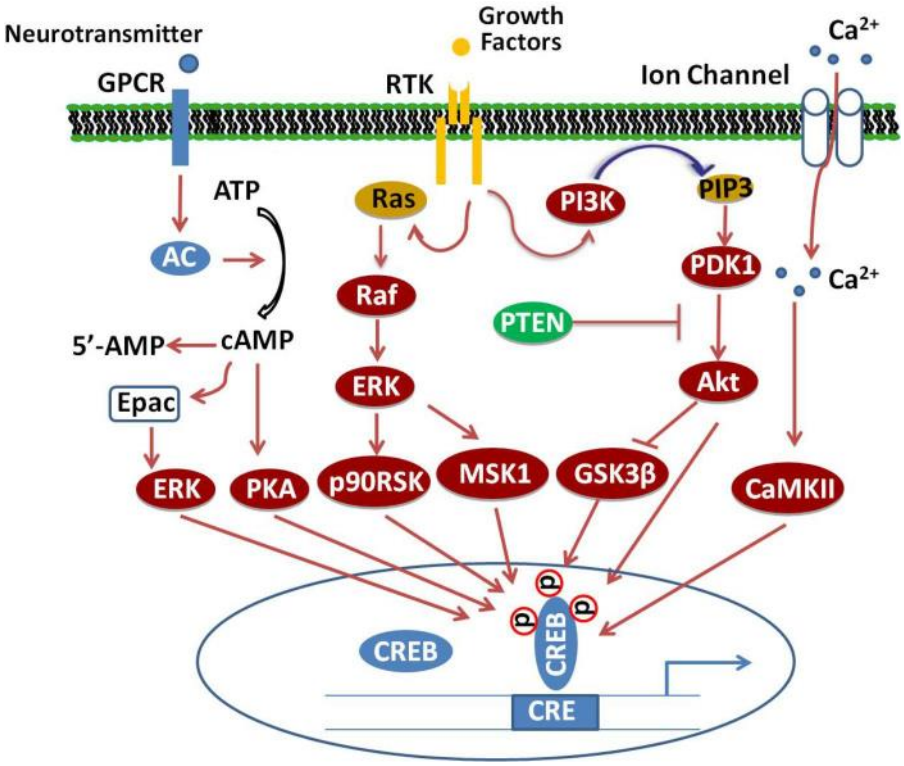

Figure 1.6 - Activation of the CREB transcription factor via upstream signalling (Adapted from Wang *et al.*, 2018).The classical pathway of CREB activation follows G-protein coupled receptor (GPCR) activation. This binds and activates adenylate cyclase (AC), which produces cAMP. This activates phosphokinase A (PKA). PKA enters the nucleus and phosphorylate CREB at Ser133, which causes its activation. Alterative pathways include growth factor activation of receptor tyrosine kinases (RTK) acting via Ras/Raf/MEK/ ERK/p90/RSK pathways, which can induce phosphorylation of CREB at alternative sites. Finally, in excitable cells, activation of excitatory NMDA receptors increases intracellular calcium, and induces CREB phosphorylation through Ca^{2+}/CaMK-dependent pathways.

The consequence of CREB activation in neurons has been well studied. Induction of CREB target genes are essential for neuronal development and promote changes in synaptic plasticity, learning and memory (Lonze and Ginty, 2002). In addition, CREB activation induces pro-survival gene expression and promotes neuronal resilience to injury.

The role of CREB in astrocytes is less well understood. Recent publications have identified that activation of CREB drives distinct transcriptional programmes in astrocytes compared to those in neurons (Pardo *et al.*, 2017) and enhancing CREB activation in astrocytes can reduce neuronal damage following focal cortical injury (Pardo *et al.*, 2016).

1.2.2. Extracellular signals.

Astrocytes receive a number of extracellular signals from other CNS cell-types that have been demonstrated to alter their transcription and phenotype.

1.2.2.1. *Neuronal contact*

Astrocytes *in vivo* differ markedly both morphologically and in their transcriptome from those cultured alone *in vitro* (Cahoy *et al.*, 2008). Specifically, *in vitro* astrocytes demonstrate both immature characteristics as well as some features consistent with a reactive phenotype

Recent work has expanded our understanding of how neurons, through direct contact with astrocytes, induce changes in function and phenotype. Co-culturing astrocytes with neurons induces the distinctive stellate shape seen *in vivo*, which is mediated through astrocytic neuroligan signalling (Stogsdill *et al.*, 2017). Co-culture with neurons also drives transcriptional changes in astrocytes towards those of a more *in vivo* signature, and induced functional maturity as measured by glutamate uptake capacity, with transcriptional and functional changes being driven by the Notch signalling pathway (Hasel *et al.*, 2017).

1.2.2.2. *Synaptic activity - consequences on neuronal transcription*

One of the most important and defining features of CNS communication is synaptic activity. Action potentials transmitted down neuronal axons induce the release of neurotransmitter substances at the synapse. Besides allowing communication and propagation of signals between neurons, synaptic activity has a profound effect on neuronal health and function by mediating changes in neuronal transcription – so called "synapse-to-nucleus" signalling (Greenberg, Ziff and Greene, 1986; Flavell and Greenberg, 2008). Transcriptional changes induced by synaptic activity promotes axonal and dendritic outgrowth, bringing together pre- and postsynaptic aspects of neuronal circuitry (Henley and Poo, 2004). Calcium-induced changes to neuronal transcription programmes also promote synapse maturation (Redmond and Ghosh, 2005).

In addition to effects on neuronal function, synaptic activity also promotes transcriptional changes that promote neuronal survival, conferring resistance to both excitotoxic and apoptotic insults. Synaptic activity, via activation of NMDAR-mediated Ca^{2+}-dependent transcription factors such as NFAT, NFI-A and CREB in neurons, leads to the expression of a family of genes called activity-regulated inhibitors of death (AIDs) (Hardingham and Bading, 2003). These genes confer resistance to neuronal death by a number of mechanisms, including increasing mitochondrial resistance to stress. Neuronal activity also promotes the expression of a number of neurotrophic factors (for example Bdnf,

Fgf2). Synaptic activity has been demonstrated (by suppressing key pro-apoptotic transcription factors such as p53 and forkhead box protein O (FOXO) to suppress components of both intrinsic and extrinsic apoptosis pathways, further promoting neuronal resilience to injury and disease (Léveillé *et al.*, 2010).

Finally, synaptic activity enhances neuronal resilience and health by boosting neuronal antioxidant defences (Baxter *et al.*, 2015, Baxter and Hardingham, 2016). Whilst neurons suppress Nrf2 and rely on astrocyte antioxidant pathways for the supply of glutathione precursors, synaptic activity is able to regulate mechanisms to utilise these precursors, as well as control other intrinsic Nrf2-independent antioxidant systems. Synaptic activity regulates both GSH pathway genes and other antioxidant genes that form part of the thioredoxin-peridoxin pathways such as *Gclc*, *Gsr*, *Srxn1* and *xCT*. Whilst some of these genes are Nrf2 dependent, neuronal activity regulates these genes in an Nrf2-independent manner by means of utilising other activity-dependent transcription factors such as AP-1 and ATF4 (Deighton *et al.*, 2014).

1.2.2.3. *Synaptic activity – consequences on astrocyte transcription*

Given that synaptic activity has such profound consequences on neuronal transcription as described above, a natural question is whether it influences astrocyte transcription to alter astrocyte function.

Astrocytes have been shown to respond to neurotransmitters such as, for example, glutamate the main excitatory neurotransmitter in the CNS. As discussed above, single synaptic activation of neighbouring neurons can lead to altered astrocytic Ca^{2+} responses. Unlike the neuronal response to glutamate, which mainly involves ionotrophic glutamate receptors such as NMDA or AMPA, the astrocyte response typically involves metabotropic glutamate receptors (mGluRs) (Panatier *et al.*, 2011).

Human studies on mature astrocytes extracted via immunopanning from human brain tissue suggest that mature human astrocytes responded to glutamate administered in the medium, and this was inhibited by mGluR5 antagonists (Zhang *et al.*, 2016). Other receptors including adrenergic, purinergic, serotonin and muscarinic receptors have also been described on astrocytes (Porter and McCarthy, 1997) and astrocytes have been shown to respond to other neurotransmitter substances such as vasoactive peptide, ATP and noradrenaline which act via GPCRs as outlined above.

Exposure to glutamate has been shown to alter astrocyte glutamate transporter levels (Yang *et al.*, 2009) and transporter position (Murphy-Royal *et al.*, 2015). Glutamate also affects key astrocyte metabolic processes including aerobic glycolysis (Pellerin and Magistretti, 1994a), mitochondrial positioning (Jackson *et al.*, 2014), and the response to hypoxia (Vanzulli and Butt, 2015).

Neuronal activity has also been suggested to increase astrocyte Nrf2 expression. Coculture of astrocytes and neurons utilising membrane-inserts physically

separating the cell-types but allowing diffusion of soluble messengers, combined with elevated neuronal activity in intact brain slices, neuronal activity was found to increase levels of astrocytic Nrf2 (Habas *et al.*, 2013). This required a well-developed synaptic network, action potential firing and was reduced by glutamate receptor inhibitors (NMDA and mGluRs) and intracellular Ca^{2+} chelation.

Finally, more recent published work from the Hardingham lab (including data from this thesis) describes the effect that that neuronal activity *in vitro* had profound influence on astrocyte transcription and function (Hasel *et al.*, 2017). And a recent study using single-cell sequencing of visual cortices from mice exposed to 1h and 4h light stimulus also revealed the capacity of neuronal activity to change astrocyte transcription (Hrvatin *et al.*, 2018). These studies will be discussed more fully in the results and discussions chapters below.

1.2.2.4. *Gliotransmission*

Given the close proximity to synapses, and the response to neurotransmitter substances, astrocytes have also been implicated to release neuroactive substances in response to synaptic signalling. These substances are hypothesised to signal back to neurons and modulate synaptic transmission. Postulated gliotransmitters include amino acids such as glutamate and D-serine (Parpura *et al.*, 1994; Schell, Molliver and Snyder, 1995); nucleotides such as

ATP (Bal-Price, Moneer and Brown, 2002) and complex peptides such as ANP and BDNF (Kržan *et al.*, 2018).

The concept of gliotransmission is controversial. Positive evidence supporting gliotransmission include the blockage of long-term potentiation (LTP) in the hippocampus by Ca^{2+} chelation in astrocytes (Henneberger *et al.*, 2010), and the induction of neuronal activity in nearby neurons by stimulating astrocytes – a phenomenon that can be transmitted through neighbouring astrocyte gap junctions (Nedergaard, 1994). *In vivo* evidence that supports glia transmission includes the reduction of cortical gamma oscillations and behavioural deficits induced by astrocyte-specific inhibition of vesicle release by tetanus toxin (Lee *et al.*, 2014).

Negative evidence against gliotransmission includes the lack of neuronal or behaviour changes seen in transgenic mouse lines that both activated astrocyte calcium signalling via a synthetic GPR or inhibited calcium signalling via blockade of the IP3 pathway (Agulhon, Fiacco and McCarthy, 2010). And astrocytes from specific brain regions *in vivo* appear to have very low levels of RNA and protein expression of the Ca^{2+}-sensitive vesicular release machinery for the commonly described gliotransmitters (Chai *et al.*, 2017).

Therefore, whilst astrocytes are closely involved in synapses, and have been implicated to be both modulated by synaptic activity, and in turn to modulate neurotransmission, the exact role of neuron-astrocyte interactions in normal physiology and in disease remains incompletely understood.

1.2.2.5. *Interactions with other CNS cell-types.*

Whilst a full discussion is beyond the scope of this introduction, it is important to note that astrocytes also have important interactions with other CNS cell-types. These include microglia, oligodendrocytes, pericytes and endothelial cells.

Astrocyte-oligodendrocyte interactions have been suggested to have a key role in promoting remyelination following injury by supplying cholesterol precursors needed for myelin formation (Itoh *et al.*, 2018). And astrocytes interact with pericytes and endothelium cells to regulate blood-brain barrier properties as described above. Finally, there is a growing body of evidence that microglia-astrocyte crosstalk is essential in regulating astrocytosis and in determining the fate of reactive astrocytes in response to CNS injury. A fuller description of how microglia may influence astrocyte phenotype in disease is detailed in section 1.3.1.

Section Summary

Astrocytes alter intracellular signalling pathways in response to extracellular signals, especially from other CNS cell-types such as neurons. However, the full consequence of these signals on astrocyte transcription and function are poorly understood. In this thesis, I describe studies aimed at better understanding the astrocyte response to neuronal signals and the consequence on key homeostatic and metabolic functions.

1.3. Astrocytes during disease.

1.3.1. Reactive astrocytes

The previous sections have described the important roles that astrocytes play during normal physiology. Since astrocytes were first described, it has been observed that they alter their characteristics in response to disease and injury: a term called reactive astrocytosis (Virchow, 1855; Liddelow and Barres, 2017).

Morphologically, reactive astrocytes hypertrophy, reduce their stellate appearance, and following some insults undergo proliferation to form a glial scar. Functionally, they demonstrate altered intracellular calcium signalling; reduced glutamate uptake capacity; production of extracellular matrix molecules; and the secretion of inflammatory mediators such as Il-6, TGF-B and TNF-alpha (Liddelow and Barres, 2017). Reactivity is a heterogeneous response, encompassing a spectrum of morphological, transcriptional and functional changes. The nature and duration of reactivity is determined by the nature and strength of injury or insult.

It is emerging that reactive astrocytes can demonstrate both neuroprotective and neurotoxic roles. Reactive astrocytes in spinal cord injury have been demonstrated to secrete inhibitory extracellular matrix molecules that inhibit neurite outgrowth and lead to regeneration failure (Yiu and He, 2006). Conversely, reactive astrocytes have also been shown to have beneficial effects. In spinal cord recovery, removal or inhibition of astrocyte scar formation

resulted in reduced spontaneous regrowth of transected axons following cord injury (Anderson *et al.*, 2016).

More detailed profiling of reactive astrocytes has become possible recently with RNA-sequencing. This has revealed distinct transcriptional signatures associated in response to different injury paradigms (Zamanian *et al.*, 2012). This study described distinct types of reactive astrocytes produced in response to an inflammatory insult (LPS injection) vs an ischaemic insult (middle cerebral artery occlusion). These two reactive astrocyte types were termed "A1" vs "A2" to reflect the "M1" vs "M2" nomenclature that has previously been utilised to describe macrophage and microglial responses.

A1 astrocytes, produced in response to inflammation, upregulate many genes that are neurotoxic (for example, genes associated with activation of the complement cascade) and were demonstrated to be detrimental to neuronal health and synapses. They had reduced ability to induce synapse formation and secreted an unidentified toxin that specifically induced neuronal and oligodendrocyte apoptosis (Liddelow *et al.*, 2017).

In contrast, A2 astrocytes, produced in response to ischaemic injury, upregulated many neuroprotective genes that are involved in the astrocyte antioxidant response and promoting synapse repair, and have been demonstrated to be broadly neuroprotective (Hayakawa *et al.*, 2014).

Whilst this simple binary classification of reactive astrocytosis (A1 – neurotoxic vs A2 - neuroprotective) is most likely an oversimplification of a complex and

heterogenous response to injury, it nevertheless serves as a useful framework to describe the manner in which astrocytes can have both neurotoxic and neuroprotective roles in the context of injury.

Whilst the signals that modulate astrocyte phenotype are incompletely understood, non-cell autonomous interactions between astrocytes and other CNS cells are believed to be important. Recently it has demonstrated that inflammatory processes that act to push astrocytes towards an A1 phenotype requires signalling via activated microglia through the release of specific cytokines (IL1a, TNFa and C1a) which modulated astrocyte phenotype into an A1 vs A2 profile (Liddelow *et al.*, 2017).

The full extent of the signals that control astrocyte phenotype, as well as a more complete understanding of what happens to astrocyte phenotype in a more chronic and complex neurodegenerative process such as dementia are not understood, and developing a better understanding of these questions forms a key aim of this thesis.

1.3.2. Astrocytes and dementia

Astrocytes have been implicated as playing important roles as both upstream mediators and downstream effectors in several neurodegenerative diseases. These include: dementias such as Alzheimer's (AD) (Cai *et al.*, 2012), frontotemporal dementia (FTD) (Radford *et al.*, 2015), Parkinson's disease

(Rappold and Tieu, 2010); Huntingtons disease (Tong *et al.*, 2014); and amyotrophic lateral sclerosis (ALS) (Nagai *et al.*, 2007; Serio *et al.*, 2013).

In this thesis I describe studies investigating how astrocytes respond to neurodegeneration in a transgenic model of human tauopathy and FTD. Therefore, I will now expand upon the general pathology involved in dementia (AD and FTD) and the current understanding of the role that astrocytes may play in these diseases.

1.3.2.1. *Dementia – definition and pathology*

The term dementia encompasses a range of different neurodegenerative conditions that lead to a progressive decline in memory, cognitive function and behavioural changes. The two most common causes of dementia are Alzheimer's disease (AD) and frontotemporal dementia (FTD). Dementia remains a massive global clinical and economic problem. It affects 48.4 million individuals worldwide and the lifetime risk of developing dementia in the western world is estimated to be as large as 25.9% for women, and 13.7% for men (Licher *et al.*, 2018), with the global cost of dementia estimated to rise to approximately $1 trillion annually by 2018 (World Alzheimer's Report, 2015). Aetiologically, these diseases are associated with ageing, as well as environmental and genetic risk-factors.

Histopathologically, dementias are characterised by the presence of intra and extracellular aggregates of misfolded proteins (Lippens *et al.*, 2007). These

include β-amyloid and hyper-phosphorylated tau protein in Alzheimer's disease, and hyper-phosphorylated tau and transactivation-response-element DNA-binding protein 43 (TDP-43) aggregates in FTD. Accumulation of misfolded protein is thought to initiate a cascade resulting in inflammation, synaptic loss, mitochondrial dysfunction and loss of antioxidant homeostasis (De Strooper and Karran, 2016), ultimately resulting in neuronal death.

β-amyloid is a 33-43 kDa peptide that constitutes the extra-cellular amyloid plaques found in AD. β-amyloid is derived from cellular amyloid precursor protein (APP), which is processed by cellular secretases to yield soluble amyloid monomers (O'Brien and Wong, 2011) . According to the amyloid cascade hypothesis, oligomerisation of amyloid protein yields toxic soluble oligomers and toxic non-soluble fibrils and plaques (Reitz, 2012).

Tau is a 55-74 kDA microtubule associated protein (Pîrşcoveanu *et al.*, 2017). In health, tau binds reversibly to the cellular microtubules and regulates cytoskeletal function and transport. Alternative splicing can generate multiple isoforms of the protein. Isoforms have different affinities for microtubule binding and abnormalities in ratios of tau isoforms have been implicated in disease. Post-translational modifications of tau, and in particular its phosphorylation state, are key modifiers of its function. Hyperphosphorylation of tau causes it to accumulate within cellular aggregates, which are the hallmark of AD and FTD.

The roles of amyloid and tau in dementia are poorly understood, and it is unclear whether accumulation of misfolded protein is a primary driver of pathology or merely represent down-stream consequences of generalised cellular malfunction. There has been a recent shift of focus on the role that tau might play in both AD and FTD (Kametani and Hasegawa, 2018). Several familial mutations in tau have been identified that can cause dementia without amyloid deposition (Wolfe, 2009), and tau aggregation appears to be more closely related to cognitive loss in AD (Huber *et al.*, 2018). Studies have also demonstrated that suppression or deletion of tau has neuroprotective effects in AD models (Shipton *et al.*, 2011). Finally, the focus on understanding tau pathology is further supported by unexpected failures trials of candidate drugs targeting β-amyloid (Doody *et al.*, 2013, 2014; Salloway *et al.*, 2014).

1.3.2.2. *Astrocyte roles in dementia*

Astrocytes have long been implicated as playing a number of roles in AD and FTD pathology. Some genes identified as being associated with Alzheimer's from genome-wide association studies (for example *Apoe and Clusterin*) are expressed more highly in astrocytes as compared to neurons (Cahoy *et al.*, 2008), and reactive and abnormal astrocytes are a well-established histopathological feature of AD (Chun and Lee, 2018) and FTD (Radford *et al.*, 2015).

Astrocytes undergo morphological and functional changes, which can include both toxic gain-of functions as well loss of normal neuroprotective and homeostatic functions. Astrocytes react to misfolded protein aggregates such as β-amyloid in plaques and uptake β-amyloid via the low-density lipoprotein receptor-related protein 1 (LRP1) transporter, with astrocytes being implicated in both β-amyloid clearance and plaque spread (Liu *et al.*, 2017). In AD, activated astrocytes surrounding plaques overexpress the serine protease inhibitor a1-antichymotrypsin (ACT). This protein has been suggest to inhibit β-amyloid breakdown and to induce tau hyperphosphorylation (Akiyama *et al.*, 2000; Padmanabhan *et al.*, 2006).

Astrocytes in AD demonstrate impaired calcium signalling. Picomolar amounts of β-amyloid induce intracellular calcium transients and spontaneous intercellular Ca^{2+} waves in cultured astrocytes and leads to upregulation of the reactivity marker Glial Fibrillary Acidic Protein (GFAP) (Lee, Kosuri and Arancio, 2014). Targeting activated astrocytes in the hippocampus of APP/PS1 mouse model of Alzheimer's with astrocyte-specific expression of VIVIT, an inhibitor of the calcineuron/NFAT signalling pathway, was shown to reduce glial activation and improve cognition (Furman *et al.*, 2012). In addition, astrocyte glutamate uptake capacity is impaired in AD, via mechanisms involving oxidative modifications of the glutamate transporters EAAT1 and EAAT2, in both patient brain samples and animal models (Beart and O'Shea, 2009).

In contrast to AD, the consequences of astrocyte activation in tauopathy or FTD are less well understood. Astrocytes in mutant-tau transgenic mouse models of FTD were found to have reduced glutamate transporter expression and transport capacity, along with reduced GLT-1 staining in tau-bearing astrocytes (Dabir, 2006). And in an IPS-stem cell model of FTD, astrocytes expressing the N279K MAPT mutation demonstrated increased vulnerability to oxidative stress, with impaired antioxidant capacity, when co-cultured with neurons (Hallmann *et al.*, 2017). Astrocytes in FTD-model transgenic mice have also been shown to demonstrate increased levels of markers associated with cellular senescence and clearance of senescent cells reduced tau-dependent pathology and improved cognition (Bussian *et al.*, 2018). Finally, transplantation of healthy glial-precursors has been demonstrated to reduce disease severity in the P301S tauopathy model of FTD (Hampton *et al.*, 2010).

Section summary

Taken together, the above studies demonstrate the emerging concept that astrocytes are influenced by neurodegenerative processes and play important roles in mediating both toxic down-stream processes as well as having neuroprotective roles. However, the manner in which astrocyte phenotype is altered in dementia, as well as the consequence on neuronal health, is poorly understood.

1.4. Thesis aims

In this introduction, I have summarised key roles that astrocytes play in health and disease, along with our current understanding of the cell-autonomous and non-cell autonomous signals that influence their function and phenotype. The signals that control astrocytes in normal physiology, and the consequences of neurodegeneration on astrocyte transcription, function and phenotype are incompletely understood.

The overall aim of the work presented in this thesis was to better understand the non-cell autonomous signals that control astrocyte transcription and function in health and disease. This was to identify astrocyte neuroprotective signalling pathways that could be manipulated to enhance CNS resilience and reduce neuronal loss in neurodegenerative conditions such as dementia.

The first results chapter describes studies investigating how neuron-astrocyte interactions alter astrocyte transcription to drive metabolic capacity of astrocytes *in vitro*. The second results chapter expands upon this *in vivo*: examining how astrocyte transcription is influenced by synaptic activity in both a controlled light-stimulus paradigm, and a more complex (yet more clinically relevant) prolonged anaesthesia paradigm.

The final results chapter investigates how astrocyte transcription is altered in a transgenic mouse model of human tauopathy and FTD. I describe how neurodegeneration drives wide-spread changes to astrocyte transcriptional signatures with alterations in antioxidant pathway genes. Enhancing expression of astrocyte antioxidant pathways achieves both transcriptional and functional rescue in this model of FTD.

Chapter 2

Materials and Methods

2.1. Neuron and astrocyte cell-culture

2.1.1. Rodent primary culture

Primary cortical neurons and astrocytes were cultured from E17.5 CD1 mice or E20.5 Sprague Dawley (SD) rat embryos using a modified version of the protocol described by Bading and Greenberg, 1991. Cortices were dissected following decapitation in dissociation medium (DM) (mM: 81.8 Na_2SO_4, 30 K_2SO_4, 5.84 $MgCL_2$, 0.252 $CaCl_2$, 1 HEPES, 0.001% Phenol Red, 20 Glucose, 1 kyurenic acid, adjusted to pH 7.35 with NaOH). Tissue was enzymically digested by incubation with DM with 10 units/mL papain enzyme (Worthington Biochemicals) for 40 mins with regular mixing, followed by two washes with DM and two washes with Neurobasal-A medium (Thermofisher) supplemented with 1% rat serum (Envigo), 1 x B-27 supplement (Thermofisher), 1 x Antimicrobial-Antifungal supplement (premixed penicillin, streptomycin and amphotericin B - Thermofisher) and 1mM glutamine (Sigma). Following washing, cortices were mechanically dissociated with repeated mixing using a 5 mL serological pipette and the resulting cell-suspension diluted with in Opti-MEM (Life Technologies) supplemented with glucose (20 mM) and Antimicrobial-Antifungal to achieve a final tissue concentration of 0.14 mouse cortical hemispheres or 0.07 rat cortical hemispheres per mL.

For neuronal culture, 0.5 mL of cell suspension was added to 24-well tissue-culture plates (with or without glass-coverslips) coated with 0.5 mLs of water

with 0.5% laminin from mouse Engelbreth-Holm-Swarm sarcoma cells (Roche) and 1.33% poly-D-lysine (Sigma). For astrocyte culture, 10 mL of cell suspension was added to 75 cm tissue-culture flasks coated with 10 mL of water with 1.33% poly-D-lysine only. All plates and flasks were pre-coated with appropriate coating mixtures for 2 h at 37ºC in a humidified 5% CO2 incubator and washed and dried prior to application of cell suspension.

Plates and flasks with cell-suspension were incubated for 2.5 h at 37ºC in a humidified 5% CO2 incubator. After this, plate or flask medium was aspirated (along with dead or non-adherent cells) and replaced with feeding medium. Neurons were fed with: 1 mL Neurobasal-A medium supplemented with 1% rat serum, B-27, Antimicrobial-Antifungal and glutamine as above as described above. Astrocytes were fed with Dubenco's Modified Eagle Medium with 4.5% glucose, L-glutamine and Phenol Red (DMEM High Glucose – Thermofisher) supplemented with 10% heat inactivated fetal bovine-serum (Invitrogen) and 1x Antimicrobial-Antifungal.

Neuronal cultures were subsequently fed at day *in vitro* (DIV) 4 with 1 mL of Neurobasal-A medium supplemented with 1% rat serum, B-27, Anti-Anti and glutamine along with 9.6 µM of the antimitotic cytosine B-D-arabinofuranoside hydrochloride (AraC) to prevent glial growth. Astrocyte cultures were fed at DIV4 with 10mLs of DMEM supplemented with 10% FBS as above.

Astrocytes were split 3:1 (by washing with 1 x PBS, followed by detachment using 0.05% trypsin-EDTA (Life Technologies), twice at DIV 7 and DIV 11 to

achieve >95% GFAP positive pure astrocyte cultures. For co-culture astrocytes were plated onto 24 well plates at astrocyte DIV 11, and primary neurons were cultured on top of confluent astrocytes 72 h later. Neuron-astrocyte cocultures were kept in serum-free medium (Neurobasal A supplemented with B-27, Anti-Anti and glutamine as above) and fed every 3-4 days. Co-cultures were utilised for experiments at neuronal DIV 9 (Astrocyte DIV 23) unless otherwise stated.

2.1.2. Human astrocytes

Primary human astrocytes were obtained from ScienCell Research Laboratories, and cultured in human astrocyte medium (ScienCell) for up to 5 passages in a similar manner to rodent astrocytes described above. Induced pluripotent stem-cell derived astrocytes were generated and maintained as previously described (Serio *et al.*, 2013). In brief, neural precursor cells obtained from human-derived induced pluripotent stem-cells were cultured as neurospheres suspended in medium enriched in epidermal growth factor (EGF) and leukemia inhibitory factor (LIF) for four to six weeks. After enrichment, neurospheres were enzyme- dissociated to a single-cell monolayer of astroprogenitor cells, and differentiated into mature human astrocytes by culturing with cilliary neurotrophic factor (CNTF). This process yielded cells with >95% positive for astrocyte markers (GFAP, s100B or aldh1l1) and < 2% of cells positive for neuronal markers (beta-3-tubulin).

2.1.3. Drug stimulations

Conditions of altered synaptic activity in co-cultures were generated by changing cells into serum-free base-medium (10% minimum essential media (MEM, Life Technologies) and 90% salt–glucose–glycine (SGG) containing in mM: 114 NaCl, NaHCO3, 5.292 KCl, 1 $MgCl_2$, 2 $CaCl_2$, 10 HEPES, 1 Glycine, 30 Glucose, 0.5 sodium pyruvate, 0.1% Phenol Red) with 100nM tetradotoxin (TTX, Tocris) on DIV8 for 22 h to inhibit neuronal action potential firing. Cells were then washed and changed into medium containing 50 µM Bicuculline (BiC, Tocris) to induce network bursting. Control conditions were washed with TTX and left in medium containing BiC in the presence of TTX to maintain activity inhibition.

2.2. Transfection

Astrocyte specific transfection was achieved by transfecting confluent astrocytes 24 h prior to neuronal co-culture. Cells were incubated for 45 mins in DNA/lipofectamine mix (0.65 µg total DNA with 2.33 µL of Lipofectamine 2000 (Life Technologies) per well) in serum free transfection medium (in mM: 114 NaCl, 26 $NaHCO_3$, 5.3 KCl, 1 $MgCl_2$, 2 $CaCl_2$, 10 HEPES, 1 glycine, 30 glucose, 0.5 sodium pyruvate, 0.001% phenol red, 1% Antibiotic-Antimitotic, 1% insulin–transferrin–selenium supplement (Thermofisher Scientific)). Following transfection, the lipofectamine-DNA mix was washed off and medium replaced with DMEM supplemented with 10% FBS and Antibiotic-Antimitotic as above.

Table 2-1 – References and sources for plasmids

Glucose FRET (FLII12Pglu-700μδ6)	Takanaga, Chaudhuri and Frommer, 2008
Pyronic FRET	San Martín *et al.*, 2014
Laconic FRET	Barros *et al.*, 2013
VP16-CREB	Klemm *et al.*, 2001
ICER	Inada *et al.*, 2004

2.3. Imaging

2.3.1. Immunohistocytochemistry

For cell culture: cells were fixed with 4% paraformaldehyde (PFA) for 20 mins at RT, washed 3x with PBS, and permeabilized for 5 mins with 1% NP40 (Life Technologies). For cortical slices: Mice were killed by perfusion-fixation with 4% PFA. Brains were removed and 50 μM slices prepared using a vibratome. Slices were washed 3x with PBS, blocked and permeabilized with 10% normal goat-serum (Thermofisher) with 0.3% Triton-X (Sigma-Aldrich). Primary antibodies were applied overnight at 4^{0}C whilst shaking, and secondary antibodies applied for 2hr at RT. Following this, cells or slices were washed 4x in PBS and mounted using Vectashield with 4′,6-diamidino-2-phenylindole (DAPI) (Vector Labs).

Table 2-2 Antibodies used for imaging

Antibody	*Source*	*Code*	*Concentration*
Anti-GFP-FITC (goat)	Abcam	Ab6662	1:500
Neuro-chrom™-CY3 (rabbit)	Millipore	Abn2300c3	1:500
Anti- ALDH1L1 (rabbit)	Abcam	Ab190298	1:500
Anti-Rabbit IgG-CY3 (donkey)	Jackson	711-165-152	1:500

2.3.2. Quantifying astrocyte perimeter

Changes in GFP-transfected astrocyte complexity in monoculture and co-culture was determined by taking cells at DIV0 vs DIV9, and an outline mask created using Adobe Photoshop. The area and perimeter measurements of the outline mask were determined and ratios calculated.

2.3.3. FRET metabolic imaging

FRET and fluorescence imaging was carried out on a Leica AF6000 LX microscope utilising a DFC350 FX digital camera operated using the LAS X imaging suite. All FRET imaging was performed at 37^{0}C in continuous perfusion with artificial-CSF (composition in mM: 150 NaCl, 3 KCl, 10 HEPES buffer, 0.1 glycine, 2 $CaCl_2$, 1 $MgCl_2$, and 10 glucose, pH 7.4). Tetrodotoxin (TTX) 100 nM was added to A-CSF perfused in all conditions to exclude acute effects of altered neuronal activity on astrocyte metabolism at the time of imaging. Imaging was carried out at 20X magnification and images were acquired every 10 s. All

probes were imaged with a standard FRET CFP/YFP filter wheel, with excitation at the CFP spectrum (472±5 nm) and measurements taken within both CFP (472±15 nm) and YFP (542±13 nm) emission spectra.

For glucose measurement, the YFP/CFP ratio of FLII12Pglu-700uδ6 FRET probe was used to determine intracellular glucose concentrations for individual astrocytes. Levels were measured at baseline in ACSF with TTX, before the addition of the glucose-uptake inhibitor cytochalasin B (20 μM) after 60s, resulting in a reduction in intracellular glucose levels corresponding to the rate of glucose consumption.

For pyruvate and lactate measurements, the CFP/YFP ratio of the Laconic and Pyronic FRET probes were used to determine intracellular lactate and pyruvate levels respectively. Levels were measured at baseline in ACSF, before the addition of the MCT inhibitor AR-C155858 (1 μM) resulting in an increase in concentration corresponding to lactate or pyruvate production.

All FRET ratios were normalised by subtracting baseline and expressed as percentage of maximum. A linear least-squares fitting routine was used to determine the line of best fit and slopes calculated for the portion of the curve corresponding to the rate of consumption or production of substrate.

2.4. Western blots

Cell-culture and tissue samples were lysed in RIPA-buffer (500 µL per half-cortex; 40 µL per well of 24-well tissue-culture plate) followed by centrifugation to remove non-lysed debris. A BCA assay (see below) was utilised to calculate protein concentrations of lysate. Protein concentration was adjusted and mixed with 4x LDS Sample Buffer (Thermofisher) and 10x Nupage Sample Reducing Reagent (Life Technologies) to achieve 1 µg/µL of protein and samples boiled at 100^{0}C for 10 mins, 15 µg of protein were loaded onto 4-12% pre-cast gradient Bis-Tris gels (Nupage, Life Technologies) and electrophoresis performed using the XCell SureLock system at 120V, in MOPS running buffer (in mM: 50 3-(N-morpholino)propanesulfonic acid (MOPS), 50 tris(hydroxymethyl)aminomethane (TRIS), 1 EDTA, 3.5 SDS, pH adjusted to 7.7).

Proteins were transferred onto a PVDF membrane (Millipore) by electrophoresis at 80V for 1h in transfer buffer (in mM: 96 glycine, 12 mM Tris, 20% Methanol). Membranes were blocked in Tris-buffered saline (TBS) (in mM: 20 Tris, 137 NaCl and 0.1% Tween-20, pH 7.6, 5% milk) and incubated with primary antibody overnight at 4^{0}C. The following day, membranes were washed in TBS three times and incubated with HRP-conjugated secondary antibody for 1 h at RT. For reprobing, membranes were stripped for 15 mins using ReBlot PLUS Strong (Merck Millipore), re-blocked with 5% milk TBS with tween for 1 h, before repeat primary antibody incubation as above.

Bands were visualised using peroxide and LumiGlo (Cell Signalling), and photographed on Kodak X-Omat film (Sigma). A range of exposures were utilised to ensure both that bands were not saturated and that faint bands were not missed. Developed photographs were digitally scanned (greyscale, 600dpi) and densitometric quantification performed using ImageJ, with subtraction of background and normalisation of band density performed using a β-actin control for each well.

Table 2-3 Antibodies used for Western blots

Antibody	*Source*	*Code*	*Concentration*
Anti-Cleaved - Caspase 3 (Rabbit)	Cell-Signalling	#9664	1:1000
Anti-Caspase-3 (Rabbit)	Cell-Signalling	#9665	1:1000
Anti-β-Actin (Rabbit)	Abcam	Ab8227	1:20000
Anti-rabbit IgG – HRP (Goat)	Cell Signalling	#7074	1:2000

2.5. Bicinchoninic acid (BCA) assay

Protein concentrations were measured using the Pierce BCA assay (Thermofisher) as per instructions. 50 µL of lysate was transferred in triplicate to a clear flat-bottomed 96 well plate, along with 50 µL of known bovine-serum albumin standards, and 200 µL of BCA protein re-agent mixture added. The plate was covered and incubated at 37^{0}C for 30 mins, and absorbance measured at 562 nM using the Lumistar Omega plate reader.

2.6. Caspase-GLO Assay

Activated caspase 3 and 7 activity was measured using the Caspase-Glo™ 3/7 luminescence assay (Promega) as instructions. 50 µL of normalised tissue extract (1 µg/µL protein) was added to 96 well plates in triplicate, along with samples from negative and positive apoptosis controls (cultured cells exposed to 24h of 100nM staurosporin). 50 µL of reconstituted Caspase-Glo reagent was added, and mixed gently at RT for 30 secs. The plate was incubated at RT for 1h and luminescence measured using a plate reader.

2.7. Fluorescence-activated cell sorting

CNS cell suspensions were prepared by enzyme and mechanical dissociation of mouse cortices as described above, with final resuspension in 10 mLs Hibernate A (Thermofisher) + 1% rat serum + B27 + A/A at 4^{0}C. Suspensions were sorted using a FACSAria IIiu flow cytometer (Beckton Dickinson Immunocytometry Systems (BD), UK) running BD FACSDiva v6 software. An electronic acquisition gate was applied to the Forward/Side scatter plot to exclude debris from intact material. Aggregates were excluded by applying gating to the FSC area vs width profile. EGFP was detected following 488 nm excitation, at emission between 530/30nm and an electronic gate applied to identify positive cells by reference to a negative control.

Cells were acquired at ~12,000 events per second and positive cells were sorted using a 85 µm nozzle at a system pressure of 45 psi into 15 mL collection tubes pre-filled with 5 mL Hibernate A medium supplemented with 20% bovine serum. Sort purity was verified by the reacquisition of 1,000 singlets from the collection tubes. Post-acquisition data was gated and analysed using FacsDiva v6 software.

2.8. RNA analysis

2.8.1. RNA extraction

RNA extraction was carried out using the High Pure RNA Isolation Kit (Roche) as per manufacturer's instructions. 3 wells of a 24 well cell-culture plate were lysed per sample and transferred into glass-fibre filter column assemblies. Following DNAse incubation for 15 minutes, the columns were washed, dried and RNA eluted in 30 µL of elution buffer.

Low-yield RNA extraction (for example following ribosomal pulldown) was carried out using the Absolutely RNA Nanoprep kit (Agilent) as per manufacturer's instructions. Samples were lysed in 100 µL of lysis buffer with β-mercaptoethanol; mixed with equal volume of 80% sulfolane and added to silica-based fibre filter columns. DNAse treatment was carried out for 15 mins; columns were washed and dried, and RNA eluted in 20 µL of pre-warmed 60ºC RNAse free water.

2.8.2. Translating Ribosome Affinity Purification (TRAP).

Isolation of cell-type specific translating mRNA was carried out as previously described (Heiman *et al.*, 2014). Briefly: tissue or cells were lysed in ice-cold lysis buffer (in mM: 20 HEPES, 10 $MgCl_2$, 150 KCl, 0.5 DTT) along with 100 µg/mL cyclohexamide (Sigma), cOmplete ULTRA protease inhibitors (Sigma) and RNAse inhibitors (Superasin – Life Technologies; RNAsin – Promega). Cell lysate was centrifuged to clear debris and solubilised with 1% NP40 and 30 mM 1,2-diheptanoyl-*sn*-glycero-3-phosphocholine (DHPC – Avanti Polar Lipids). Following further centrifugation, supernatants were added to pre-prepared anti-GFP (19C8 and 19F7 antibodies – Sloan Kettering Memorial Centre) coated magnetic beads (Dynabeads MyOne Streptavadin T1 – Life Technologies). Following immunoprecipitation overnight at 4^{0}C with continuous rotation, beads were washed four times. Cell-type specific mRNA, attached to immunoprecipitated GFP-tagged ribosomes, was isolated and purified using the Agilent Nanoprep kit described above. 50 µL of solubilised lysate ("input sample" – representing total RNA) was taken prior to immune-precipation and spun overnight at 4^{0}C (same conditions as TRAP samples) before RNA-purification with TRAP samples.

2.8.3. Reverse-transcription PCR (rtPCR)

cDNA was generated using the Transcriptor First Strand cDNA Synthesis Kit (Roche). 7 µL of RNA was added to the RT and buffer mixture prepared with random hexamers and oligoDT primers as per kit instructions, and rtPCR

carried out with the following programme: 10 min at 25°C, 30 min at 55°C and 5 min at 85°C.

2.8.4. Quantitative PCR (qPCR)

qPCRs were performed on a Mx3000P QPCR machine (Agilent Technologies) using the FastStart Universal SYBR Green QPCR Master (Rox) (Roche) reagent. 6 ng of cDNA was used for each reaction and all qPCR results were carried out in duplicate or triplicate, along with no template controls and no RT controls where appropriate. The following cycling programme was used: 10 min at 95°C; 40 cycles of: 30 s at 95°C, 40 s at 60°C (with fluorescence detection), 1 min at 72°C; ending with dissociation curve: 1 min at 95°C and 30 s at 55°C with a ramp up to 30 s at 95°C with fluorescence detection. All data was normalised to house-keeping gene controls (*Rpl13a*).

Table 2-4 Mouse-specific primer sequences

Gene	*Forward (5'-3')*	*Reverse (5'-3')*
Aif1	GCAATGATGAGGATCTGCC	CCACTGGACACCTCTCTAATTAATC
Aldh1l1	GTTGCTAGCCCAGAGCC	GGAACTTAAACACGGGCAC
Aqp4	GAGAGTCGTCACACCAGTG	TCCCAGCCAGGAAGTAACTA
Arc	AGTGGTGGGAGTTCAAGCAG	TCCTCAGCGTCCACATACAG
Bdnf	AAAGTCCCGGTATCCAAAGG	CTTATGAATCGCCAGCCAAT
Cx3cr1	CTGGTGGTCTTTGCCTTC	GCACTTCCTATACAGGTGTCC
Dio2	CCCTTCTGAGCGAATTGATCCA	CACATCGTAAGTATGTATCTGGG
Eno2	GCCATCTCCTGTAACTCTCC	ATTCTGTAAAGTTCCGAGCTTC
Fos	CCATGATGTTCTCGGGTTTC	TGGCACTAGAGACGGACAGA
Gfap	GCAAAAGCACCAAAGAAGGGGA	ACATGGTTCAGTCCCTTAGAGG
Hes5	TGCAGAGTTGTCATTTGGGG	AACGGGCCCTGAAGAAAGT
Hey2	GAATGTAACGTAGCACAAGATCAG	AGGTCTTTCGACTTAATTTCCC
Hk2	GTTCCCTCCCCTGTTCTAC	TCCTCTTCCTCCTCCTCC
Ldha	GTACAGTGGTGTTGAGATGGTG	CAGGGCAGCAATGCAG
Mbp	CCAGTCTAATAATGTCCATCGAC	CAGATTAACAAGATGCAGTATTGG
Mog	AAAGAATACCGACCAGAGAAATAC	CACATTGGTTCTCAGAGAAATAAG
Npy	AGACCTCTTAATGAAGGAAAGCAC	CAGGCAGACTGGTTTCAGG
Ptg	CTGCGTGAACAGGACAAG	GACAGTGTGGAGCGGAC
Rpl13a	GATGAATACCAACCCCTCC	CGAACAACCTTGAGAGCAG
Slc1a2	TATCATCTCCAGTTTAATCAC	TTCATTCAACATGGAGATGACC
Slc1a3	CAAGACACTGACACGCAAGGAC	CTTAACATCTTCCTTGGTGAGGC
Slc2a1	TGCAGCCCAAGGATCTC	TGAATATCCTCCTGGACTTCAC
Slco1c1	GATCCAGACCCTTGCGAACAT	GATATCCGACTGTAAAGGATGG
Tubb3	CCGACAACTTTATCTTTGGTC	TCCACCACAGTGTCCG

Table 2-5 Human specific primer sequences

Gene	*Forward (5'-3')*	*Reverse (5'-3')*
ALDH1L1	CTCCCTCTTGAGCCTGG	GACGGTCTCTCTTCAGAAGC
AQP4	GAGAGTCGTCACACCAGTG	TCCCAGCCAGGAAGTAACTA
HES5	TCTTCTGCCAAGTGTCTGAC	CCGGCACTACAAATATCATAGA
HEY2	TGAGAGAGTCGTGTTTCGTAAG	CAACTTGAAAATTATTTTCAGCAG
HK2	TTATAAGATGTCATCCCCTTGTG	TGATGCATGTGAACAAATCC
LDHA	GGAAAAACATCAACTCCTGAAG	CACACGGTAAACATCCACC
PFKFB3	GCGAAAGAAGGGGGAC	CTGTAGGGTCGTCGCAC
PPP1R3C	GGGAGGTCTGATCATTGTTG	AATACCACCCACATTCTTAAAGG
RPL13A	CCACTACCGGAAGAAGAAACAG	CAGGGCAACAATGGAGG
SLC16A3	CCACTGCTATGCTCAAGG	CACTCAAGAGGGGTGGG
SLC1A2	TTATTTATGTTCGGTTTGCCT	CTAGGACGATGAGATGATGACT
SLC1A3	ACCTGCCCTCTGTTTCC	ATGAATAATCCCACTCCTGG
SLC2A1	TTCCAAACCTGACAGATGTC	GTGGGCACAGGAGACTC
SLCO1C1	GATCACACAGACTACCAAACAC	GTTTGTACGTCACCATGCCG
SOD3	CCACCATCCTTCCATCC	AGATCGTCAGGTCAAAGGC

2.8.5. RNA-sequencing

Total RNA sequencing was performed by Edinburgh Genomics using Trueseq Stranded Total RNA V2 library preparation along with next-generation sequencing on the Illumina Novaseq 6000 platform. At-least 1 µg RNA per sample was utilised, with RNA-integrity number (RIN) > 7. TRAP-sequencing (along with sequencing of matched inputs where appropriate) was performed by Cambridge Genomic Services, utilising the Clonetech - SMART-Seq v4 Ultra Low input RNA library preparation, along with sequencing on the Illumina Nextseq 500 platform. At least 1ng RNA was used per sample with RIN > 7. All sequencing utilised 75 paired-end reads at the following requested depths:

Table 2-6 Requested depth for RNA-sequencing

Experiment	***Approximate sequencing depth (per sample)***
Light Stimulus TRAP	Input: 50 million TRAP: 30 million
Co-culture Mixed-species TRAP	Input: 60 million TRAP: 30 million
Anaesthesia TRAP	Input: 60 million TRAP: 30 million
P301S TRAP	Input: 60 million TRAP: 30 million
P301S- NRF2	50 million

2.8.6. Bioinformatics

Bioinformatics was performed by Owen Dando and Xin He. RNA-seq reads were mapped and analysed using Spliced Transcripts Alignment to a Reference (STAR) version 2.5.3a. Subsequently, per-gene read counts were summarised using featureCounts version 1.5.2. For read-mapping and feature counting, genome sequences and gene annotations were downloaded from Ensembl version 94. Differential expression analysis was then performed using DESeq2 (R package version 1.18.1), with a significance threshold calculated at a Benjamini–Hochberg-adjusted P value of <0.05.

Gene Ontology enrichment analysis on differentially expressed genes was performed with topGO (R package version 2.30.1), using gene ontology annotations described by the R package org.Mm.eg.db (version 3.5.0), using the Fisher's exact test statistic. The "weight01" graph processing algorithm was used to improve relevance of results.

Mixed-species sorting was carried out using the SARGASSO (Sargasso Assigns Reads to Genomes According to Species-Specific Origin) python tool as described in Hasel *et al.*, 2017 and Qiu *et al.*, 2018 *(source code available: http://statbio.github.io/Sargasso).* This utilises a strategy that aims to minimize reads misallocated to the incorrect species whilst maximizing the number of reads unambiguously assigned to the correct species. Briefly, the protocol first maps reads to the genomes of each species. All reads that map to mouse genome and not to rat are provisionally assigned to the mouse, and vice-versa. If

alignments to both genomes exist, these alignments are examined in more detail, including examining the number of mismatches, and the structure of read alignments, along with further checks, to finally assign reads with high confidence to each species, whilst rejecting ambiguous reads.

For analysis seeking to discover genes altered differentially at the level of translation compared to transcription by experimental conditions, per-gene read counts were modelled with DESeq2. In short, read counts were modelled with generalized linear models of the negative binomial family, as is standard in differential gene expression studies. A model design was used containing main effects of experimental condition (for example, mono or coculture), sample type (input or TRAP) and an interaction term between experimental condition and sample type. Genes with different translation and transcription behaviour were then discovered by testing for statistical significance of this interaction term, using a significance threshold of adjusted p-value of <0.05.

Analysis of transcription factor enrichment was carried out using the Gene2Promoter tool (Genomatix Software GmbH, Munich). Promoter regions were selected using Genomatix optimised lengths (1000 bp upstream of first transcription start site (TSS) and 100bp downstream of last TSS) from genes upregulated >2 fold in response to treatment conditions, and analysed for statistical overrepresentation of transcription factor binding sites using TRANSFAC 7.0 Library matrices, with the Z-score for enrichment over promoter background calculated.

2.9. *In vivo* methodologies

2.9.1. Animal husbandry

All procedures described were performed in compliance with the UK Animals (Scientific Procedures) Act 1986 and University of Edinburgh regulations, and carried out under project license numbers 70/9008 and P1351480E. Mice were group-housed in environmentally-enriched cages within humidity and temperature controlled rooms, with a 12-hour light dark cycle (unless otherwise stated), with free access to food and water.

2.9.2. Transgenic mouse lines

The Aldh1l1-EGFP-Rpl10a (referred to as *astro-TRAP* in this thesis) transgenic mouse line expresses an EGFP-tagged ribosomal protein l10a under the astrocyte-specific aldh1l1 promoter, was generated as previously described (Doyle et al., 2008) and re-derived on a C57B/6 background from frozen sperm imported from Jackson Laboratories (Mouse Strain Number – 030248). Animals were utilised as heterozygotes in all experiments and mixed-sex unless otherwise stated.

The Thy1-hTau.P301S (referred to as *P301S* in this thesis) transgenic mouse line over-expresses human mutant P301S tau under the neuron-specific Thy 1.2 promoter and was generated as previously described (Allen et al., 2002). Female mice were used for all experiments as they both demonstrate less fighting and

exhibit more rapid-onset pathology than males. Animals were used as homozygotes at 12 or 20 weeks for experiments described in this thesis, or culled humanely if they demonstrated rapidly progressive pathology (20% body weight loss persisting for 48 hours or hind limb paralysis). Mice were culled by perfusion with ice-cold PBS with cyclohexamide, followed by rapid dissection of the superficial frontal cortices and cervical spinal cord (C2 – C7 vertebral levels).

2.9.3. Light stimulus experiments

4 week or 24 week old mice were transferred from standard lighting conditions to a temperature and ventilation controlled light-proof cabinet and housed in constant darkness for 7 days. Mice were then exposed to a further 24 h of darkness or 24 h of continuous light, following which they were decapitated and visual cortices rapidly dissected.

2.9.4. Prolonged anaesthesia

8 week old mice were induced in an anaesthesia chamber with 4% isoflurane in oxygen, followed by maintenance anaesthesia via facemask with 1.5 % isoflurane. Mice were actively warmed to 36^{0}C, and temperature, pulse, respiratory rate and oxygen saturations continuously monitored and maintained within normal physiological range using the Physiosuite monitoring system (Kent Scientific). 0.1 mL subcutaneous warmed sterile 0.9% saline solution was administered every 1-2hrs to maintain hydration.

2.9.5. Transcranial electrical stimulation

Mice were anaesthetised and monitored as above. A small area of scalp above the right cortex and left cheek was shaved. Silver-wire electrodes were applied using electrode conducting gel (SignaGel – Parker Labs). Sinusoidal alternating current was applied at 20 min intervals via a NeuroConn DC Stimulator Plus device (NeuroCare Group, Germany) using a 10Hz frequency, with a 10 cycle fade-in and fade-out period. A ramp period of 100 μA for 5 mins followed by 250 μA for 5 mins was used before a final stimulation current of 500 μA.

1.5. Statistics and data analysis

Unless otherwise stated, all data are presented as mean, with error bars representing standard-error of the mean. Statistical tests used to analyse each result are detailed in figure legends. In general, comparisons between two means were made using two-tailed t-tests: unpaired for independent data, and paired for non-independent data. Comparisons between groups were made using 1-way or 2-way ANOVA, with correction for multiple comparisons with the Dunn-Sidak method. A significance level of $p < 0.05$ was used.

In RNA-sequencing experiments, significantly changed genes were selected as those: i) expressing >1 FPKM expression in any condition; ii) achieving significance threshold calculated at a Deseq2 Benjamini–Hochberg-adjusted p-adjusted value of < 0.05 as outlined above; and iii) demonstrating greater than

1.3 fold change. Statistical analysis was done using Graphpad Prism v7.0 for Windows (Graphpad Software Inc., San Diego, USA).

Chapter 3

Synaptic activity regulates astrocyte transcription to control metabolism.

3.1. Chapter Introduction

The consequences of activity-dependent neuron-to-neuron signalling for the CNS have been extensively studied. Synaptic activity alters neuronal transcription, and drives cellular and circuit-level changes necessary for memory and neuronal health (Hardingham *et al.*, 2018). Non-cell autonomous signals from neurons to astrocytes were also implicated to have important consequences for CNS homeostasis and function. However the manner in which neuron-astrocyte signalling influences astrocytes was not fully understood.

In this chapter, I describe investigations seeking to understand how neurons and synaptic activity alter astrocyte transcription. A key challenge in understanding non-cell-autonomous signalling between different cell-types is the requirement to physically separate cells before transcriptomic analysis. Several approaches have been traditionally used. Co-culturing astrocytes and neurons utilising membrane-inserts allows cell-types to be physically separated whilst allowing diffusion of soluble messengers (Habas *et al.*, 2013). However, this prevents direct cell-cell interactions. Other powerful and useful methods that can be used include flow-cytometry sorting, magnetic sorting and single-cell sequencing. However these methods are susceptible to contamination from off-target cell-types and require tissue to be dissociated into a single-cell suspension prior to RNA-extraction, which can induce transcriptional stress responses (Liu, Morgan and Pine, 2014).

A novel technique recently developed by our lab exploits inter-species differences in RNA sequences between closely-related species to separate and assess the transcriptional responses of cocultured cells *in silico (*Qiu *et al.*, 2018*).* Rat neurons are cocultured with mouse astrocytes, and RNA-seq reads separated according to species (and hence cell-type) post sequencing. This approach allows the investigation of the interactions between co-cultured astrocytes and neurons, without the use of physical separation prior to analysis. Data from this approach revealed that neurons induced wide-spread transcriptomic changes in astrocytes both as a result of direct cell-to-cell contact with neurons, as well as further transcriptomic changes induced by altered synaptic activity (Hasel *et al.*, 2017) **(Figure 3.1)**.

In this chapter, I validated findings from the above study (done on mouse astrocytes) in a human-astrocyte coculture system and describe conservation between human and mouse astrocytes in the transcriptional response both to direct neuronal contact and altered synaptic activity.

The largest family of upregulated genes due to synaptic activity are involved with astrocyte metabolic flux, with upregulation of key components of the astrocyte-neuron lactate shuttle. I proceed to demonstrate, using intracellular metabolic optical FRET probes, the manner in which synaptic activity alters astrocyte metabolic flux, and describe a novel role of the CREB-

signalling pathway in driving activity dependent transcriptional and metabolic changes.

Data presented in this chapter has been published (Hasel *et al.*, 2017**).**

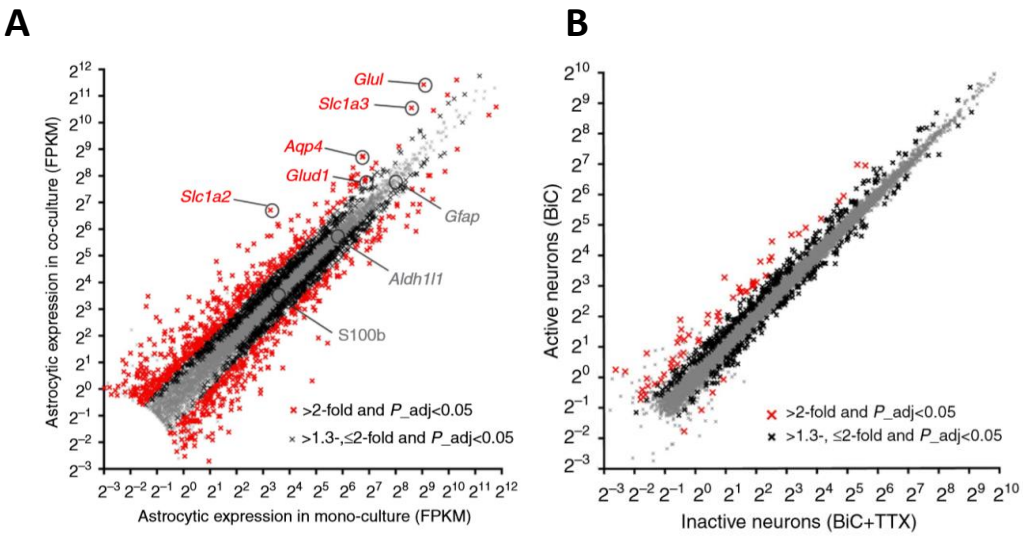

Figure 3.1 - Neurons and neuronal activity alter a wide-programme of mouse astrocyte transcription. (Figure modified from Hasel et al., 2017). **A**. **Neurons alter mouse astrocyte transcription.** Mouse astrocytes were kept as monoculture or cocultured with rat neurons for 9 days. RNA was extracted and species-specific gene expression analysed using the SARGASO species-sorting work flow. Coculture with rat neurons alters the expression of a large number of astrocyte genes. **B. Synaptic activity alters mouse astrocyte transcription.** Mouse astrocytes cocultured with rat neurons were transferred into TTX-containing medium for 22h, after which cells were washed and transferred to medium with either bicuculline (BiC) to create network firing or remained in TTX (BiC+TTX) to achieve silent neurons. RNA was extracted at 16 h post-wash. Expression of genes (FPKM) in astrocytes in the presence or absence of neurons is plotted for all genes expressed >0.5 FPKM average across mono- and co-cultures. Red and black crosses indicate the astrocytic genes induced or repressed by neurons more than twofold or >1.3, <2-fold respectively (DESeq2 P_adj<0.05, N=4 cultures).

3.2. Results

3.2.1. Co-culture with neurons alters human astrocyte morphology and gene expression.

It is well established that neurons alter rodent astrocyte morphology. However, there are significant inter-species differences between human and rodent astrocytes. Human astrocytes are larger and more complex, with increased cell volume. They have an increased number of processes, and make contact with a greater number of synapses (Oberheim *et al.*, 2009).

I therefore asked to what extent the transcriptomic changes induced in astrocytes in response to neurons were conserved between rodents and humans. I developed and characterised an *in vitro* co-culture system in which primary human astrocytes were co-cultured with rat neurons. By transfecting astrocytes with green-fluorescent protein (GFP) prior to co-culture, I visualised and measured morphological complexity and found that co-culture with neurons dramatically alters human astrocyte morphology. **(Figure 3.2 A, B).** Astrocytes become more complex and resemble *in vivo* astrocytes, in a manner similar to rodent astrocytes (Hasel *et al.*, 2017).

I next investigated whether coculture with neurons induced similar changes to human astrocyte gene expression as in mouse astrocytes. I designed and validated human-specific primers for specific genes that were found to be most upregulated in mouse astrocytes with rat neuronal coculture, and used

quantitative PCR (qPCR) to assess the response of these genes in human primary astrocytes co-cultured with rat neurons. Coculture with neurons pushes human astrocytes towards a more mature state, with upregulation of genes that act as markers for maturity (glutamate transporters *Slc1a2*, *Slc1a3* and the water channel *Aqp4*) **(Figure 3.2C).**

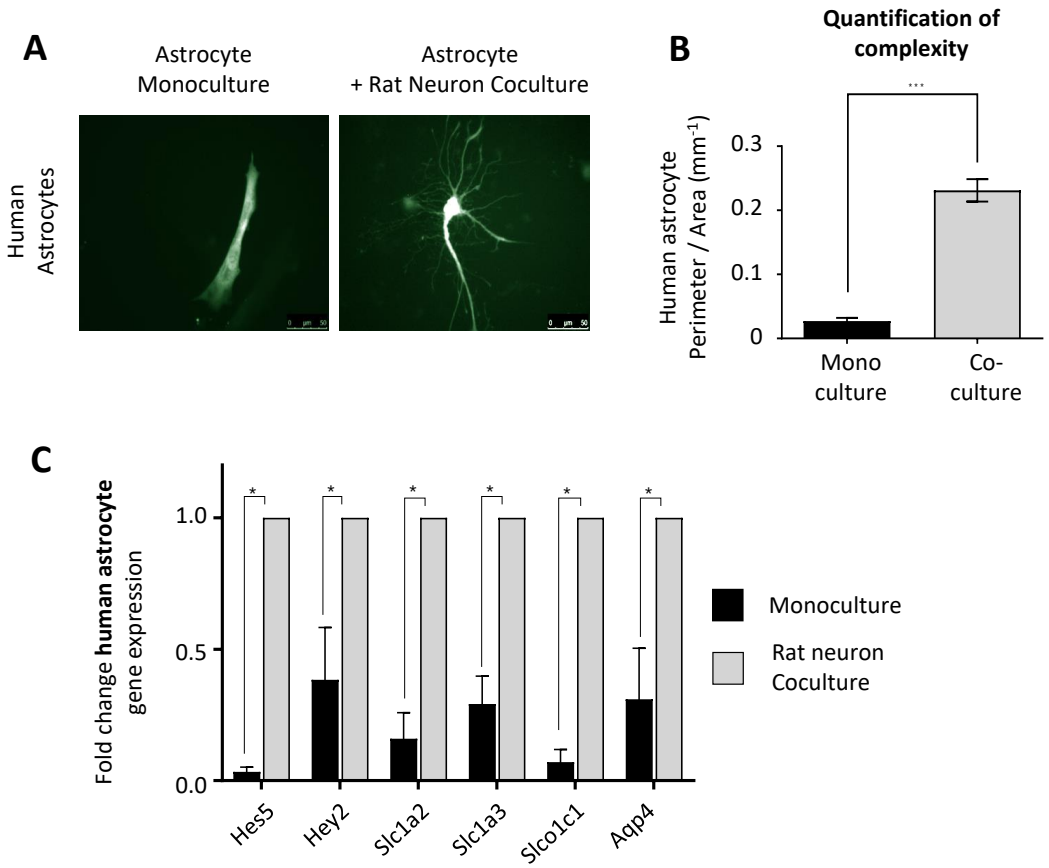

Figure 3.2 - Neurons alter human astrocyte morphology and gene expression. A, B. Human primary astrocytes co-cultured with rat neurons for 9 days undergo morphological changes leading to increased complexity (n = 12 in each group from three independent cultures, ***p<0.001 - two-tailed t-test). **C.** Neurons induce gene expression changes in human astrocytes. Astrocyte gene-expression changes were analysed using human-specific primers and compared with astrocytes kept in monoculture. Neurons upregulate genes for notch signalling (*Hes5*, *Hey2*) to increase astrocyte maturity markers for glutamate uptake (*Slc1a2*, *Slc1a3*), thyroid hormone uptake (*Slo1c1*) and water regulation (*Aqp4*) (N=5, *p < 0.05 - 2-way ANOVA with Sidak's correction for multiple comparisons).

3.2.2. Synaptic activity alters gene expression in human astrocytes

Using the coculture system developed and characterised above, I next addressed whether altered synaptic activity altered human astrocyte gene expression. To alter neuronal activity, cocultured cells were incubated overnight in tetrodotoxin (TTX), to block neuronal firing. Cells were then washed in the presence of bicuculline (BiC- a γ-aminobutyric acid-A (GABA-A) receptor antagonist), to achieve increased action potential firing (confirmed using electrophysiology - **Appendix Figure 7.1**). Cocultures were either exposed to 15 h of bicuculline to achieve high activity or washed with and kept in TTX to maintain electrically quiescent neurons. Following this, RNA was extracted and astrocyte-specific gene expression measured using human-specific primers with qPCR.

I selected genes that were demonstrated to be significantly upregulated by synaptic activity in mouse astrocytes from our previous RNA-seq data. I found that increased synaptic activity upregulates the same genes in human astrocytes – with upregulation of gene-sets responsible for key homeostatic pathways including thyroid hormone activation (*Dio2*, *Slco1c1*), antioxidant protection (*Sod3*) and glucose uptake and metabolism (*Pppc1r3c*, *Ldha*, *Slc1a2*) (**Figure 3.3**).

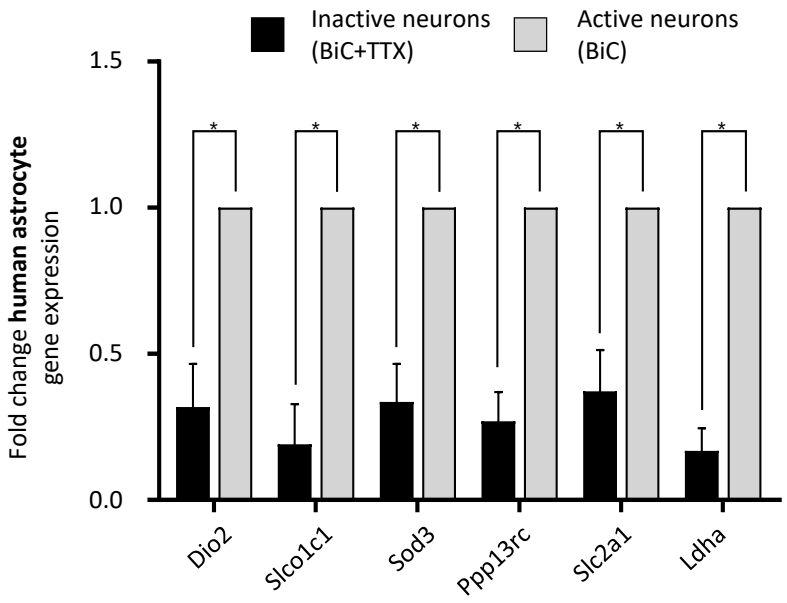

Figure 3.3 - Neuronal activity alters human astrocyte gene expression. Primary human astrocytes were co-cultured with rat neurons and cocultures stimulated to create conditions of high vs low neuronal activity. Cells were exposed to tetradotoxin (TTX) overnight to suppress neuronal activity. TTX was then either replaced with bicuculline (BiC) for 15hrs to generate a condition of high neuronal activity or left on (TTX+BiC) to generate reduced neuronal activity. Human-specific primers were used to assess changes in astrocyte gene expression. Increased neuronal activity upregulates human astrocyte genes for thyroid hormone activation (*Dio2* and S*lco1c1*), antioxidant protection (*Sod3*), and glucose uptake and metabolism (S*lc2a1, Ppp1r3c, Ldha*) (N=3, * = $p < 0.05$, 2-way ANOVA with Sidak's correction for multiple comparisons).

3.2.3. Neuronal activity increases astrocyte metabolic flux.

Having determined that human and mouse astrocytes demonstrated conservation in their morphological and transcriptional response to neuronal signals, I next set out to investigate if transcriptional changes led to alterations in astrocyte function.

The largest battery of genes upregulated by synaptic activity consisted of genes involved in the astrocyte-neuron lactate shuttle pathway (ANLS). Strikingly, every single step along this pathway had genes that were upregulated between 50% - 200% , including genes for astrocytic glucose uptake, glycolysis and the production and export of lactate **(Figure 3.4)**. In total, out of 32 genes involved in glycolysis and lactate export (wikipathways.org), 14 were significantly upregulated ($p_{adj} < 0.05$, fold-change >1.3), and a further 6 genes (total of 20 genes) were trending upwards using less strict criteria (>1.2 fold change only). The mean fold change across all glycolytic genes was an increase of 1.33 fold.

In contrast genes involved in mitochondrial import of pyruvate or the astrocyte Kreb's cycle were unaltered. Out of a total of 95 genes involved in mitochondrial function, Kreb's cycle and oxidative phosphorylation, none were significantly upregulated ($p_{adj} < 0.05$, fold-change >1.3), and only 2 were upregulated using less strict criteria (>1.2 fold change only). The mean fold change across all mitochondrial genes was 0.97. These data suggested that neuronal activity had a specific effect on the astrocyte-neuron lactate shuttle pathway, boosting the ability of astrocytes to provide fuel for metabolically active neurons.

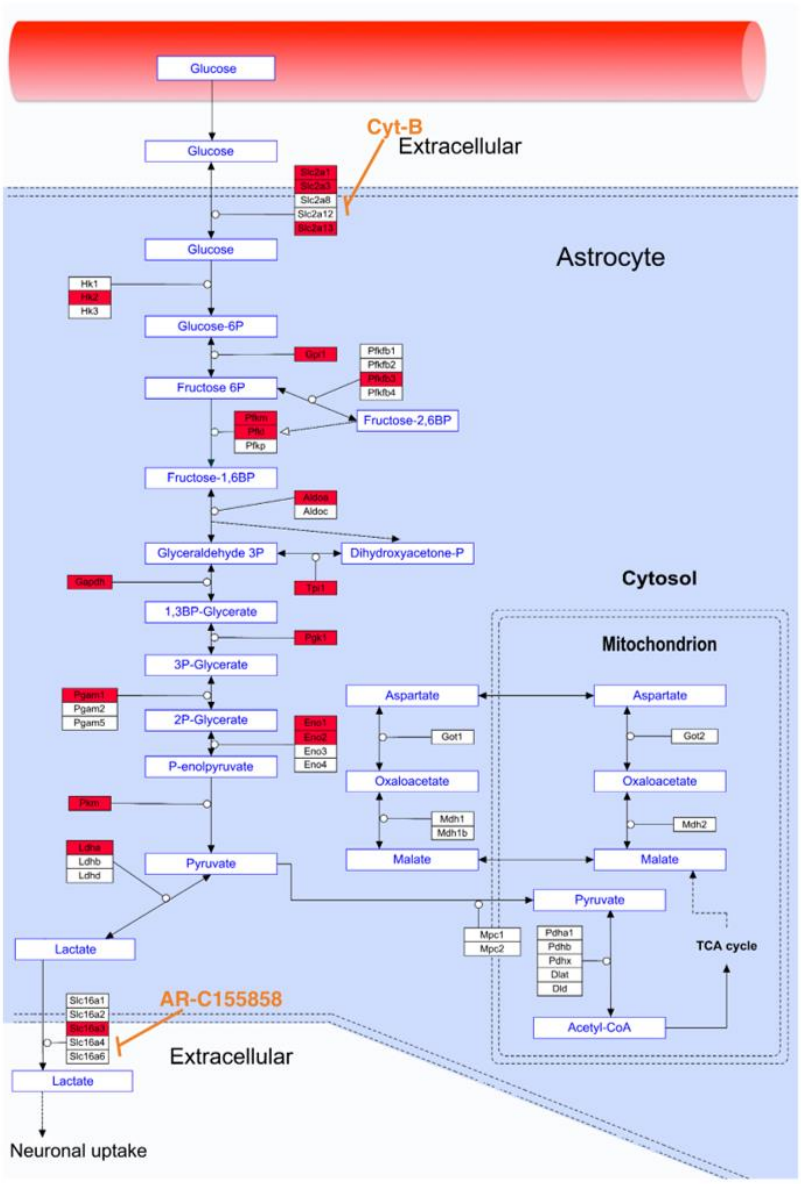

Figure 3.4 - Synaptic activity increases astrocyte expression of genes in the astrocyte-neuron lactate shuttle pathway. (Figure from Hasel *et al.*, 2017). Mouse astrocytes co-cultured with rat neurons, and gene expression assessed using RNA-seq and *in silico* read separation. Genes in red were significantly upregulated (deseq2 padj<0.05). Neuronal activity enhances genes along each step in glucose uptake, glycolysis, and conversion of pyruvate to lactate and lactate export.

Given these transcriptional changes, I wanted to confirm whether synaptic activity drove a functional increase in the ability of the astrocyte to utilise glucose and produce pyruvate and lactate. Measuring metabolic flux in co-culture systems has specific challenges. There is a requirement to distinguish between neuronal and astrocytic metabolic changes. Furthermore metabolism can change rapidly in any cell in response to internal and external conditions. Hence any method must have appropriate spatial and temporal resolution to measure changes in metabolic flux in individual cells.

To achieve the above, I utilised recently developed high resolution intracellular genetically-encoded florescent resonance-transfer (FRET) metabolic optical nanosensors, specific for glucose, pyruvate and lactate. FRET nanosensors have two fluorescence domains. Binding to a particular metabolic substrate results in a conformational change in the probe, resulting in energy transfer and an alteration in the ratio of emitted light from each of the two fluorescent domains. A measure of the ratio between the intensities within the two spectra corresponds to the intracellular concentration of the metabolic substance of interest. Plasmids for these sensors are transfected into astrocytes prior to co-culturing with neurons, ensuring all metabolic measurements are specific for astrocytes. This cell-type specificity is also further confirmed by the morphological shape of transfected cells at the time of imaging.

I used a glucose-specific-specific FRET nanosensor (FLII12Pglu-700uDelta6). The FRET ratio obtained gave me an indication of the concentration of glucose

present within the cell. By inhibiting glucose uptake using the glucose transporter inhibitor cytochalasin B (CytoB), and by determining the rate of decline in intracellular glucose concentrations, I was able to measure the rate of glucose flux and the rate of utilisation via glycolysis (specifically the rate of conversion of glucose into glucose-6-phosphate by hexokinase). All imaging was done with astrocytes from both conditions perfused continuously with TTX, to ensure that any changes in metabolic activity found was as a result of exposure to prior neuronal activity.

Mouse and human astrocytes co-cultured with active neurons (BiC) overnight demonstrated enhanced glucose utilisation vs those cocultured with silent neurons (TTX) **(Figure 3.5 A, B, C)**. Furthermore, the effect on astrocyte metabolism appears to be long-lasting. Astrocytes exposed to high neuronal activity overnight, and then switched back into low-activity conditions, maintain an increased metabolic flux. This appears to slowly return back to baseline **(Figure 3.5 D)** and would fit with the prediction that observed metabolic changes are due to changes at the level of transcription and protein expression, leading to the long-lasting changes observed.

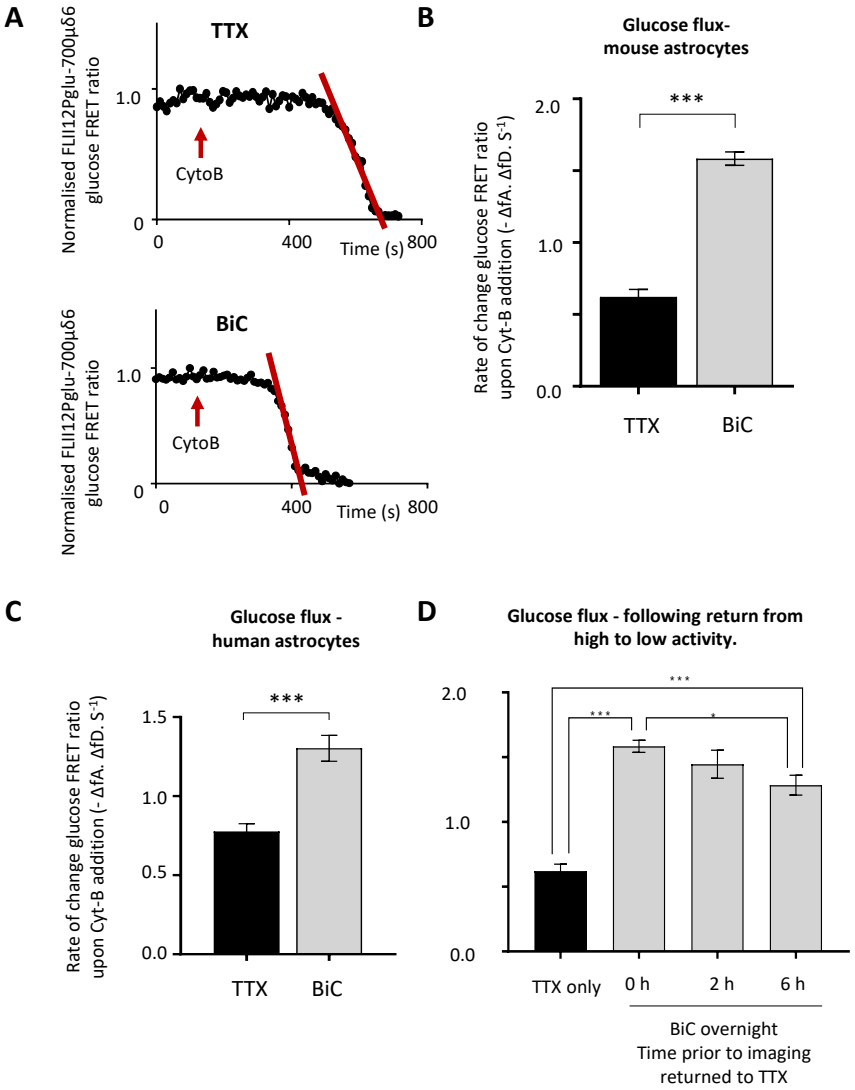

Figure 3.5 - Increased synaptic activity enhances astrocyte glucose utilisation. A, B. Mouse astrocytes exposed to high synaptic activity (BiC) vs low synaptic activity conditions (TTX) demonstrate increased rate of glucose utilisation following inhibition of glucose uptake with cytochalasin (TTX: n=14, BiC n=14, from 3 cultures ***p<0.001 unpaired t-test). **C.** These findings are replicated in human astrocytes (TTX: n=16, BiC n=16, from 3 cultures *** p<0.001 unpaired t-test). **D.** Exposure to increased neuronal activity has long-lasting effects on astrocyte metabolism. Returning to low-activity conditions for >6h is still associated with increased rates glucose utilisation compared with astrocytes always kept in low-activity conditions (TTX: n=14, 0 h: n=12, 2h: n=12, 6h n=14, cells from three cultures ***p<0.001, *p<0.05, unpaired t-test using cells as replicates).

3.2.3.1. *Neuronal activity increases astrocyte lactate and pyruvate flux.*

To measure astrocyte lactate and pyruvate production, I utilised the Laconic and Pyronic FRET probes together with inhibition of lactate export using the lactate-transporter blocker arc-C1558558 (AR-C). The subsequent rate of rise of intracellular lactate or pyruvate corresponds to a measure of the rate of production. I found that exposure to increased neuronal activity leads to an increased pyruvate and lactate rate, consistent with the transcriptional changes observed **(Figure 3.7)**.

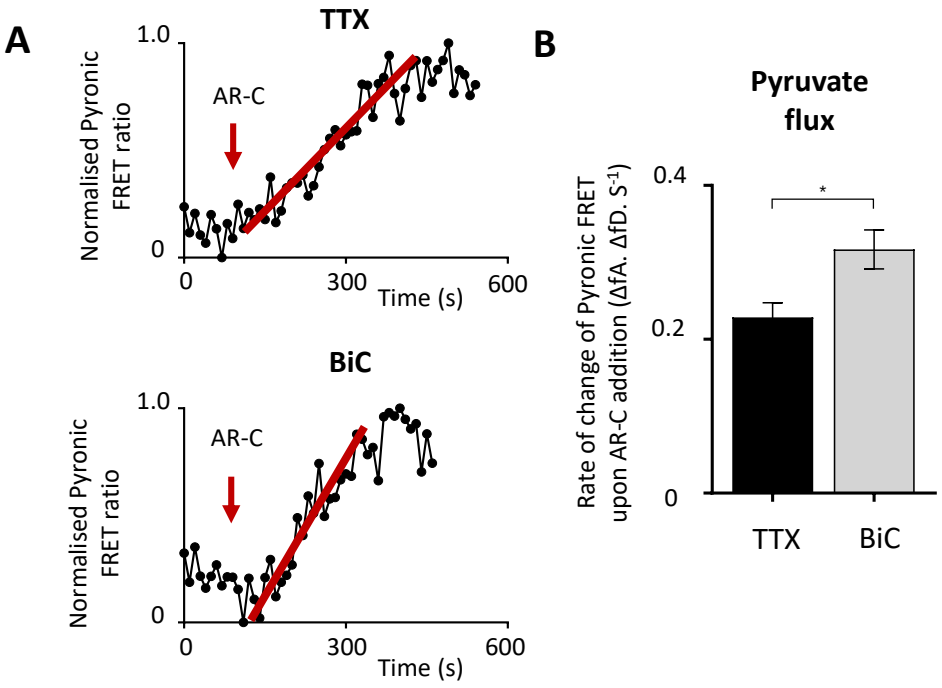

Figure 3.6 - Increased synaptic activity enhances astrocyte pyruvate production. Mouse astrocytes are cocultured with rat neurons, and neuronal activity manipulated over night to create low (TTX) vs high (BiC) activity conditions. Pyruvate levels are measure using the Pyronic FRET sensors. **A.** Samples traces demonstrating increased rate of pyruvate production in astrocytes exposed to high activity (Bic) conditions vs low activity (TTX). **B.** Pyruvate flux calculated as the rate of change of normalised Pyronic fret ratios after addition of MCT blocked with 1 µM arc-C1558558 (AR-C). High activity conditions lead to increased pyruvate production (TTX: n=41, BiC n= 37 cells from four cultures *p <0.05 unpaired t-test using cells as replicates).

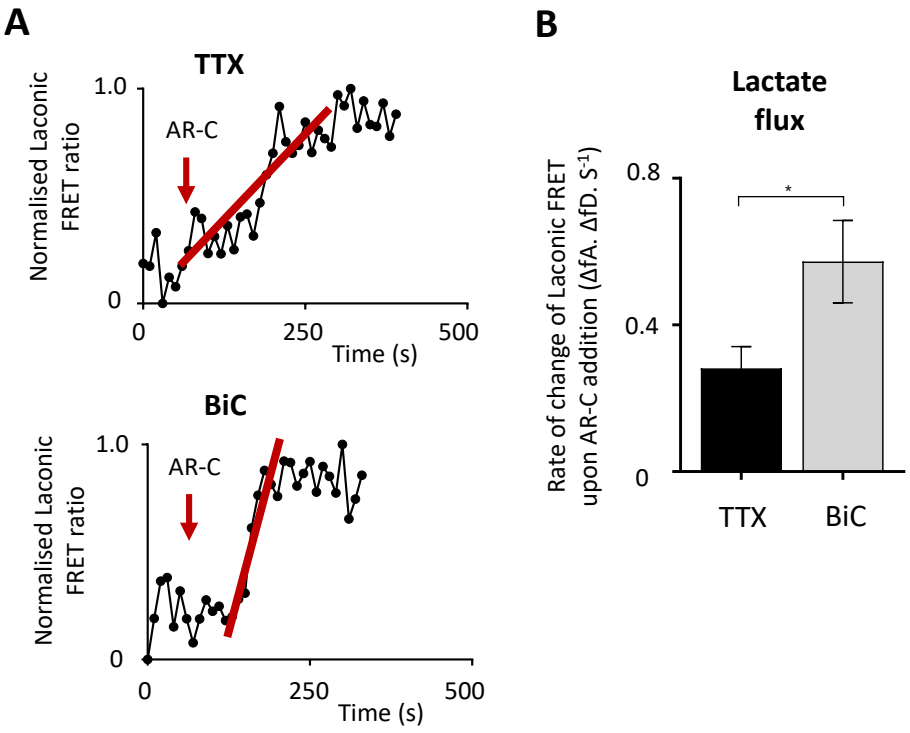

Figure 3.7 - Increased neuronal activity enhances astrocyte lactate production Similar to previous figures, mouse astrocytes are cocultured with rat neurons, and neuronal activity manipulated over night to create low (TTX) vs high (BiC) activity conditions. Lactate levels are measure using the Laconic FRET sensor. **A.** Samples traces demonstrating increased rate of lactate production in astrocytes exposed to high activity (Bic) conditions vs low activity (TTX). **B.** Lactate flux calculated as the rate of change of normalised Laconic fret ratios after addition of MCT blocked with 1uM arc-C1558558 (AR-C). High activity conditions lead to increased lactate production (TTX: n=13, BiC: n= 12 cells from three cultures, *p <0.05- unpaired t-test, using cells as replicates).

3.2.4. Metabolic changes are driven via activation of the CREB pathway

3.2.4.1. *Upregulated genes demonstrate enrichment for the CREB promoter motif*

I next set out to determine the intracellular signalling pathways by which neuronal activity drives the above alterations in astrocyte metabolism. A promoter analysis of genes induced more than twofold by both BiC and BiC+TBOA found the highest enrichment was for members of the cAMP response element binding protein (CREB) family. CREB family transcription factors are responsive to both Ca^{2+} and cAMP/PKA signalling **(Figure 3.8)**. The role of the CREB pathway has been well described in neurons, where it is important for learning and memory (Benito *et al.*, 2010). However, its role in astrocytes is less well-studied.

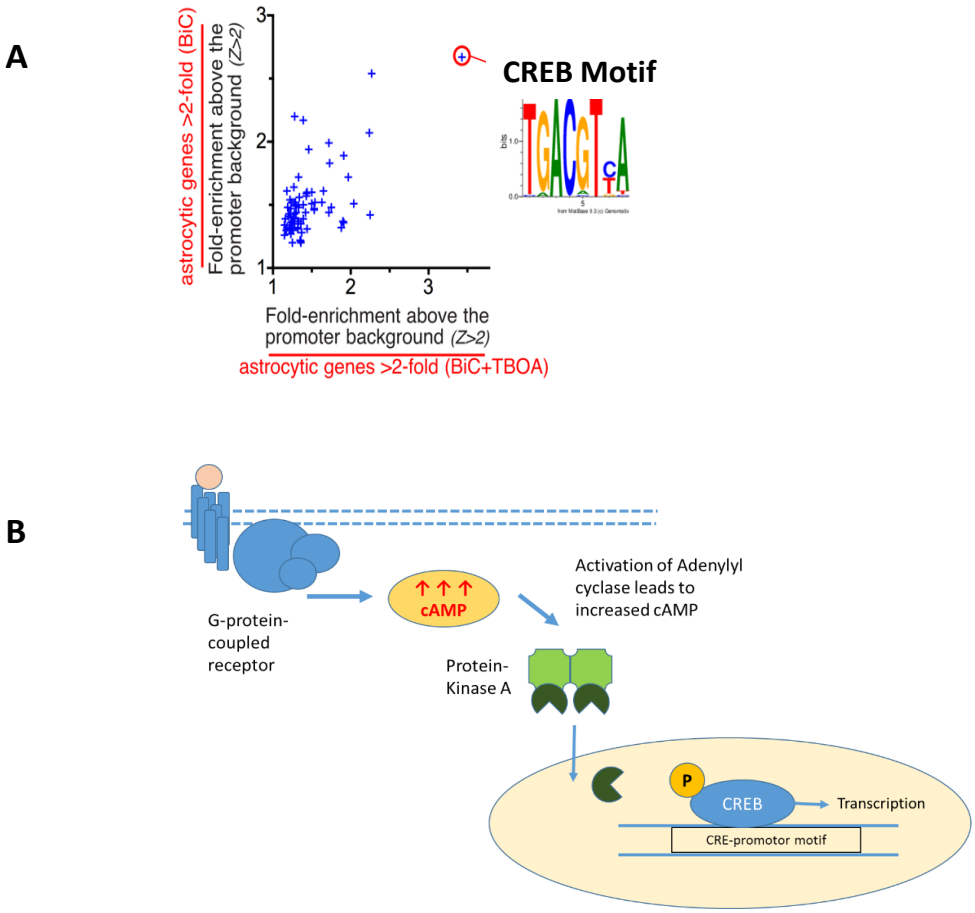

Figure 3.8 - Promoter analysis of activity-regulated genes reveals enrichment for the CREB promoter motif. A. Promoters of astrocytic activity-responsive genes (induced more than twofold) were analysed within Genomatix for enrichment in TRANSFAC Library matrices, with the Z-score for enrichment calculated. The CREB family matrix is the most enriched and is highlighted. **B.** Example of the CREB signalling pathway. Extra-cellular signals are transduced via a transmembrane receptor, resulting in second-messenger production of cAMP. These then activate protein kinases (PK) by causing dissociation of PK-dimers. The activated PK translocates to the cell nucleus and phosphorylates CREB-protein. This activates the CREB transcription factor, allowing it to bind to CRE-response elements via its basic leucine-zipper domain, and initiating transcription of down-stream genes.

3.2.4.2. *CREB activation is sufficient and necessary to drive activity-dependent metabolic changes.*

To test whether CREB signalling was sufficient to enhance astrocyte glucose flux, I transfected astrocytes with a constitutively-expressed variant of CREB (VP16-CREB, formed by fusing CREB with the Herpes Simplex virus protein VP16). I found that constitutively driving CREB was sufficient to increase astrocyte glucose utilisation and lactate production even when neurons were kept in low-activity (TTX) conditions. I then inhibited CREB by transfecting astrocytes with the Inducible cAMP Early Repressor (ICER) protein. This is an endogenous inhibitor of the CREB pathway (Jaworski *et al.*, 2018). Co-transfection of astrocytes with the CREB inhibitor ICER, was able to reverse activity-dependent changes in astrocyte glucose metabolism in both mouse and human astrocytes (**Figure 3.9**). These data suggest that the CREB-activation is sufficient and necessary in mediating neuronal-activity mediated changes to astrocyte metabolism.

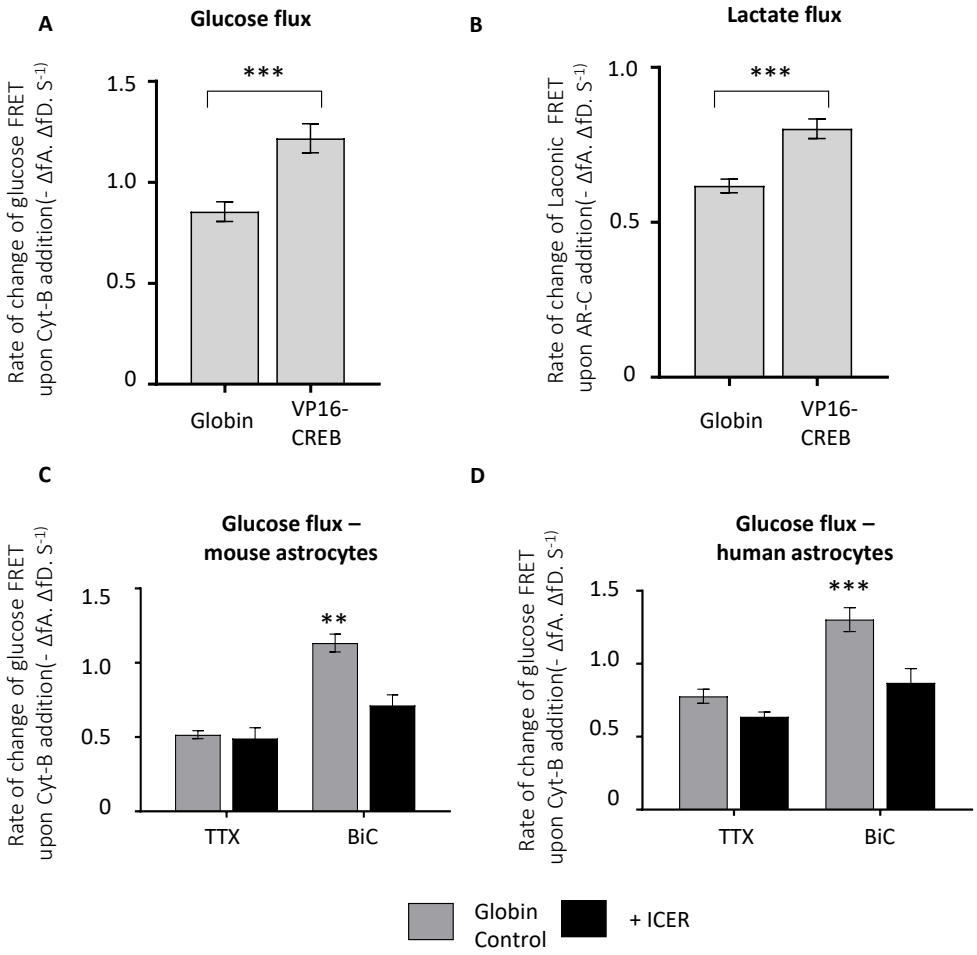

Figure 3.9 - CREB activation is sufficient and necessary to drive synaptic-activity mediated changes in astrocyte metabolism. **A, B.** Expression of constitutively-expressed CREB (VP16-CREB) is sufficient to enhance glucose utilisation (globin: n=36 globin, VP16-CREB: n=29, cells from three cultures *** p <0.001 unpaired t-test) and lactate production (globin: n=47, VP16-CREB: n=30, cells from three cultures ***p < 0.001 unpaired t-test, using cells as replicates) in co-cultured astrocytes kept in low-activity conditions (TTX). **C, D.** Activity-mediated changes in astrocyte glucose metabolism are reversed by co-transfecting cells with the CREB inhibitor ICER in mouse and human cells. (TTX globin: n=33, BiC globin: n= 26, TTX ICER: n=10, BiC-ICER: n=13, cells from 3 cultures; ***p<0.001 compared to TTX or Bic + ICER, 2-way ANOVA with Sidak's multiple comparisons, using cells as replicates).

3.2.4.3. *Drugs promoting upstream CREB activity boost astrocyte metabolic flux.*

Having elucidated a key role for the CREB-signalling pathway in driving neuronal activity mediated changes to astrocyte transcription and metabolism, I was next interested in whether drugs acting upstream off CREB could also increase astrocyte metabolic flux. I found that the cAMP activator forskolin potently enhanced metabolic gene-expression along with glucose flux. In addition, other drugs that act on the cAMP pathway such as the phosphodiesterase inhibitors 3-isobutyl-1-methylxanthine (IBMX) and the PDE type-3 specific inhibitor cilostazol, as well as Gs activators (noradrenaline) increased astrocyte metabolic flux **(Figure 3.10 B)**. Finally, I confirmed that the action of forskolin in boosting astrocyte metabolism was through activation of CREB, by confirming that any increase in metabolic flux could be reversed by CREB inhibition using ICER (**Figure 3.10 C**).

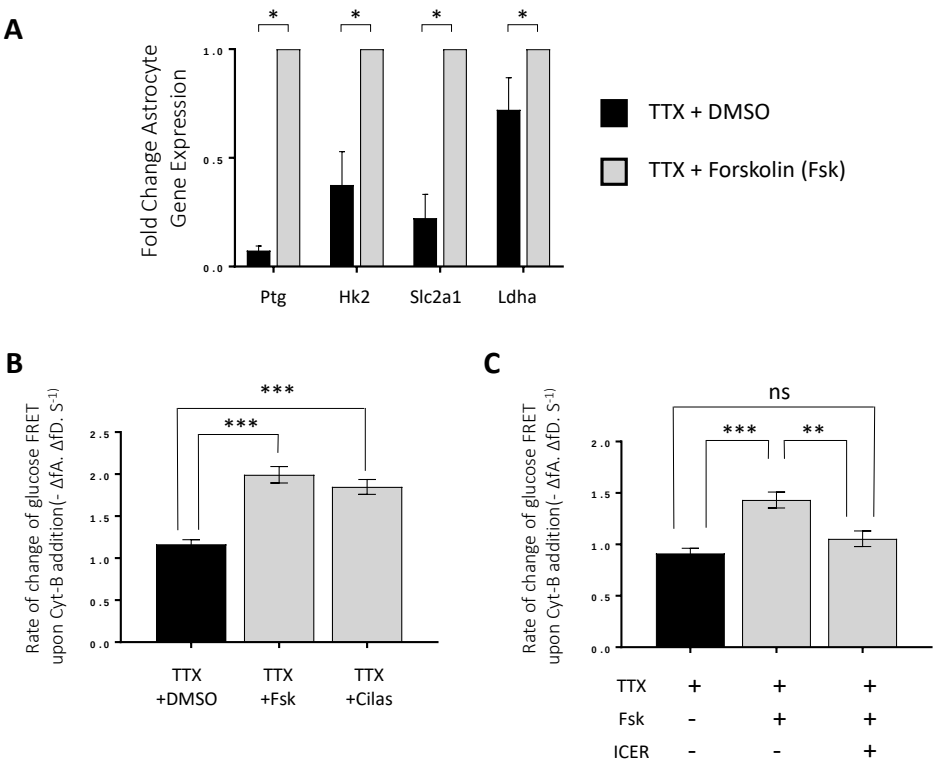

Figure 3.10 - Drugs acting upstream of CREB by elevating cAMP levels enhance astrocyte metabolic flux. A. Treatment of cocultured astrocytes with the adenylate-cylase activator forskolin (Fsk) increases astrocyte metabolic gene expression. Mixed rat neuron/mouse astrocytes were treated with forskolin (10 μM for 16 h) and gene expression measured by qPCR using mouse-specific primers. (N=3, *P<0.05 (2-way ANOVA plus Sidak's method for multiple comparisons). **B.** cAMP boosting drugs enhance astrocyte metabolic flux. 10 μM forskolin (cAMP activator) treatment and 2 μM cilostazol (PDE3 inhibitor) boost astrocyte glucose utilisation (n= 29 DMSO, n=25 forskolin(Fsk), n = 25 cilostazol (Cilas), 2 cultures ***= p<0.001, 1-way ANOVA with Sidak's multiple comparisons, using cells as replicates). **C.** Forskolin mediated increases in astrocyte metabolism occur via the CREB pathway. Co-expression of the CREB inhibitor ICER reverses forskolin mediated increase in glucose flux. (n= 11 DMSO, n=14 Fsk, n= 11 Fsk+ICER , cells from two cultures ** p <0.01, ***p<0.001, 1-way ANOVA plus Sidak's multiple comparisons, using cells as replicates).

3.3. Chapter Discussion

3.3.1. Summary of findings

The data presented in this chapter demonstrate that neurons induce transcriptomic and functional changes in astrocytes. I first extended and confirmed previous transcriptomic findings from our lab in human astrocytes. I next went on to confirm that activity-induced transcriptomic changes translated into activity-induced metabolic changes in astrocytes. Neuronal activity increases astrocyte glucose uptake and lactate production. Finally, I demonstrated that activity-induced changes occur via activation of the astrocyte CREB pathway, and can be enhanced by drugs acting upstream of CREB.

3.3.2. Conservation between rodent and human astrocytes

Prior work in our lab elucidated that coculture with mouse neurons, as well as altered synaptic activity, altered gene expression in mouse astrocytes. However, there are significant inter-species differences between human and rodent astrocytes. Human astrocytes are larger and more complex, making contact with a greater number of synapses (Oberheim *et al.*, 2009, Han *et al.*, 2013). Compared with other CNS cell-types, marked differences in gene-expression have also been found between murine and human astrocytes (Zhang *et al.*, 2016). Therefore, it was important to check to what extent the neuron-astrocyte signalling pathways that we were investigating were conserved between rodents and humans to provide confidence that any further

investigations using rodent models would be applicable to human physiology and disease.

The data presented above demonstrate that human astrocytes undergo similar morphological changes in response to neurons. They also demonstrate conservation with rodent astrocytes in their transcriptional response to neurons and synaptic activity, and in the manner in which synaptic activity regulates metabolic flux.

An important limitation with the above data is that utilisation of only a small selection of genes from the rodent datasets. This approach is biased and may miss pathways that are differentially regulated between species. An unbiased panel of genes that are upregulated, down-regulated and not changed (or utilising RNA-sequencing) would allow us to investigate the true extent of conservation between humans and mouse astrocytes.

However, with the above limitation considered, the overall conservation of both contact-mediated and activity-dependent functional responses suggest that there is evolutionary conservation in these selected key pathways between human and rodent astrocytes, thus providing confidence in the translatability of using rodent models going forwards to investigate neuron-astrocyte crosstalk.

3.3.3. Consequences of activity-dependent regulation of astrocyte metabolism.

The main finding described in this chapter was that synaptic activity drives long-lasting transcriptional changes in astrocyte metabolic flux. This has important implications for how neuron-astrocyte signalling regulates metabolic homoeostasis in the CNS. Astrocytes are the largest uptakers of glucose in the CNS during periods of strong synaptic activity (Zimmer *et al.*, 2017). According to the ANLS hypothesis, synaptic activity leads to glutamate uptake and glutamine synthesis in astrocytes. This in turn, by the laws of mass-action, triggers increased lactate export from astrocytes (Pellerin and Magistretti, 1994b). This lactate can then serve as an important fuel source for nearby neurons.

The data presented in this chapter reveal that synaptic activity regulates transcription to drive an enhanced capacity of an astrocyte to utilise glucose and produce lactate. This ensures that the ability of the astrocyte to supply metabolic substrates is tuned to the neuronal activity of nearby neurons, hence ensuring that metabolic supply meets metabolic demand in the CNS. This reveals a novel pathway by which synaptic activity tunes astrocyte transcription to regulate metabolic homeostasis in the neuroglial unit.

3.3.4. Utilising the CREB pathway for future therapeutic use.

I also describe the role of the CREB signalling pathway, demonstrating that CREB activation was sufficient and necessary for mediating activity-dependent astrocyte transcriptional and metabolic changes. CREB has previously been demonstrated to have important roles in mediating activity-dependent neuroprotection in neurons (Shaywitz and Greenberg, 1999). Its role in astrocytes is much well less understood, although recently it has been demonstrated that CREB activation in astrocytes leads to the activation of distinct transcriptional programmes different from those seen in neurons (Pardo *et al.*, 2017). Activation of CREB in astrocytes also has a neuroprotective role and has been shown to reduce injury in a stroke model (Pardo *et al.*, 2016).

Consistent with its role in mediating activity-dependent transcriptional and metabolic changes, targeting the CREB pathway boosts astrocyte metabolic flux. This offers a potential drug target that might be of future therapeutic benefit. Interestingly, phosphodiesterase (PDE) drugs that target the cAMP and CREB pathways (e.g. rolipram, a Type 4 PDE and cilostazol, a Type 3 PDE) have already been trialled in neurodegenerative conditions. Whilst their actions on astrocytes have not been considered, it may be that some of their consequences on CNS health may come from effects via activation of astrocyte pathways. This is discussed further in chapter 6.

3.3.5. The role of other transcriptional pathways altered by neuronal activity.

In this chapter, I have focused on the consequences of neuronal activity on one pathway uncovered by transcriptional data – that of astrocyte metabolic flux. However other notable gene clusters identified include those involved in thyroid hormone signalling (*Slco1c1, Dio2* and *Slc7a5*) and antioxidant capacity (*Sod3* and *Grx3*). These suggest that synapse-astrocyte signalling is also essential for regulating other key trophic and protective pathways in the brain, and investigating the functional consequences of these pathways, and whether they are disrupted in neurodegeneration, offers an interesting avenue for future investigation.

3.3.6. Limitations and future work.

The main limitation of these studies is that they are carried out in a mixed-species coculture system. Astrocytes grown in culture are different from those found *in vivo* (Cahoy *et al.*, 2008). Whilst we have discovered that coculturing astrocytes with neurons does push astrocytes somewhat towards a more *in vivo* state, differences still exist. Furthermore, our co-culture system lacks other important cell types such as oligodendrocytes, microglia or vascular cells. Interactions with these cells may alter astrocyte gene-expression and function further. I address these limitations in the next experimental chapter.

It is also important to consider artefacts that may be induced by mixing cells from different species. Mouse and rats CNS cells demonstrate a high level of evolutionary conservation, and similarities in transcription and functional changes between human and rodent astrocytes further support the high level of conservation in these important pathways. Furthermore, astrocyte genes that could be tracked in single-species co-culture (due to being >10 fold expressed in astrocytes vs other cell-types) which changed with rat neurons were also significantly changed in mouse-astrocytes cultured with mouse neurons (Hasel *et al.*, 2017 - Supplementary Table 5), again supporting that neuron-astrocyte signalling pathways demonstrate a high-level of conservation between rat and mouse. However, whilst this increases confidence that the findings in this chapter are applicable in normal physiology, there will nevertheless be differences that will influence some aspect of transcription and function. Therefore, there is a requirement to test and confirm these findings in a more complicated *in-vivo* system. These investigations are described in the next chapter.

3.3.7. Chapter conclusion

The studies in this chapter demonstrate how synaptic activity alters astrocyte transcription to drive long-lasting enhancement of pathways for astrocyte–neuron metabolic support. Activity-dependent changes occur via activation of

the CREB transcription factor, and astrocyte metabolic flux can be enhanced in low-activity conditions by drugs acting upstream of CREB signalling.

Chapter 4

In vivo consequences of altered synaptic activity on astrocyte transcription.

4.1. Chapter Introduction

In the previous chapter, I described investigations seeking to understand how synaptic activity regulates astrocyte gene-expression using an *in vitro* co-culture model. These revealed that synaptic activity led to widespread transcriptomic changes in astrocytes. However, given the caveats with using cultured cells (discussed previously), it was important to confirm to what extent synaptic activity regulated astrocyte transcription *in vivo*.

To answer this question, I was required to overcome two separate methodological challenges. First, I had to distinguish astrocyte-specific gene-expression changes from those in other CNS cell-types. Second, I had to determine a paradigm for generating conditions of high vs low neuronal activity *in vivo*.

With regards to separating astrocyte vs other CNS cell-type transcription: *in vitro*, we utilised mixed-species coculture and exploited inter-species differences in genetic sequence to separate cell-type specific reads post-sequencing. However, *in vivo* this approach would not be possible.

Current methods for achieving cell-type specific gene expression include: 1) Florescence-assisted cell sorting (FACS), 2) Magnetic sorting 3) Single-cell RNA sequencing. Whilst these are all powerful tools that allow physical separation of cells prior to RNA-sequencing, they have important caveats. Firstly they require tissue homogenisation and cell-dissociation into a single cell suspension prior to separation. This homogenisation can induce transcriptional changes that

may mask any activity-induced effects (Liu, Morgan and Pine, 2014). Secondly the time-delay between homogenisation and RNA-sequencing when the cell is still alive can further influence transcriptional changes. Astrocytes, being highly reactive cells with multiple fine processes, are particularly prone to damage and artefact following sorting.

For these reasons, I decided to utilise an alternative technique: translating ribosome affinity purification (TRAP - **Figure 4.1**). In TRAP, cell-type specific expression of GFP-tagged ribosomes is driven by a cell-type specific promoter. Immunoprecipitation of GFP-tagged ribosomes allows isolation of attached cell-type specific mRNA. In the first part of this chapter I describe validation and optimisation of the TRAP methodology to successfully allow measurement of astrocyte-specific transcriptional changes.

TRAP has benefits over the other methods described above. First, it does not require tissue dissociation into a single-cell suspension prior to RNA collection. Instead, dissected tissue is rapidly homogenised in buffer containing cyclohexamide which fixes the ribosome-mRNA complexes. Hence, the transcriptional state of the cell is preserved to the time the animal is culled, minimising transcriptional artefacts induced by tissue dissociation and delay. Second, TRAP isolates actively translating mRNA. Therefore any changes found in gene-expression may better reflect functionally relevant pathways than those detected by total mRNA isolation.

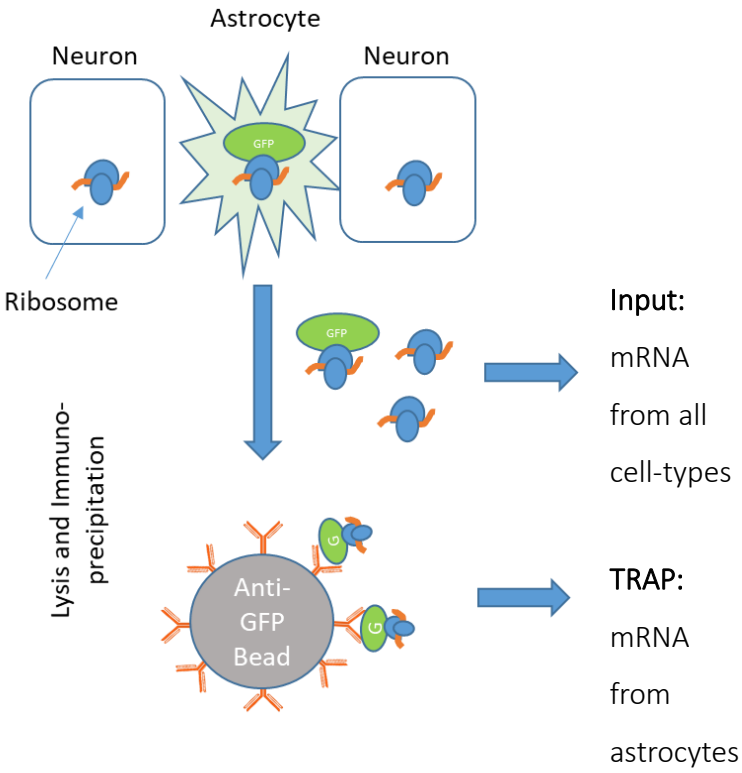

Figure 4.1 - Schematic of translating ribosome affinity purification (TRAP) method. Tissue from the astro-TRAP mice brains are lysed and incubated (in the presence of RNAse and proteinase inhibitors) overnight with anti-GFP coated beads. The beads bind to the EGFP-tagged rpl10a protein of the 60S unit of the ribosome. This pulls down ribosomal complexes along with translating mRNA. An input sample taken prior to IP contains mRNA from all cell-types.

The second challenge was to develop a suitable paradigm to manipulate synaptic activity *in vivo*. In the second part of this chapter I describe optimising a light-stimulus paradigm to achieve conditions of high vs low neuronal activity in the visual cortex. By combining light-stimulus along with astrocyte-specific TRAP, I was able to investigate how altered synaptic activity controls astrocyte gene-expression *in vivo*.

In the final part of the chapter, I explore the consequences on CNS transcription in a clinically relevant model where synaptic activity is suppressed: prolonged anaesthesia. I describe how anaesthesia suppresses activity-dependent neuronal and astrocyte gene-expression, and investigate the functional consequences of these transcriptional changes on pro-survival and death pathways in the CNS. Finally, I demonstrate that anaesthesia-induced transcriptional changes during anaesthesia might be reversed when synaptic activity is upregulated using non-invasive transcranial electrical stimulation.

4.2. Results

4.2.1. Validation of Aldh1l1-EGFP-Rpl10a transgenic mouse line

Cell-type specificity of TRAP is achieved by driving EGFP expression under a cell-type specific promoter. We utilised a transgenic mouse (Aldh1l1-EGFP-Rpl10a - referred to in this thesis as the *astro-TRAP* mouse) where EGFP is driven under the expression of the *Aldh1l1* gene promoter. *Aldh1l1* is expressed specifically in astrocytes in the CNS **(Figure 4.2A)** and is generally considered as being the archetypical astrocyte marker, demonstrating the best sensitivity and specificity for astrocytes compared to alternative astrocyte markers or promoters such as *Gfap*, *S100B* and *Slc1a3* (Srinivasan *et al.*, 2016). The transgenic mouse had already been previously generated and described (Heiman *et al.*, 2008) and the line was re-derived from frozen sperm on a C57B/6JN background as outlined in methods.

To confirm that EGFP was correctly expressed only in astrocytes in the re-derived line, I took slices of cortex from 8 week old astro-TRAP mice and co-stained with anti-EGFP and either anti-ALDH1L1 or a pan-neuronal antibody (Neurochrom) **(Figure 4.2B)**. Confocal imaging of the cortex using coronal sections demonstrated that EGFP staining was present only in astrocytes (as confirmed by both morphology and anti-ALDH1L1 costaining), and not present in neurons.

To further validate the identity of EGFP expressing cells, I isolated EGFP+ cells using fluorescence-activated cell sorting (FACS). The gene-expression profile in eGFP+ vs GFP- cells was determined by qPCR with a panel of cell-type specific gene-markers. These markers were selected from Ye Zhang *et al.*, 2014, as genes that demonstrated >10 fold specific expression in an individual cell-type vs expression in other cell-types. EGFP+ cells showed enrichment for astrocyte-specific genes, and depletion of neuronal, oligodendrocyte and microglial genes **(Figure 4.2D)**.

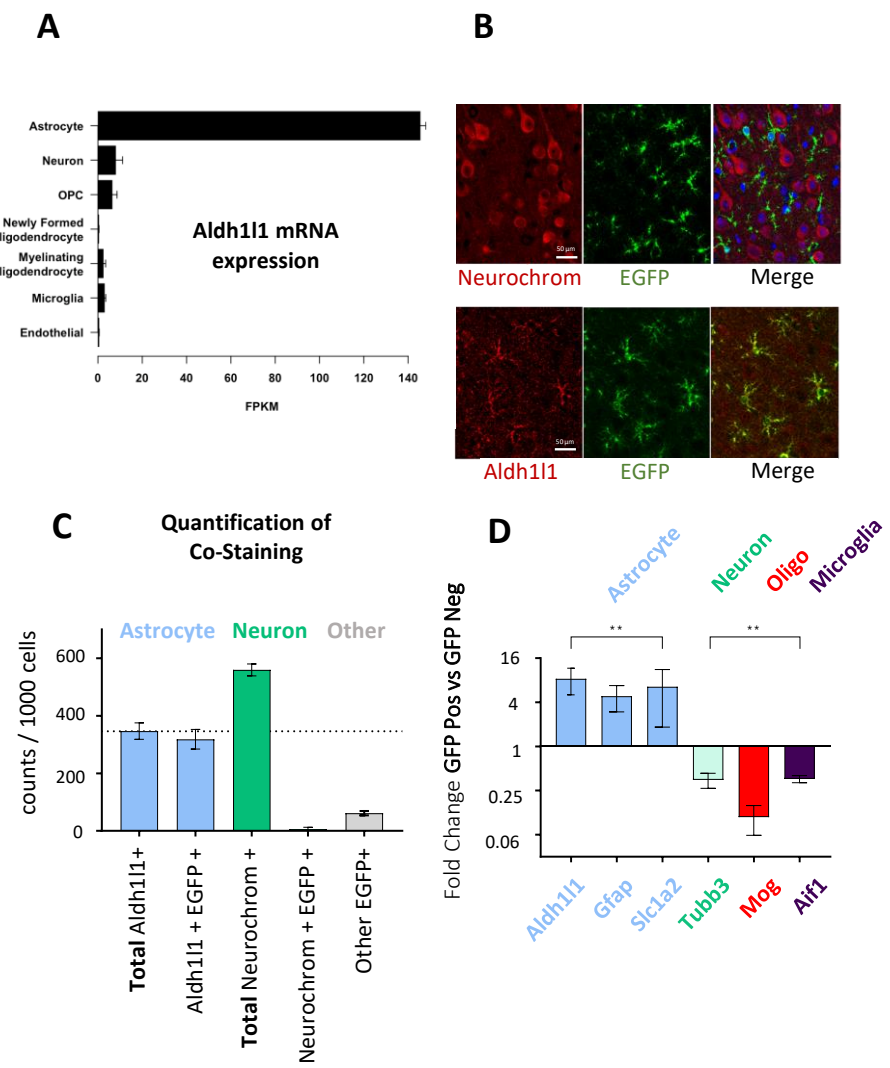

Figure 4.2 - Validating astrocyte-specific GFP expression in the Alh1l1-egfp-rpl10a transgenic mouse. A. *Aldh1l1* is an astrocyte-specific marker, demonstrating enrichment in astrocytes vs other CNS cell-types. Data taken from Ye Zhang *et al*., 2014. **B. C.** Confocal images, along with quantification of cell counts, confirms EGFP is selectively expressed along with *Aldh1l1* (mean ± SD, N=4) in astro-TRAP mice. Neurons, labelled with the polyclonal pan-neuronal marker Neurochrom, do not exhibit EGFP expression. **D.** Separation of EGFP + cells by flow-cytometry and assessment of cell-type specific genes by qPCR confirms enrichment of astrocyte-specific markers (*Aldh1l1, Gfap, Slc1a3*) and depletion of markers for other cell-types (*Tubb3, Mog, Aif1*). (N = 3, **p<0.01 – 1 way ANOVA on each gene-set).

4.2.2. Optimisation of TRAP protocol to obtain cell-type specific mRNA

Having successfully confirmed that astro-TRAP transgenic mouse expressed EGFP in an astrocyte-specific manner, I next set out to validate and optimise a protocol for isolating astrocyte-specific mRNA by immunoprecipitation. This involved modifying previously published methodology (Heiman *et al.*, 2014) until satisfactory enrichment of astrocyte vs other CNS cell-types genes was achieved.

I first determined the optimal ratio of anti-GFP coated beads to tissue to determine the optimal balance between maximising mRNA yield and minimising background contamination. I carried out immunoprecipations using different amounts of mouse cortex and assessed RNA yields and quality using an Agilent bioanalyser. To determine the amount of background mRNA contamination that was not reliant on EGFP-pulldown and to confirm that the above enrichment was indeed due to the expected mechanism of EGFP-specific ribosome pulldown, the TRAP method was repeated with two specific controls. Firstly, immunoprecipation was performed on brain samples from wild-type mice. Second, immunoprecipitation was performed on astro-TRAP mice, with substitution of the anti-EGFP antibodies with a control antibody (anti-myc). In both controls, neglible RNA amounts were obtained following TRAP. This demonstrates that the mechanism of RNA pulldown required IP of GFP-tagged ribosomes, and confirmed that there was minimal background mRNA contamination.

Table 4-1: RNA extraction requires anti-GFP binding to GFP-tagged ribosomes. Post-TRAP RNA yields only significant in Astro-TRAP mice with anti-GFP antibodies, and negligent with wt mice or using control (c-myc) antibody. (N=2, mean (±SD)).

	ASTRO TRAP MOUSE + ANTI-GFP	**WT MOUSE + ANTIGFP**	**ASTRO-TRAP MOUSE + ANTI-MYC**
INPUT RNA CONCENTRATION (NG/ML)	59.4 (±5.4)	70.6 (±7.35)	53 (±3.4)
POST-TRAP CONCENTRATION (NG/ ML)	28.5 (±1.5)	1.5(±0.45)	1.2 (±0.64)

I next checked if the RNA obtained by TRAP demonstrated successful enrichment of astrocyte vs other cell-types genes. This was done by comparing the expression of cell-type specific gene markers from the TRAP samples vs the input samples. Cell-type specific markers were identified as genes from the Ye Zhang *et al.*, 2014 dataset that were >10 fold enriched in a particular cell-type vs other cell-types. TRAP successfully enriched for astrocyte-specific markers and depleted for markers from other cell-types **(Figure 4.3A)**.

Finally, I confirmed that there was minimal background contamination by looking for depletion of mitochondrial mRNA. Mitochondrial mRNA is translated by mitochondrial ribosomes rather than cytoplasmic ribosomes (Greber and Ban, 2016). As mitochondrial ribosomes in the astro-TRAP mice are not EGFP-tagged, mitochondrial RNA would not be expected to be isolated by TRAP. Hence it serves as a useful marker for determining the success of the TRAP method and assessing the level of background RNA contamination. I found that TRAP samples demonstrated a strong reduction of all mitochondrial genes compared to input samples following RNA-sequencing **(Figure 4.3B)**.

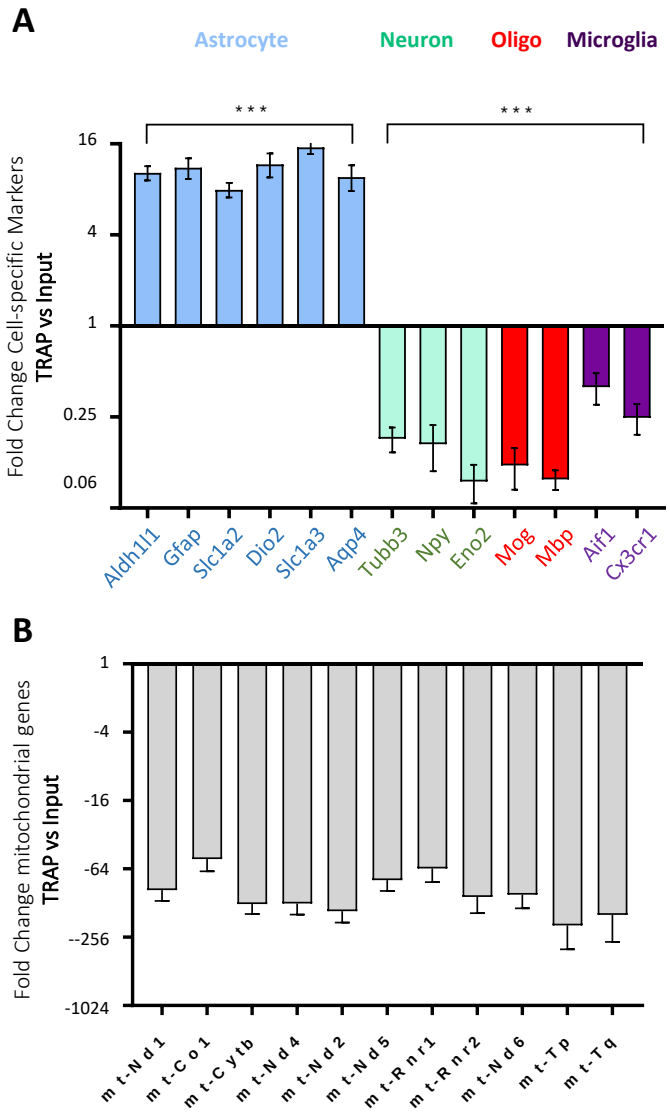

Figure 4.3 - TRAP allows isolation of cell-type specific mRNA from whole brain. A. TRAP successfully allows isolation of astrocyte-specific mRNA from cortical samples, confirmed by enrichment of astrocyte-specific genes and depletion of markers of other cell-types (N=4, *** p<0.001, 1-way ANOVA on each gene-set). **B.** TRAP samples have a strong depletion in mitochondrial mRNA (translated by non-GFP tagged mito-ribosomes) vs input samples (N=4, *** p<0.001, 1-way ANOVA).

4.2.3. Using light-stimulus to manipulate synaptic activity *in vivo.*

Having selected and confirmed TRAP as a suitable method for measuring astrocyte-specific transcription *in vivo*, I next required to establish paradigms by which I manipulate synaptic activity upwards and downwards. In cell culture, we utilised drugs (bicuculline and TTX) to achieve high vs low neuronal activity states. However, these cannot be used *in vivo* as they would result in animal death.

It was important for any suitable paradigm to be as non-invasive as possible. This was both for animal welfare purposes and to minimise changes in gene-expression due to injury or CNS trauma that may occur with invasive methods. Astrocytes are very reactive and alter their gene-expression profile rapidly to injury. This would mask transcriptional changes resulting from altered neuronal activity.

For these reasons, I decided to utilise a light-stimulus paradigm to manipulate neuronal activity *in vivo*. This exploits the fact that the primary visual cortex (V1) is innervated mainly from the retina by a neuronal circuit through the lateral geniculate nucleus **(Figure 4.4B)**. Exposing mice to light vs darkness creates conditions of high vs low neuronal activity in the V1 visual cortex. The visual cortex does receive input from other cortical areas (Macaluso, Frith and Driver, 2000). Whilst this means that in darkness there would not be the total absence of synaptic activity, we predicted that exposure to light vs darkness would lead to a sufficient difference in synaptic activity to drive changes to

astrocyte transcription. This method has been extensively described previously as a method to achieve altered neuronal activity, and well established to alter activity-dependent transcription in the visual cortex (Majdan and Shatz, 2006). Benefits of this method were that it was easy to implement and non-invasive, thereby minimising non-specific gene-expression effects.

Mice were first kept in total darkness for 7 d. A period of 3- 14 days of darkness prior to light-exposure is consistently used in studies employing light-stimulus (Ataman *et al.*, 2016, Hrvatin *et al.*, 2018, Murase, Lantz and Quinlan, 2017) as a means to achieve a low baseline on which to measure subsequent effects of light-stimulation. Following 7 d dark exposure, mice were then exposed to different periods of light (4 h – 48 h). Visual cortices were then dissected and gene-expression measured by RNA extraction and qPCR.

Changes in neuronal activity was confirmed by measuring expression of two immediate-early genes (IEGs) *Arc* and *Bdnf*. These genes were selected as established activity dependent markers that have been previously described to respond robustly to increased neuronal activity (West and Greenberg, 2011). I determined that light stimulus upregulates neuronal activity in the visual cortex and that the optimum time-point when there was greatest upregulation appeared to be 24 h of light-exposure **(Figure 4.4C)**. Finally, I also checked the expression of these genes in mice kept in a normal light-dark cycle (Normal light). These consistently appear to have higher levels of IEG gene expression compared to mice exposed to darkness for 7 d.

Using the 24 h light-stimulus time-point, I next investigated if there was difference between younger (post-natal day 28) and older (24 week old) mice. I predicted that older mice would have reduced plasticity in their visual cortices, and therefore demonstrate reduced change in gene-expression in response to light-stimulus compared to younger mice. However, I found no difference between the two ages in the induction of *Arc* and *Bdnf* by light-stimulus **(Figure 4.4D)**.

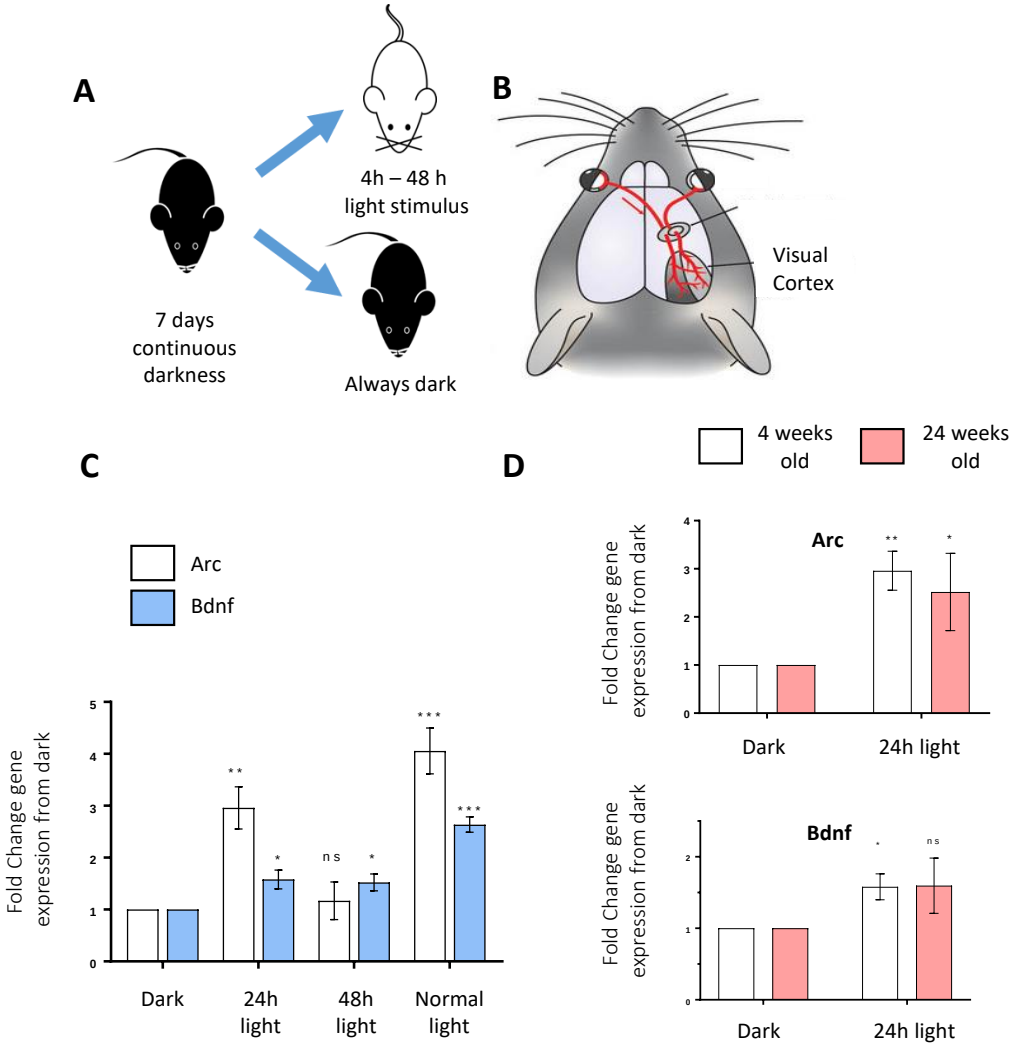

Figure 4.4 - Light stimulation allows regulation of neuronal activity. A. Schematic of stimulation paradigm. Mice were exposed to continuous darkness for 7d followed by either being kept in darkness, or variable period of light exposure. **B.** Visual cortex is innervated by a neuronal pathway from the retina. Hence, light vs dark exposure creates conditions of high vs low synaptic activity. **C.** Light exposure increases expression of immediate-early genes *Arc* and *Bdnf* (dark: N=6, 24h light: N =6, 48h light: N=3; Normal light: N=4. *p<0.05, **p<0.01, ***p<0.001 compared to dark, 2-way ANOVA with Sidak's multiple testing,). **D.** Light-induced changes in *Arc* and *Bdnf* expression are similar between old and young mice (4 week old mice: N=5; 24 week old mice: N = 3; *p<0.05, **p<0.01 compared to dark, 2-way ANOVA with Sidak's multiple testing).

4.2.4. Neuronal activity alters astrocyte transcription *in vivo.*

Combining the above two approaches, I next investigated how synaptic activity altered astrocyte transcription *in vivo.* This was done by exposing astro-TRAP mice to 24 h light v dark stimulus, and subsequently isolating astrocyte-specific mRNA using TRAP. P28 astro-TRAP mice were kept in 7 days of complete darkness and then either exposed to 24 h light or a further 24 h of darkness. In addition a control group were kept in normal light-cycle conditions. RNA-seq of TRAP mRNA isolated from the visual cortex revealed that 24 h light alters a wide-programme of astrocyte gene-expression **(Figure 4.5A)**. Furthermore a larger number of genes were found to be altered in mice kept in normal light cycles vs darkness, as compared to 24 h light stimulus vs darkness **(Figure 4.5B)**.

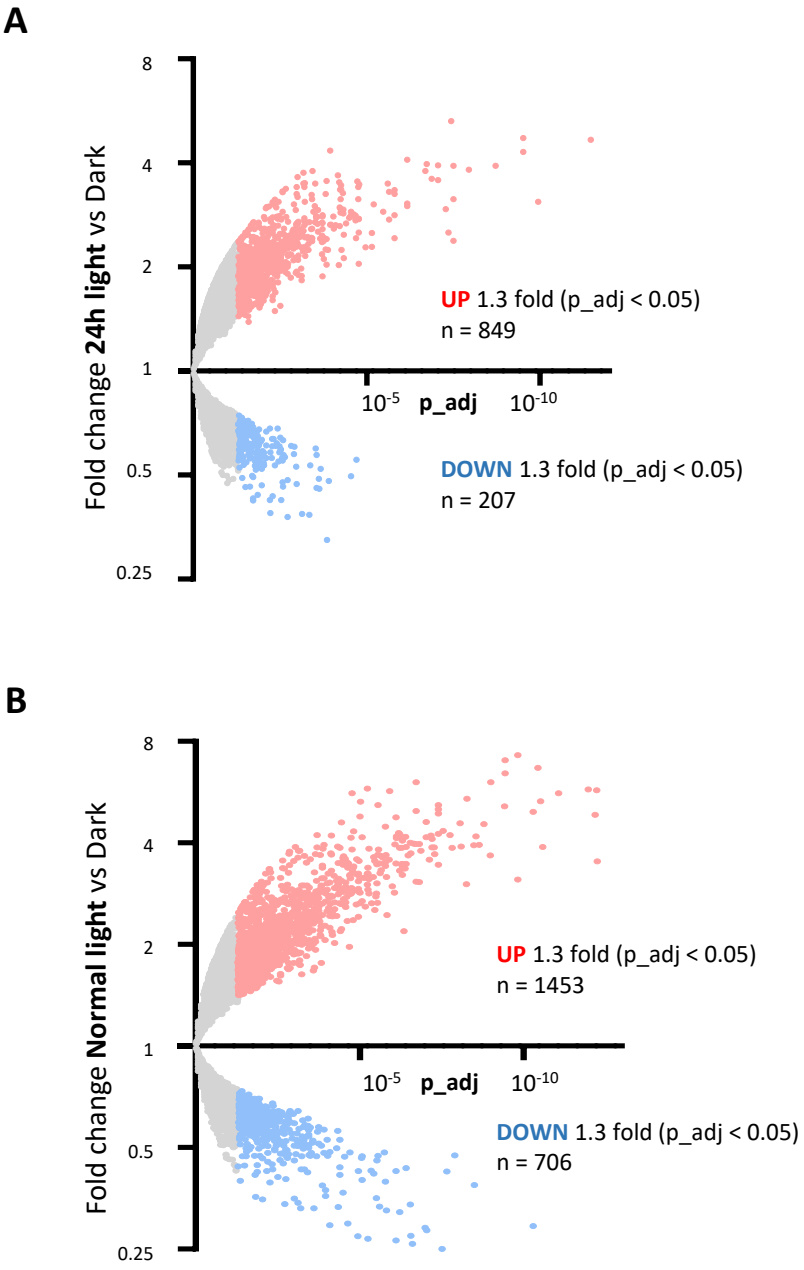

Figure 4.5 - Light-stimulus alters a wide-programme of astrocyte gene expression. A. Astrocyte gene expression measure by TRAP and compared between mice kept in darkness and mice exposed to 24 h light. A large number of genes have significantly altered gene-expression (Red – genes upregulated >1.3 fold, p_adjusted < 0.05, Blue - genes downregulated >1.3 fold, p_adj <0.05, N=4 mice in each condition) **B.** Similar to above, but utilising mice exposed to normal light-dark cycle vs those kept in darkness (N=4 mice in each condition).

4.2.5. *In vivo* transcriptional changes correlate with *in vitro* changes

I next investigated whether the astrocyte transcriptional changes seen with light stimulus correlated with our previous *in vitro* transcriptomic findings. Comparisons were done using both 24 h light vs dark **(Figure 4.6A, B)** and normal light vs dark **(Figure 4.6 C, D)** transcriptomic changes. These were compared to changes seen in astrocytes in cocultures exposed to 24 h of bicuculline or bicuculline+TBOA, vs TTX, to increase synaptic activity.

I found that i*n vivo* transcriptomic changes broadly overlapped and correlated well with gene-sets regulated by altered synaptic activity *in vivo,* with slightly stronger correlations between genes changed with 24h light vs dark than those changed with normal light vs dark.

Activity-dependent astrocyte genes identified in our experiment were also compared to other recently published datasets **(Figure 4.7)**. We found activity-dependent astrocyte genes identified from the above study overlapped with astrocyte genes identified in a recent publication utilising a light-stimulus paradigm of 1 h or 4 h light with single-cell sequencing of the visual cortex (Hrvatin *et al.*, 2018). Activity-dependent astrocyte genes also overlapped with those that are regulated during sleep (Bellesi *et al.*, 2015). Finally, utilising data from a study examining astrocyte gene-expression in aged (2 y) vs adult mice (4 month old) (Boisvert *et al.*, 2018), we found that activity-dependent genes are significantly down-regulated with ageing.

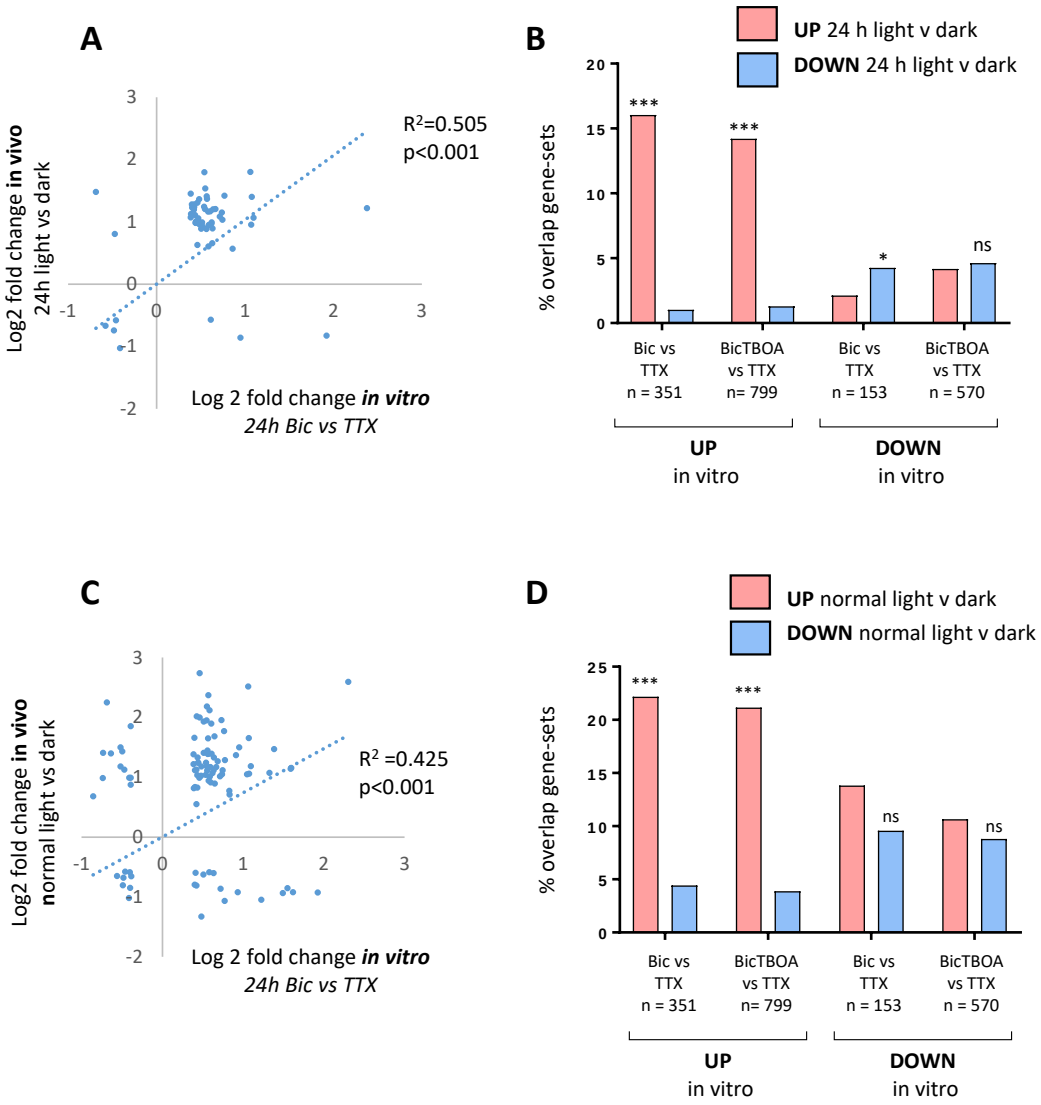

Figure 4.6 - Astrocyte genes regulated by light stimulus overlap with genes regulated by neuronal activity *in vitro*. A. Changes in astrocyte gene-expression following 24h light-stimulus vs dark or normal light exposure vs dark correlate to changes seen in astrocyte gene-expression *in vitro*. (N=4 mice or cultures, Spearman's rank correlation). **B**. Overlap between genes changing *in vitro* (Bic vs TTX, or Bic vs TTX with the addition of TBOA) vs genes upregulated (red) or downregulated (blue) with 24 h light stimulus vs dark. Percent overlap is fraction of genes from each gene-set that are significantly up or down-regulated , n = total number of genes in each set (***p<0.001, Fisher's exact test) **C, D.** Similar to above, but for genes altered with mice kept in normal light cycle vs dark.

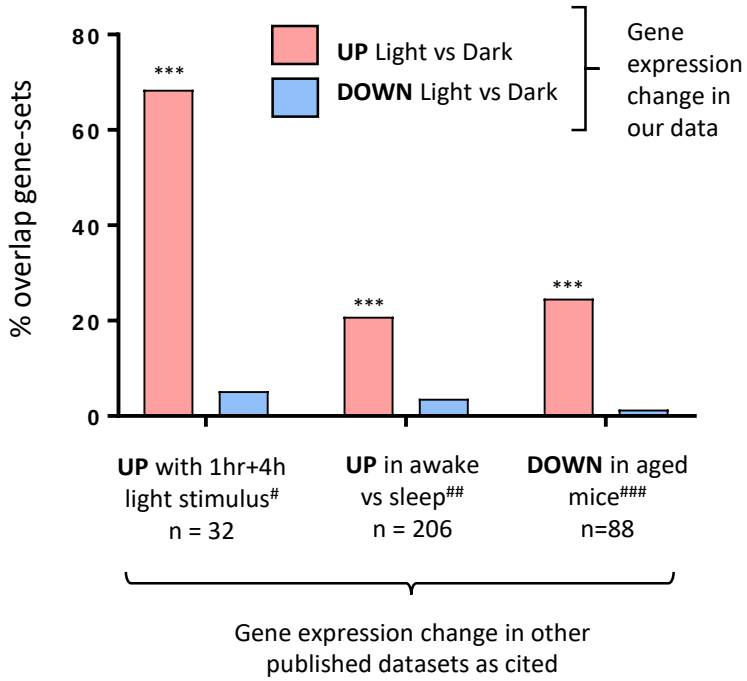

Figure 4.7 - Investigating overlap of activity-dependent astrocyte genes with datasets from other studies. Changes in astrocyte gene expression between mice kept in normal light vs those in dark were compared to published datasets. There was strong overlap found in gene-sets between astrocyte genes changes with 1 and 4 hr light stimulus isolated by single-cell sequencing (#Hrvatin *et al.*, 2018), and with genes that were increased in awake and sleep-deprived mice vs asleep mice (##Bellesi *et al.*, 2015), and astrocyte genes that are downregulated in aged (2y old) vs adult (8 week old) mice (###Boisvert *et al.*, 2018). Percent overlap is fraction of genes from each gene-set that are significantly up or down-regulated , n = total number of genes in each set (***p<0.001 Fisher's exact test).

4.2.6. Comparing activity-dependent transcription with activity-dependent translation.

Gene expression is a multistep process involving transcription of DNA to produce mRNA, and then subsequent translation of mRNA into protein. Transcriptional levels of mRNA may not correlate with protein levels. Post-transcriptional modification regulates mRNA translation and protein levels are also controlled by degradation. Whilst total mRNA levels correlate poorly with cellular protein levels, the cellular abundance of proteins is predominantly controlled at the level of translation (Schwanhäusser *et al.*, 2011).

Normal RNA isolation methods purifies all mRNA in the cell, whilst the mRNA isolated using TRAP is that which is being actively translated. Whilst we found a large overlap between gene-sets changed by neuronal activity *in vivo* (light vs dark) with those changed in cell-culture (Bic vs TTX), there were some genes that were differentially regulated. These differences could be due to the differences between neuron-astrocyte interactions *in vitro* vs *in vivo*, or might represent a difference between total transcribed mRNA and translated mRNA.

I therefore set out to investigate to what extent neuronal contact and synaptic activity effected astrocyte gene-transcription vs gene-translation. I did this by developing a novel method employing a combination of the mixed-species coculture methodology along with TRAP. By coculturing astro-TRAP astrocytes with rat neurons, and by sequencing both the input (total transcribed mRNA) vs that obtained by ribosomal pull-down (translating mRNA), I could

distinguish astrocyte-specific transcribed and translated mRNA. Furthermore the use of the species-specific sorting algorithm allowed me to distinguish and remove the rat neuronal reads from mouse astrocyte reads in both total mRNA (transcribed) and TRAP mRNA (translated). Hence, this approach allowed the investigation of non-cell autonomous effects of neurons and neuronal activity on astrocyte transcription vs translation.

I discovered a very strong correlation between astrocyte genes that are altered at the level of transcription with their subsequent change at the level of translation in response to both neuronal contact and synaptic activity **(Figure 4.8 A, B)**. The correlation was stronger with activity-dependent changes, vs contact dependent changes.

We next investigated whether any genes demonstrated significantly different regulation between transcription and translation levels. This was done by building a statistical model that included the interaction between input (transcribed mRNA) vs TRAP (translating mRNA) into the Deseq2 statistical framework. This approach revealed a large number of astrocyte genes exhibiting a statistically different change (Deseq2 $p\_adj < 0.05$, n= 345) between transcriptional and translational change in response to neuronal contact **(Figure 4.8 C, D)**. In contrast, very few genes appear to be differentially regulated between transcription and translation in response to altered neuronal activity (Deseq2 $p\_adj < 0.05$, N = 8). Furthermore, some of the activity-induced astrocyte genes in this group, whilst demonstrating statistical significance in

difference between transcriptional vs translational change, the overall fold-change is very small. Hence the difference in these genes is unlikely to be biologically important.

Gene ontology analysis of the genes differentially regulated at the level of transcription and translation in response to neuronal contact revealed enrichment for pathways related to astrocyte oxidative phosphorylation and ATP production (**Figure 4.8E**).

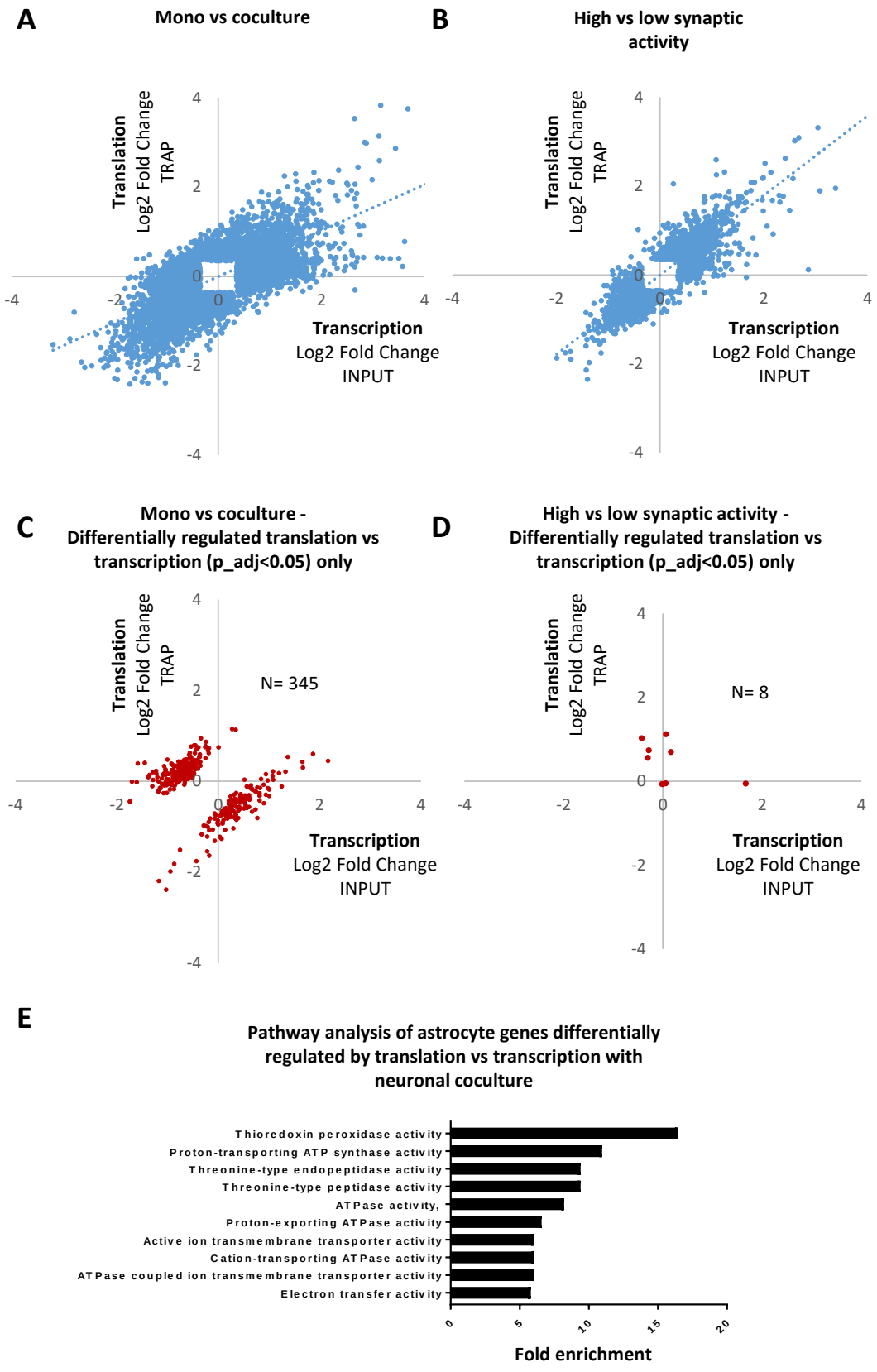
A
Mono vs coculture
Translation
Log2 Fold Change
TRAP
Transcription
Log2 Fold Change
INPUT
B
High vs low synaptic activity
Translation
Log2 Fold Change
TRAP
Transcription
Log2 Fold Change
INPUT
C
Mono vs coculture -
Differentially regulated translation vs transcription (p_adj<0.05) only
N= 345
Translation
Log2 Fold Change
TRAP
Transcription
Log2 Fold Change
INPUT
D
High vs low synaptic activity -
Differentially regulated translation vs transcription (p_adj<0.05) only
N= 8
Translation
Log2 Fold Change
TRAP
Transcription
Log2 Fold Change
INPUT
E
Pathway analysis of astrocyte genes differentially regulated by translation vs transcription with neuronal coculture
Thioredoxin peroxidase activity
Proton-transporting ATP synthase activity
Threonine-type endopeptidase activity
Threonine-type peptidase activity
ATPase activity,
Proton-exporting ATPase activity
Active ion transmembrane transporter activity
Cation-transporting ATPase activity
ATPase coupled ion transmembrane transporter activity
Electron transfer activity
Fold enrichment

Figure 4.8 - Combining TRAP with mixed-species coculture to investigate changes in astrocyte transcription vs translation. A. Astro-TRAP astrocytes were cocultured with rat neurons for 9 days or maintained as monoculture. Total mRNA was extracted and TRAP utilised to investigate only translating mRNA. The fold change in total mRNA levels (transcribed gene-expression) correlates well with TRAP mRNA levels (translated gene expression). **B.** Astro-TRAP astrocytes cocultured with neurons were exposed to high vs low activity conditons (24h of Bic vs Bic+TTX). Transcriptional vs translational change in gene-expression determined as above. **C.D.** Only genes that exhibit a significant difference between transcriptional and translational fold change (Deseq2 p_adj<0.05) are shown. Changes to astrocyte gene-expression in response to neuronal contact appear to show a greater degree of post-transcriptional control than changes in astrocyte gene-expression in response to altered synaptic activity. **E.** Panther over-representation pathway analysis of astrocyte genes that are differentially regulated at the level of translation vs transcription in response to neuronal coculture reveals upregulation of pathways for ATP synthesis and antioxidant action. Top 10 over-represented pathways shown (all p_adj <0.05).

4.2.7. Prolonged anaesthesia suppresses neuronal and astrocyte transcription.

Having determined that synaptic activity *in vivo* altered astrocyte transcription, I next set out to investigate if a more clinically relevant paradigm associated with reduced neuronal activity - that of prolonged sedative anaesthesia – also had consequences on CNS transcription. Anaesthetics are well established to be potent suppressors of neuronal activity. They are typically GABA receptor agonists or NMDA receptor antagonists (Franks and Lieb, 1994), and suppress neuronal firing (Ries and Puil, 1993), inducing burst suppression on EEG (Lukatch, Kiddoo and MacIver, 2005).

In clinical studies, anaesthesia has been implicated in increasing perioperative delirium, memory impairment and longer-term cognitive impairment in humans and animals (Dutton *et al.*, 2002; Culley *et al.*, 2004; Bratzke *et al.*, 2018). However the pathways by which anaesthesia drives these long-term effects is unclear. Furthermore many previous studies have focused on neuronal consequences, with the effects of anaesthesia on glia being less well understood.

To investigate whether anaesthesia alters CNS and astrocyte transcription, I exposed mice to 6 h anaesthesia using the volatile anaesthetic agent isoflurane. Animals were monitored throughout to ensure adequate oxygenation, temperature and hydration. Following the anaesthetic period, RNA was extracted from the cortex and analysed by RNA sequencing. By anaesthetising

astro-TRAP mice, I was able to use TRAP to investigate effects of anaesthesia on astrocyte vs other CNS cell-type gene expression.

6 h isoflurane anaesthesia has a profound effect on total CNS gene expression **(Figure 4.9A)**, altering the expression of thousands of genes. Confirming its action as a potent suppressor of neuronal activity, anaesthesia suppresses a large number of known immediate-early genes and activity-dependent CNS genes **(Figure 4.9B)**.

Anaesthesia also influences a wide-programme of astrocyte gene expression, (**Figure 4.10A)**. Genes that were significantly changed by both anaesthesia and dark-exposure demonstrated a very good correlation in induction and overall direction of change. Interestingly, both activity-dependent and activity-independent populations of genes altered by anaesthesia were identified **(Figure 4.10C)**. Some activity-dependent upregulated astrocyte genes that would be expected to be suppressed by anaesthesia were upregulated – demonstrating there is a complex astrocyte response to the anaesthetic insult, and that transcriptional changes are not purely the result of suppression of synaptic activity.

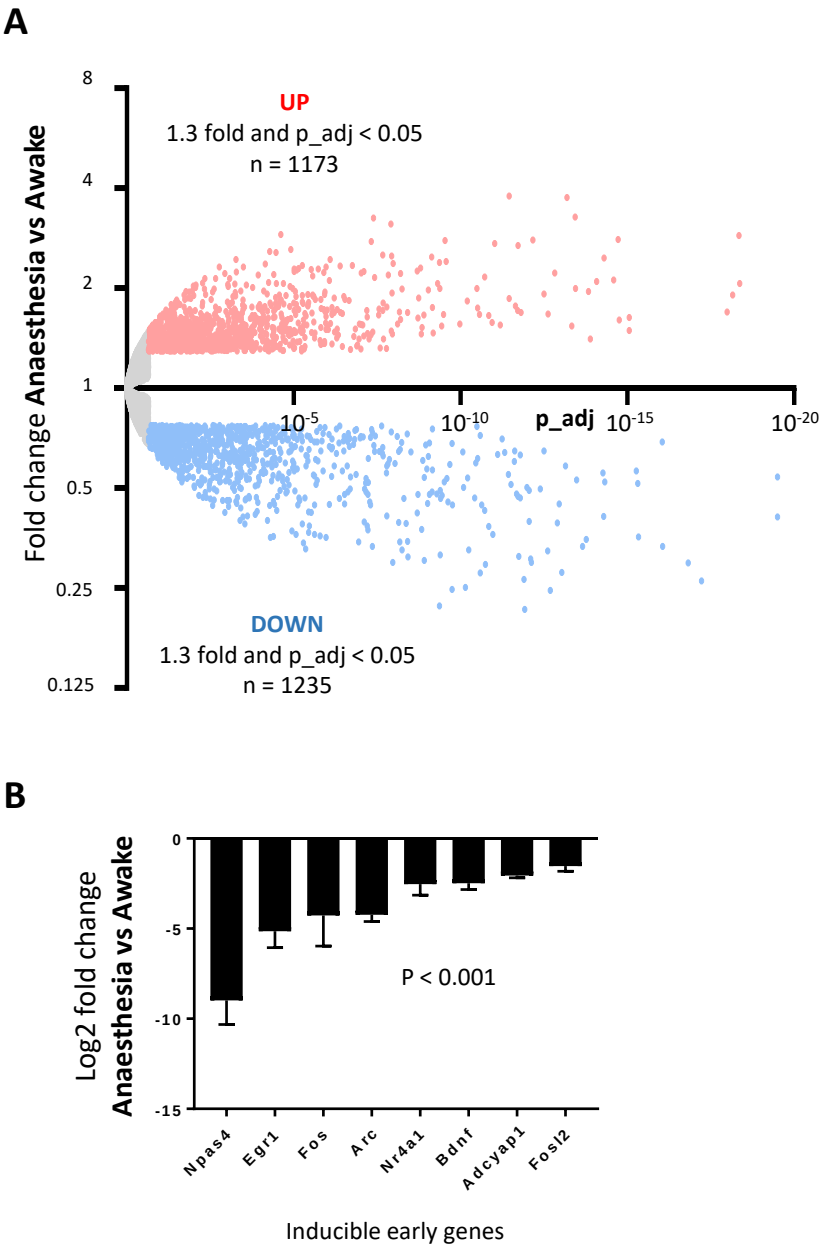

Figure 4.9 - Prolonged anaesthesia alters CNS gene expression. A. RNA-sequencing of brains exposed to 6 h isoflurane anaesthesia vs awake mice demonstrates that anaesthesia induces a change in a large number of genes (Red – genes upregulated >1.3 fold, p_adj<0.05, Blue- genes downregulated >1.3 fold, p_adj <0.05, N=5 mice awake vs anaesthetised). **B.** Anaesthesia reduces expression of activity-dependent immediate early genes (N=5, p<0.001, 1-way ANOVA).

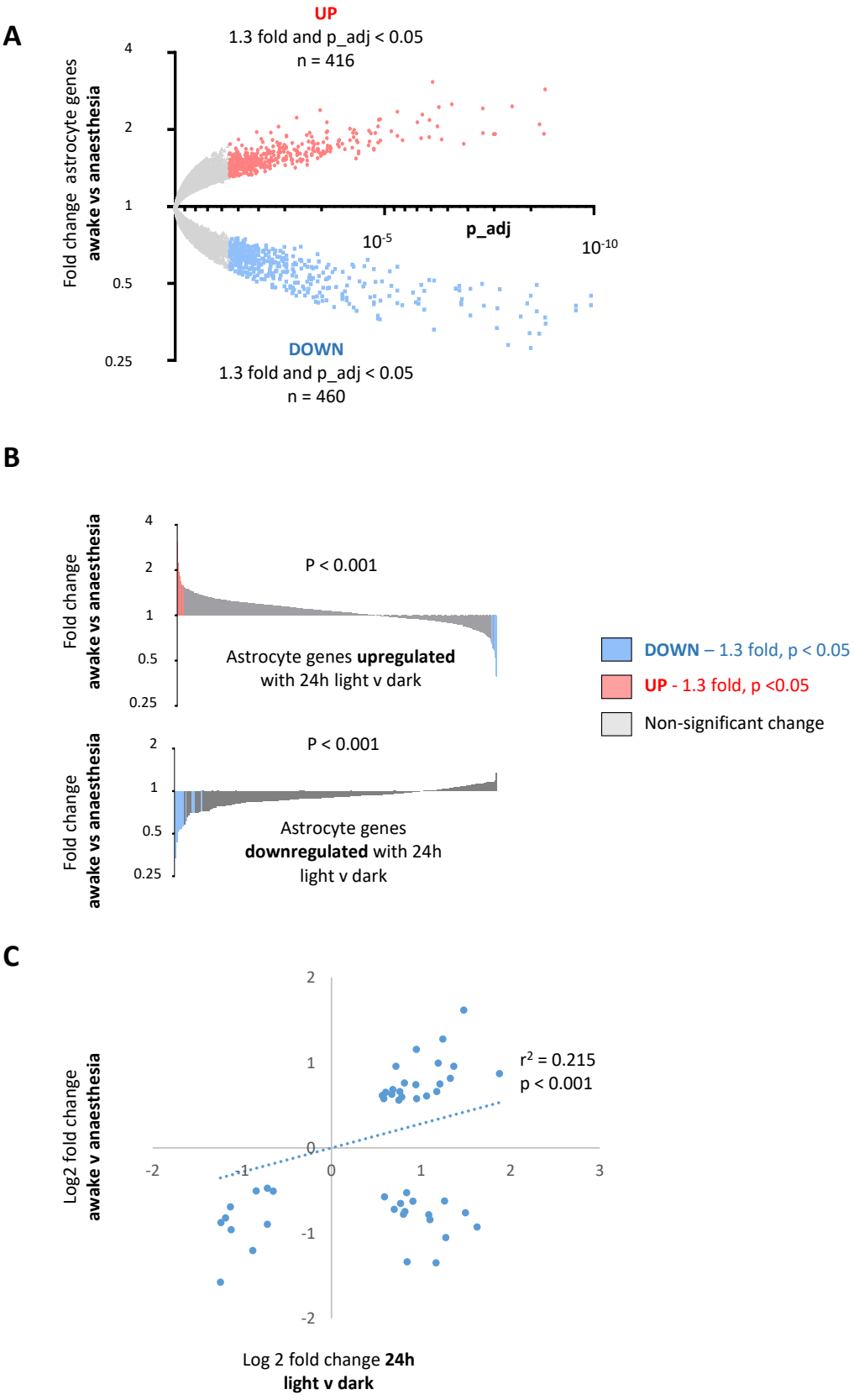
A
UP
1.3 fold and p_adj < 0.05
n = 416
Fold change astrocyte genes
awake vs anaesthesia
4
2
1
0.5
0.25
p_adj
10-5
10-10
DOWN
1.3 fold and p_adj < 0.05
n = 460
B
Fold change
awake vs anaesthesia
P < 0.001
Astrocyte genes upregulated
with 24h light v dark
P < 0.001
Astrocyte genes
downregulated with 24h
light v dark
DOWN – 1.3 fold, p < 0.05
UP - 1.3 fold, p <0.05
Non-significant change
C
Log2 fold change
awake v anaesthesia
r2 = 0.215
p < 0.001
Log 2 fold change 24h
light v dark

Figure 4.10 - Prolonged anaesthesia alters astrocyte transcription, with correlation with genes driven by synaptic activity. A. TRAP-seq used to measure astrocyte-specific transcriptomic changes in mice undergoing 6h isoflurane anaesthesia vs awake mice. A large number of astrocyte genes are dysregulated. **B. C.** Expression of genes upregulated by 24h light stimulus is overall suppressed by anaesthesia and vice-versa ($p<0.001$, 2-way ANOVA). **C.** Genes significantly changed (Deseq2 $p_{adj}<0.05$) in both light-stimulus and anaesthesia demonstrate correlation ($p<0.001$, Spearman's rank correlation).

4.2.8. Anaesthesia induces changes in pro-survival and pro-death CNS transcriptional pathways.

Some of the activity-driven genes that were dysregulated by anaesthesia were activity-regulated genes that are known to have a key role in protecting CNS cells from cell-death. These are well established genes that are driven by neuronal activity which increase neuronal resilience and inhibit apoptosis (Léveillé *et al.*, 2010; Bell and Hardingham, 2011). Anaesthesia suppresses activity-regulated inhibitor of death (AID) genes and increases activity-suppressed pro-apoptotic genes **(Figure 4.11A**). In fact many of the genes essential in both the intrinsic and extrinsic apoptosis pathways are significantly upregulated by anaesthesia **(Figure 4.11B)**.

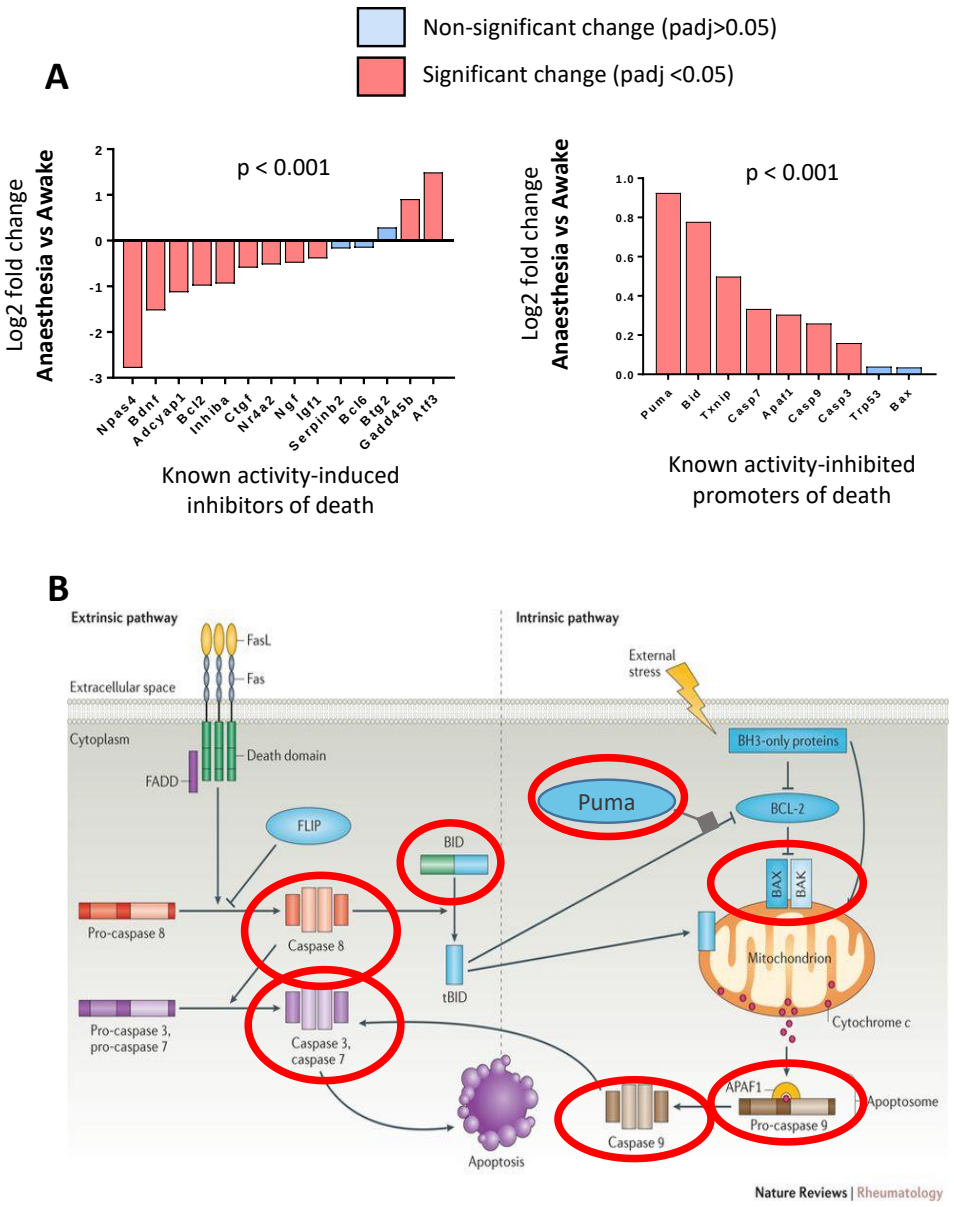

Figure 4.11 - Anaesthesia results in an increased vulnerability transcriptional signature. A. 6h anaesthesia significantly decreases expression of activity-induced inhibitor of death (AID) genes and increases apoptotic genes (N=5 awake and anaesthetised, ***p<0.001 two-way ANOVA). **B.** A large number of genes in both intrinsic and extrinsic apoptotic pathways are significantly upregulated by anaesthesia. Circled in red are all genes upregulated by anaesthesia with Deseq2 p_adj <0.05.

Given the strong dysregulation of survival and pro-death genes, I investigated if these transcriptional changes had a functional consequences on CNS apoptosis. Activation of Caspases 3 and 7 represents the common step in the intrinsic and extrinsic apoptosis pathways. I measured protein levels of Caspase 3 (inactive) and cleaved-caspase 3 (active) using western blot, finding (consistent with the transcriptional changes observed) significantly increased caspase 3 protein levels in brains from mice anaesthetised for 6h vs awake mice **(Figure 4.12B)**.

However, there was no increase in levels of the activated cleaved-caspase 3 **(Figure 4.12C)**. I next looked at functional caspase 3/7 activity by using a caspase activation luminescence assay (Caspase 3/7 Glo). Whilst a good induction of apoptosis in positive control samples was confirmed, there was no increase in caspase 3/7 activity in anaesthetised vs awake brains **(Figure 4.11D)**.

Taken together, these data suggest that prolonged anaesthesia alters transcription to boost the apoptotic potential of CNS tissue but without actual increase in apoptosis. This might lead to a primed CNS that demonstrates increased vulnerability to secondary insults, for example inflammation or hypoxia.

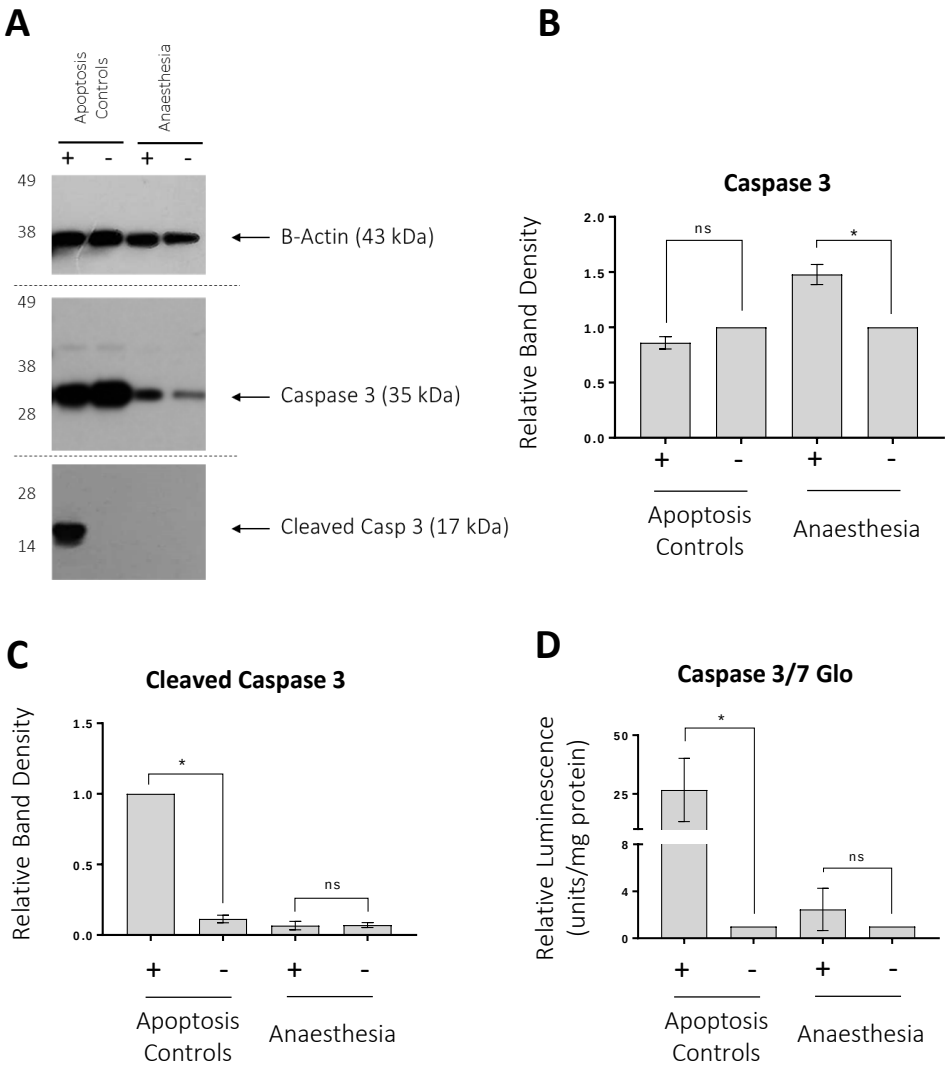

Figure 4.12 - Anaesthesia primes apoptotic pathways in the CNS but does not increase apoptosis. A Example Western blot for caspase 3 and cleaved caspase 3, with quantification of band-densities. Positive control samples were cultured cells exposed to 24h of 100 nM staurosporin, a potent inducer of apoptosis. **B, C.** Quantification of Western blots. 6h anaesthesia increases absolute caspase 3 but not cleaved caspase 3 levels (N=3 awake and anaesthetised, *p<0.05, two-tailed t-test vs awake mice or negative apoptosis control). **D.** Caspase Glo 3/7 functional caspase activity assay finds no change in apoptosis between anaesthetised and awake animals (N=3, * p<0.05, unpaired two-tailed t-test vs awake mice or negative apoptosis control).

4.2.9. Using transcranial electrical stimulation to rescue anaesthesia-induced changes.

Finally, I wanted to determine whether it was possible to reverse transcriptional changes induced by anaesthesia by enhancing synaptic activity. This would reveal which set of genes are indeed being altered by anaesthesia due to its effect on suppressing neuronal activity vs genes that were changing due to other consequences of anaesthesia. In addition, the ability to reverse anaesthesia-mediated effects on activity-dependent CNS prosurvival and death pathways would useful for possible future therapeutic strategies.

I decided that the optimal method for enhancing electrical activity in the brain would be to use non-invasive transcranial electrical stimulation (NTES). NTES has the benefit of avoiding damaging surgical interventions that may alter gene-expression. It is a well-established technique in humans and animals (Matsumoto and Ugawa, 2017) and has been shown to enhance neuronal activity (Grossman *et al.*, 2017).

To investigate whether transcranial electrical stimulation could reverse some of the transcriptional effects of anaesthesia, I applied NTES to cortical tissue during prolonged isoflurane anaesthesia. Stimulation was with a 10Hz electrical sinusoidal current (500mA), with a protocol involving 20 mins stimulation, followed by 10 mins rest to allow neuronal recovery. This was for 5 stimulation episodes for a total time of 100 mins stimulation during the 180 min

anaesthesia. CNS RNA was extracted and compared with both a sham stimulation (using a 0 mA current) along with RNA from the contralateral non-stimulated side **(Figure 4.13A)**. The level of expression of three selected IEGs (*Fos, Bdnf* and *Arc)* were measured using qPCR. I found NTES enhanced the expression of *Fos* and *Bdnf* but did not alter levels of *Arc*. Expression levels were boosted both compared to sham stimulation, as well as to the contralateral non-stimulated cortex **(Figure 4.13B)**.

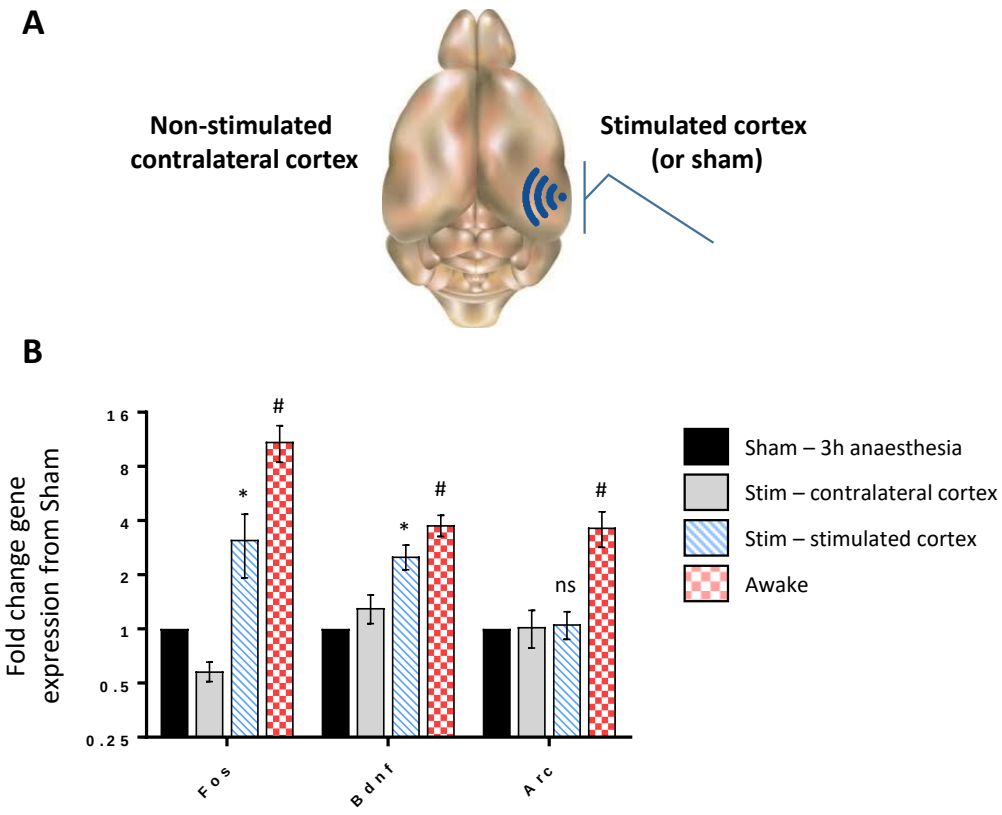

Figure 4.13 - Transcranial electrical stimulation reverses anaesthesia-induced suppression of activity-dependent genes. A. Schematic demonstrating the use of electrical stimulation to locally enhance neuronal activity. RNA from this area is compared to contralateral non-stimulated tissue and tissue from sham stimulation. **B.** RNA from stimulated cortex extracted and assessed by qPCR. Electrical stimulation significantly boosts *Fos* and *Bdnf* levels. *Arc* remains unchanged (N=3, *p<0.05 paired two-tailed t-test against contralateral non-stimulated side; #p<0.05 unpaired two-tailed t-test against sham stimulation).

4.3. Chapter discussion

4.3.1. Synaptic activity regulates astrocyte transcription in the visual cortex

In this chapter, by combining a light-stimulus paradigm with the TRAP method to measure astrocyte-specific gene expression, I have determined that altered synaptic activity in the visual cortex drives changes to the expression of a large number of astrocyte genes.

These changes correlate well with data from Chapter 3 using an *in vitro* coculture approach. We found upregulation of a number of genes involved in the cAMP pathway as well as genes involved in metabolic flux. However, there were some important differences in genes regulated between *in vivo* and *in vitro* datasets. The number of metabolic genes upregulated is much smaller. And there are some genes that are regulated in the opposite direction (for example the thyroid hormone activating enzyme *Dio2 i*s upregulated by synaptic activity in vitro but down-regulated in vivo).

Reasons for these differences could be: i) intrinsic differences between *in vitro* and *in vivo* astrocytes; ii) the presence of other CNS cell-types that modify activity-dependent signals; iii) Region-specific differences between visual cortex and other cortical astrocytes; iv) differences in the intensity or of the stimulation paradigm. Bic vs TTX drug treatment will lead to a much stronger difference in synaptic activity than light vs dark in the visual cortex, and this may account for transcriptional changes between the two approaches; v) Differences in levels

between transcribed mRNA (measured *in vitro)* and translated mRNA (measured by TRAP *in vivo*). This is discussed and addressed in more detail below.

The findings correlate well with other studies that have looked at how CNS activity may influence astrocyte gene expression *in vivo*. A recent study by the Greenberg group examined a limited set of astrocyte genes determined by single cell-sequencing of mouse visual cortices exposed to 1 h and 4 h of light stimulus. Due to the limitations of single-cell sequencing, and the fact that sequencing is only possible to a much lower depth due to the number of cells involved, they found changes in 32 astrocyte genes. My data agrees well with the findings of this study. I found approximately 80% overlap with the genes uncovered in that study and have further expanded the data-set by finding approximately a thousand more genes that are altered by light exposure.

One interesting finding was that we found that many of the activity regulated astrocyte genes are those that are found to be reduced in brains taken from aged vs adult mice (2 y vs 4 month). This could be due to : i) Reduced neuronal activity due to ageing; or ii) Reduced responsiveness of aged astrocytes to neuronal signals. This interesting finding will now require further study, and may imply a reduction in activity-induced pathways that ultimately lead to increased vulnerability and CNS susceptibility during ageing.

4.3.2. Using mixed-species culture and TRAP to reveal differences between cellular transcription and translation.

One important reason for differences between *in vitro* and *in vivo* data could be due to differences in measuring total transcription in our previous *in vitro* experiments vs measuring translating mRNA in the TRAP studies. To examine the effect of this, I developed a novel approach combining the power of the mixed-species coculture approach with the TRAP methodology. This allowed me to investigate the non-cell autonomous effects of neurons and neuronal activity on astrocyte gene-expression changes at the level of transcription and translation.

I discovered that there was an almost perfect correlation between changes at the level of transcription and translation in astrocyte genes that change in response to synaptic activity. This appears to make physiological sense: with acute signals to the cell driving transcriptional and translational flux to alter protein production and cellular function.

In contrast, I found that astrocyte genes altered as a result of neuronal contact demonstrate reduced correlation between transcription and translation. We identified 345 genes that were significantly differentially regulated. Many of these genes were related to astrocyte mitochondrial and ATP synthesis activity. This reveals an important novel method of non-cell autonomous control that regulates gene-expression in astrocytes in response to neurons. The

mechanisms by which this translational control occurs is unknown and the focus of current study.

Finally, whilst cellular abundance of proteins has been demonstrated to be controlled at the level of translation (Schwanhäusser *et al.*, 2011), there may be further differences at the level of translated mRNA and total protein levels in astrocytes. Ongoing studies in our lab are now using mass-spectrometry proteomics to quantify and understand this difference.

4.3.3. Anaesthesia reduces neuron and astrocyte activity-dependent gene expression

Anaesthesia represents a clinically relevant paradigm when neuronal activity is altered for prolonged periods of time. Whilst the exact mechanism of action of anaesthetics agents is yet to be established, it is generally considered that they globally inhibit neuronal activity by acting as GABA receptor agonists or NMDA antagonists (Franks and Lieb, 1994). Furthermore it is well established that anaesthesia leads to increased CNS vulnerability in both infants and in the elderly, where it can manifest as delirium and post-operative cognitive impairment (Leslie, 2017; Bratzke *et al.*, 2018). The mechanisms by which this occurs are unknown and I wanted to establish whether prolonged suppression of neuronal activity by anaesthesia suppressed neuronal and astrocyte activity-dependent pathways related to CNS homeostasis and resilience.

I found that 6 h exposure to isoflurane anaesthesia led to a wide-spread changes in the CNS transcriptional programme. This is not too surprising given the diffuse and generalised effects of anaesthesia. Most known immediate-early and activity-dependent CNS genes were driven profoundly down by anaesthesia confirming that it is a potent suppressor of activity-dependent pathways.

It has been well-described that neuronal activity is essential for maintaining neuronal health, with activity boosting the expression of a gene-programme known as AIDs and inhibiting pro-apoptotic neuronal genes (Hardingham and Bading, 2003; Léveillé *et al.*, 2010) . Here, I have shown that during anaesthesia these pathways are deregulated. Anaesthetised brains demonstrate low levels of AIDs and high levels of pro-apoptotic genes.

I was unable to find evidence of an acute increase in apoptosis using both western blot and functional assays for caspase activity. One reason for this might be related to timing, with 6 h being too soon for functional apoptosis to have begun. Hence we are now undertaking studies to check for apoptotic markers 48 – 72 h following recovery from anaesthesia. An alternative explanation is that anaesthesia does not induce apoptosis per se, but by switching of activity-dependent protective pathways, primes the brain for apoptosis, leaving it more vulnerable to secondary insults.

This explanation fits well with clinical observations. Many patients can undergo anaesthetic procedures with no evidence of long-term neurological sequelae. However, patients with already injured brains (due to dementia or ageing) or

those exposed to a secondary insult (such as hypoxia or inflammation) are at much higher risk of demonstrating delirium and neurological consequences following prolonged anaesthetic episodes.

Finally, I utilised non-invasive transcranial electrical stimulation (NTES) to increase neuronal activity during anaesthesia. The exact mechanism by which NTES alters neuronal activity is poorly understood, but it is thought to cause generalised network synchronisation (Roche, Geiger and Bussel, 2015). It is a technique that is routinely used in humans and has been suggested to confer neuroprotection and improve outcomes in several conditions.

In the preliminary work outlined here, I have found that exposure to NTES partially rescued the anaesthesia induced effects on activity-regulated genes. This gives confidence that some of the transcriptional changes described above are indeed due to anaesthesia-mediated suppression of synaptic activity rather than other non-specific effects of anaesthesia. Further work is now required to determine the ideal frequency and duration paradigm of NTES that induces the maximum rescue of gene-expression changes. It is also required to test whether NTES has a functional change with regards to apoptotic markers and cognitive outcomes.

4.3.4. Limitations and future work.

The TRAP methodology used to investigate cell-type specific gene expression has some limitations common to all methods that attempt to separate cell-type gene expression: namely that of off-target contamination. Utilising our mixed-

species coculture approach, and by analysing the amount of rat reads that we got in our samples, we were able to calculate this contamination to be at 12(+/-0.37)%.

There are also a few specific limitations. EGFP expression is linked to expression of the *Aldh1l1* gene, which is assumed to be astrocyte-specific. Whilst *Aldhl1l1* is considered to be the best marker (Srinivasan *et al.*, 2016) for distinguishing astrocytes from other cell-types in the CNS, it is also expressed in low amounts in oligodendrocyte precursors and neural stem cells (Foo and Dougherty, 2013). This may mean that some of the gene-expression changes detected may reflect contamination from these alternative cell-types.

Furthermore, the approach pools mRNA from all astrocytes in the cortex and hence assumes their response to be heterogeneous. It is known that astrocytes demonstrate regional and functional differences (Zamanian *et al.*, 2012; Bayraktar *et al.*, 2018) and this method will not enable investigation of these differences.

The light stimulus paradigm has some important limitations. Even in darkness, there is some spontaneous retinal activity (Colonnese, Shen and Murata, 2017). Furthermore, it is known that the visual cortex receives innervation from other cortical areas (Macaluso, Frith and Driver, 2000). This means that (especially in rodents) darkness does not mean the complete absence of neuronal activity and will reduce the sensitivity of detecting activity-induced changes. Furthermore, altered light dark cycles will have other non-specific effects, for example on

circadian rhythm and motility. Therefore confirming findings using an alternative stimulation paradigms such as whisker stimulation or auditory stimulation would help augment and support the findings in this chapter.

Finally, an important limitation to consider with all transcriptomic studies is that mRNA levels may not necessarily correlate with protein levels. The TRAP methodology extracts actively translating mRNA, and hence would be expected to correlate more closely with changes in cellular protein abundance and function as compared with measurement of total cellular. In fact cellular abundance of proteins has been demonstrated to be controlled at the level of translation (Schwanhäusser *et al.*, 2011). However ongoing proteomic and functional studies in our lab are investigating whether changes in astrocyte translating mRNA levels correlate with changes in protein and function.

4.3.5. Chapter conclusion

The studies in this chapter support that synaptic activity alters astrocyte transcription using *in vivo* experimental approaches. Anaesthesia (a potent suppressor of synaptic activity), has wide-spread consequences on CNS and astrocyte transcription, reducing expression of CNS survival genes and boosting apoptotic genes. Combined, these transcriptional changes may lead to increased anaesthesia-related CNS vulnerability, and dysregulation of these pathways may contribute towards the increased risk of neurological dysfunction clinically observed in the post-operative period.

Chapter 5

Consequences of neurodegeneration on astrocyte transcription and phenotype.

5.1. Chapter Introduction

In the previous two chapters, I have described the manner and extent to which astrocyte transcription and function are regulated by an important physiological signal: neuronal synaptic activity. The next natural question that I aimed to address was whether astrocyte transcriptional pathways are disrupted in the context of neurodegenerative disease.

As expanded in section 1.3 of the thesis introduction, the role of astrocytes in neurodegeneration is complex and incompletely understood. They are proposed to play roles as upstream modulators and downstream effectors of neurodegenerative pathology (Phatnani *et al.*, 2015; Radford *et al.*, 2015). Recent studies have identified heterogeneity in the astrocyte response to acute injury and disease, with the capacity to play both neurotoxic and neuroprotective roles (Zamanian *et al.*, 2012). Whilst this response encompasses a complex and broad spectrum of different roles, the transcriptional responses have been divided into two groups: A1 vs A2 responses (Liddelow and Barres, 2017). Whilst this binary polarisation is an oversimplification of a multifaceted astrocyte response, it serves as a useful template to discuss broadly neurotoxic vs neuroprotective consequences of reactive astrocytosis.

A1 responses were discovered in response to inflammatory stimuli and are considered generally neurotoxic. For example, A1 responses involve upregulation of complement cascade genes; to be destructive to synapses and

to have neurotoxic effects. In contrast, an alternative A2 response was identified in astrocytes profiled from brains exposed to ischaemic injury. These astrocytes demonstrated upregulation of neurotrophic and antioxidant pathways, demonstrating a response considered broadly neuroprotective.

Most neurodegenerative conditions involve a complex interplay of a number of downstream cellular and molecular pathological processes. These include metabolic dysfunction; free-radical damage; vascular compromise; inflammation; and ultimately cell-death (De Strooper and Karran, 2016). It was unclear to what extent these processes would influence astrocyte phenotype, and to what extent the response from astrocytes would be neuroprotective vs neurotoxic in the context of dementia. Specifically, we wished to investigate how the disease processes involved in dementia alter the balance of one or both of the A1 neurotoxic vs A2 neuroprotective transcriptional responses.

To address the above, I utilised the P301S transgenic mouse - a model of human tauopathy and frontotemporal dementia (FTD). The P301S mutation is a familial mutation on chromosome 17 (Sperfeld *et al.*, 1999) that leads to the substitution of proline with serine at amino acid position 301 of the human tau protein. This increases hyper-phosphorylation of mutant tau, causing aggregation and accumulation. Patients with the P301S mutation develop early-onset FTD and corticobasal degeneration (CBD) in their 20s and 30s.

The P301S transgenic mouse (first described by Allen *et al.*, 2002) sets out to model human tauopathy. It drives the expression of the mutant human-tau gene with the P301S substitution, under the neuron-specific Thy1.2 promoter.

The phenotype of the mouse has been well characterised and described (Hampton *et al.*, 2010). The region of the CNS that exhibits greatest phosphorylated tau accumulation and hence neurodegeneration is the spinal cord. Neurodegeneration also has been characterised in superficial layer 1 and 2 specific frontal and motor cortex. Regions of neurodegeneration demonstrate essential pathological features of tauopathies, including accumulation of phosphorylated tau filaments **(Figure 5.1A)** leading to progressive neuronal loss **(Figure 5.1 B, C)**. Synapse loss and neuronal loss begin at 10 weeks of age, and mice begin to exhibit weightless and hind-leg paralysis by 18-20 weeks. The functional effects of neurodegeneration can be tested by horizontal bar grip strength testing **(Fig 5.1F)**. Strengths of the P301S transgenic mouse as a model for FTD are that it mimics progressive, region-specific, tauopathy-induced neurodegeneration along with associated vascular and inflammatory responses.

In this chapter, I describe studies investigating CNS and astrocyte-specific transcriptional consequences of tauopathy-induced neurodegeneration in the P301S transgenic model. By crossing these mice with the astro-TRAP line, I was able to study effects of tauopathy-induced neurodegeneration on astrocytes at end-stage of neurodegeneration. These studies revealed that astrocytes undergo changes in both neurotoxic and neuroprotective astrocyte signatures.

Finally, I proceed to describe how boosting a specific aspect of the neuroprotective A2 response (by driving astrocyte-specific activation of Nrf2, the master antioxidant cellular regulator), reversed both transcriptional and functional phenotypes seen in this human tauopathy model.

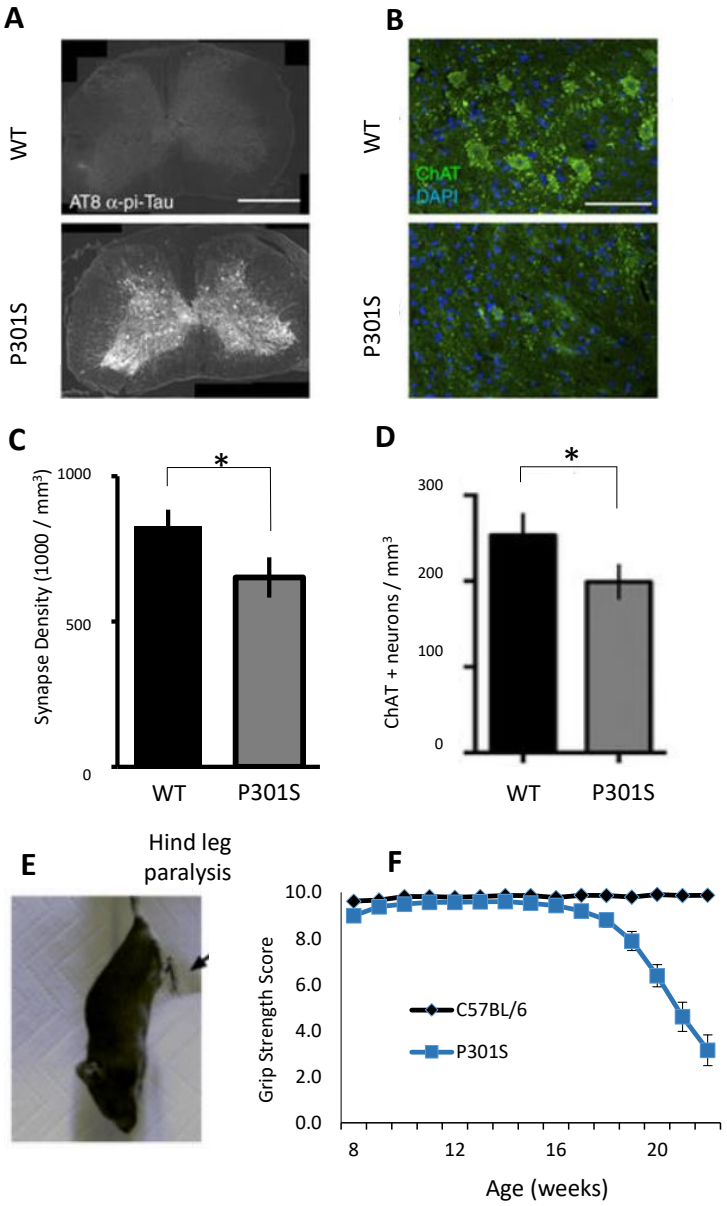

Figure 5.1 - The P301S mouse as a model for focal progressive neurodegeneration. (Data taken from experiments carried out by members of Chandran lab group). **A.** Hyper-phosphorylated tau accumulates in the cortex and spinal cord. **B, C.** Staining for neurons using the neuron-specific marker ChAt (Cholinesterase Acetyl Transferase) reveals neuronal loss at 20 weeks **D.** Neuron loss is associated with synapse loss. **E.** Spinal cord neurodegeneration is the most severe phenotype of the model leading to progressive hindleg paralysis **F.** This can be functionally measured using the horizontal bar grip test, which reveals a progressive deterioration in the p301S mouse from 16 weeks.

5.2. Results

5.2.1. Tauopathy induces CNS transcriptional changes consistent with neurodegeneration and inflammation.

To investigate the consequence of tauopathy-induced neurodegeneration on total CNS transcription, I extracted RNA from superficial frontal cortex and spinal cord from P301s mice vs control mice and analysed the transcriptional changes using RNA-sequencing. Tissue was extracted at 20 weeks, when mice exhibit severe neurodegeneration. Transcriptomic analysis was carried out on extracted cortical or spinal cord total CNS tissue (utilising the input samples from TRAP analysis) using RNA-seq.

As predicted, we confirmed that P301S mice exhibited wide-spread transcriptomic changes in both the cortex and spinal cord **(Figure 5.2 A, B)** at 20 weeks vs WT control mice. A larger number of genes are changed in the spinal cord vs the cortex, consistent with the increased amount of neurodegeneration observed in this area.

The transcriptomic changes demonstrated an increased inflammatory signature. Gene-ontology analysis for gene-sets that are significantly upregulated or downregulated reveals upregulation of gene-sets associated with inflammation and down-regulation for genes associated with neuronal function **(Figure 5.2C)**. Utilising cell-type specific gene markers (those from Ye Zhang *et al.,* 2014 which are >5 fold enriched in a particular cell-type), I examined which

cell-types had the greatest number of transcriptomic changes. This revealed an upregulation of a large number of microglia-specific genes (**Figure 5.2 D**).

Overall these data suggest increased inflammation and decrease in neuronal activity and health at the end-stage of tauopathy-induced disease.

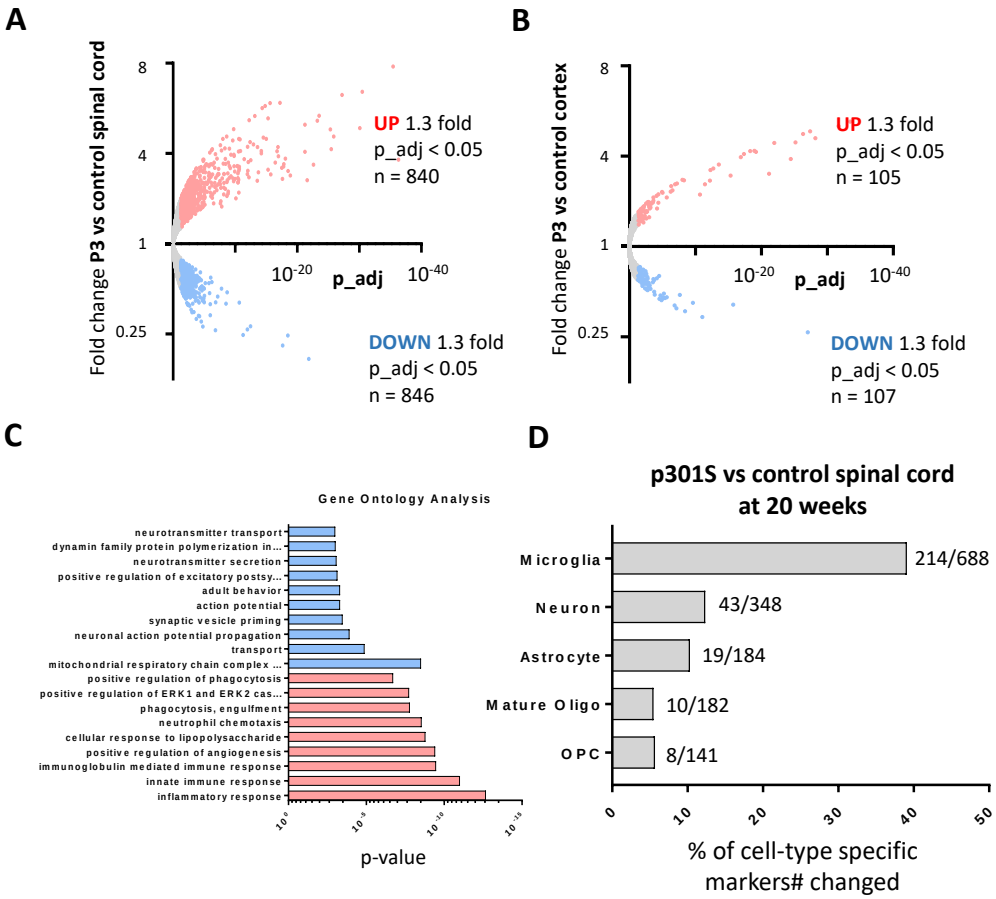

Figure 5.2 - Tauopathy induces wide-spread changes to the total CNS transcriptome. A, B. Pre-TRAP input samples (containing mRNA from all cells) were analysed by RNA-seq. A large number of genes are significantly upregulated and downregulated. The spinal cord (SC) demonstrates greater transcriptomic changes than cortex (Cx) consistent with the greater neurodegeneration seen in this area (SC-WT:N=4, SC-P301S: N= 4, Ctx-WT: N=4, Ctx-P301S: N=3). **C.** Gene-ontology analysis reveals significant upregulation of inflammatory pathways (red) and downregulation of neuronal activity and function pathways (blue). **D.** The largest number of cell-type specific markers (#from Ye Zhang *et al.*, 2014 which are >5 fold increased in a particular cell-type over other cell-types) that change are from microglia, fitting with the increased inflammatory signature present.

5.2.2. Transcriptional changes in the P301S transgenic mouse correlate with those in human FTD.

To understand how well the P301S transgenic mouse modelled human tauopathy and frontotemporal dementia (FTD), I compared the transcriptomic changes from the above study to transcriptomic data obtained from human post-mortem samples. These utilised post-mortem brain samples from the superior temporal gyrus (STG) from patients with FTD and non-affected controls. Patient characteristics are summarised in **Table 5-1**. A large number of patients in the FTD group (12/15) exhibited the tau-specific 10+16 mutation. This is a common human tau mutation that results in abnormal alternative splicing and an increased rate of inclusion of exon 10. This increases the proportion of four-repeat (4R) tau isoforms leading to early onset FTD (Hutton *et al.*, 1998).

Table 5-1 – Patient characteristics of human post-mortem samples

	Control group	***FTD group***
Sample N	21	15
Sex (% Female)	75%	71%
Age (Mean +/- SD)	63(+/-18)	60 (+/-6)

RNA extraction from post-mortem brains and sequencing of human post mortem samples was carried out by Paul Baxter and Jamie Mcqueen from the Hardingham and Spire-Jones groups.

Comparison of the transcriptional data from the P301S mouse with that from Human FTD samples reveals that there is strong overlap in gene-sets (**Figure 5.3**). Genes that are found to be both significantly changed (Deseq2 p_adj <0.05, >1.3 fold upregulated or downregulated) in the spinal cord of P301S mice are also significantly changed in human FTD post-mortem brain samples.

Transcriptional changes between P301S cortex and human FTD samples do not correlate. This may be due to the less severe neurodegeneration seen in the cortex vs spinal cord, which may not match as well with the level of neurodegeneration seen in end-stage post-mortem FTD brain samples.

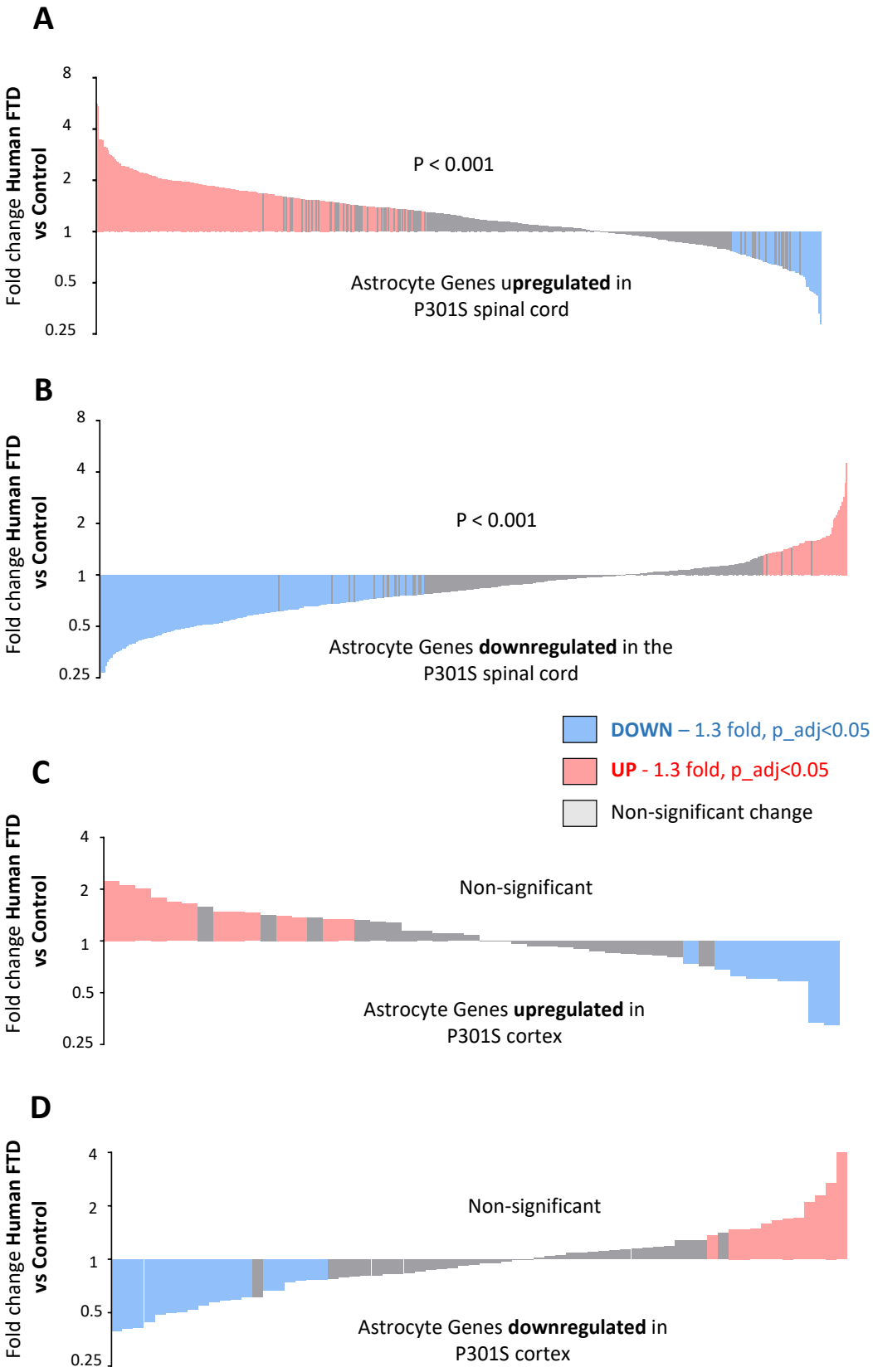
A
Fold change Human FTD vs Control
8
4
2
1
0.5
0.25
P < 0.001
Astrocyte Genes upregulated in P301S spinal cord
B
Fold change Human FTD vs Control
8
4
2
1
0.5
0.25
P < 0.001
Astrocyte Genes downregulated in the P301S spinal cord
DOWN – 1.3 fold, p_adj<0.05
UP - 1.3 fold, p_adj<0.05
Non-significant change
C
Fold change Human FTD vs Control
4
2
1
0.5
0.25
Non-significant
Astrocyte Genes upregulated in P301S cortex
D
Fold change Human FTD vs Control
4
2
1
0.5
0.25
Non-significant
Astrocyte Genes downregulated in P301S cortex

Figure 5.3 - Transcriptional changes in the spinal cord of p301S tauopathy mouse model correlates with those found in human FTD. **A,B.** Expression levels of genes that were significantly ($p_{adj}<0.05$, fold change >1.3) changed in the spinal cord of P301s vs WT mice at 20 weeks was compared in samples extracted from post-mortem human STG from healthy controls and those diagnosed with FTD. Gene-expression changes in FTD correlate with those seen in P301S spinal cord. **C.D.** Similar to above but for cortex, and this time no correlation found. (P301S and control mice- N = 4 each group. Human brain samples - Control: N= 21, FTD: N =15; 2-way ANOVA).

5.2.3. Neuronal tauopathy and neurodegeneration drives changes to astrocyte transcription.

Next, I investigated how tauopathy-induced neurodegeneration specifically altered astrocyte transcription. By crossing the P301S mouse with the astro-TRAP line, I was able to use the TRAP method to isolate astrocyte-specific changes in gene-expression. Mutant tau expression in the P301S line is expressed in a neuron-specific manner. Therefore astrocyte transcriptional changes would occur via non-cell autonomous consequences of tau-mediated neurodegeneration, rather than a direct toxic effect of mutant tau expressed in astrocytes.

Astrocyte specific gene expression was assessed by TRAP-sequencing spinal cord and cortex samples from 20 week old mice, and comparing to WT control mice. I first confirmed that TRAP was able to successfully enrich astrocyte mRNA from older brains experiencing neurodegenerative changes, ensuring enrichment of astrocyte-specific markers and depletion of other cell-type markers between TRAP and pre-TRAP input samples.

Tauopathy-induced neurodegeneration alters a large number of astrocyte genes, with changes greater in spinal cord vs cortex, fitting with the more severe neurodegeneration in that region **(Figure 5.4)**.

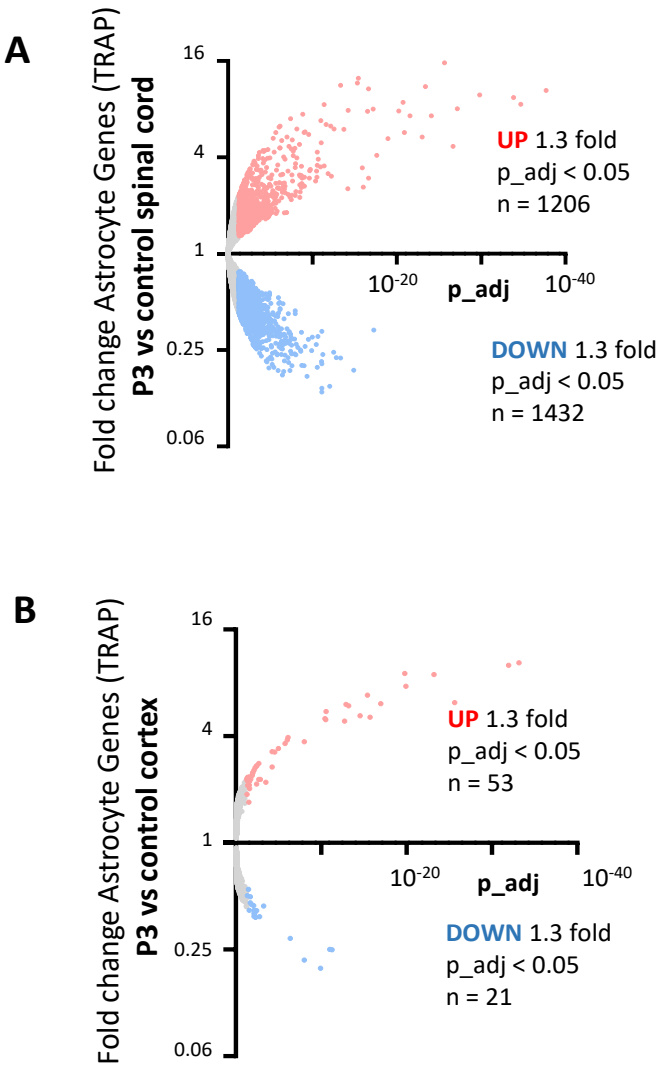

Figure 5.4 - TRAP-seq reveals that tauopathy-inducd neurodegeneration induces wide-spread changes to astrocyte transcription. . TRAPseq used to isolate astrocyte-specific transcriptional changes in P301S vs WT mice at 20 weeks in **A**. spinal cord and **B.** Cortex. Spinal cord demonstrates a greater number of genes significantly altered (p_adj <0.05) vs cortex. (Spinal cord: N=4 P301S, N=4 control. Cortex: N = 4 P301S, N=3 Control).

5.2.4. Astrocyte activity-dependent genes are suppressed by neurodegeneration.

Given the marked neurodegeneration and synapse loss seen in FTD, I was interested in whether there was any consequence on synaptic activity-dependent astrocyte genes identified in chapters 3 and 4. I compared the expression of genes altered *in vivo* by 24h light with those changed in the P301S model. I found that astrocyte genes that are both up and down-regulated by light-exposure are significantly dysregulated in P301S vs WT spinal cord **(Figure 5.5).** Overall, these data present a picture of activity-dependent astrocyte genes being dysregulated following tauopathy-induced neurodegeneration.

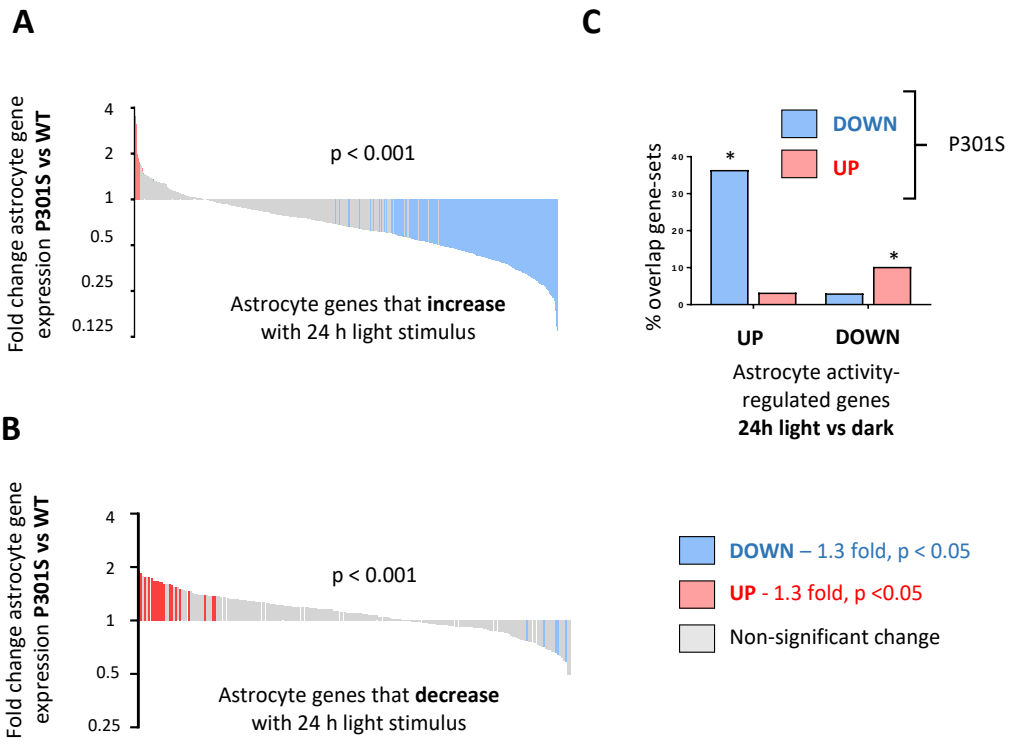

Figure 5.5 - Neuronal tauopathy drives changes to astrocyte activity-dependent genes. A. Activity-regulated astrocyte genes (upregulated by 24h light v dark exposure) are significantly down-regulated in the spinal cords of P301S mice at 20 weeks. **B.** Conversely, activity-suppressed genes (downregulated by 24h light v dark) are significantly increased in P301s vs wt spinal cord at 20 w. (N = 4 animals P301s and WT. Red and blue bars are significantly changed genes with deseq2 p_adj < 0.05. Overall p-value calculated using 2-way ANOVA). **C.** The data in A and B is re-presented as percentage overlap of gene-sets between genes up and down-regulated in P301S vs WT, with genes up and down-regulated by 24h light stimulus (***p<0.001 Fishers exact test).

5.2.5. Tauopathy induces reactive astrocytosis – promoting both neurotoxic “A1” and neuroprotective “A2” signatures.

Next, I investigated whether astrocytes in the P301S model demonstrated transcriptional changes for reactivity. In Zamanian *et al.*, 2012, reactive astrocyte transcriptional changes were profiled in response to two different acute injury models – lipopolysaccharide (LPS) injection and middle cerebral artery occlusion (MCAO). The Zamanian *et al.* study identified two distinct populations of reactive astrocytes along with their transcriptional signatures. “A1” astrocytes, found in response to LPS challenge, were shown to have a neurotoxic effect. A2 astrocytes, found to increase in response to MCAO, were neuroprotective. I identified genes that are considered specific cell-markers for A1 vs A2 astrocytes (Liddelow *et al.*, 2017), along with an expanded panel generated by considering genes that change > 4 fold to LPS stimulation (A1) or MCA injury (A2), which are not upregulated in the alternative set.

Table 5-2 - Reactive Astrocyte Genes: Genes that have been used in key papers (Liddelow *et al.*, 2017, Clarke *et al.*, 2018) as representing specific markers of reactive A1 and A2 astrocytes. List derived from Zamanian *et al*, 2012, as those that are highly upregulated (>7 fold) in response to both LPS and MCAO injury (pan-reactive), or selectively upregulated (>10 fold) to either LPS injury alone (A1) or MCAO injury alone (A2).

Pan-reactive	Gfap	S1pr3	Cxcl10	Serpina3n	Cp	Steap4	Lcn2
	Hspb1	Timp1	Osmr	Vim	Cd44	Aspg	
A1 Genes	H2-D1	Srgn	Ggta1	Fkbp5	Gbp2	C3	Amigo2
	H2-T23	Serping1	Iigp1	Psmb8	Fbln5	Ugt1a1	
A2 Genes	S100a10	Sphk1	Cd14	Tm4sf1	Ptgs2	Ptx3	Clcf1
	B3gnt5	Emp1	Tgm1	Cd109	Slc10a6		

Table 5-3 - Expanded panel of reactive astrocyte genes. Genes from Zamanian *et al*, 2012 that are upregulated >4 fold in response to LPS and MCAO injury (pan-reactive expanded), or either LPS injury alone (A1 expanded) or MCAO injury alone (A2 expanded).

Expanded Pan Reactive Panel	Galntl2	Tspan4	Rhoj	Serping1	Cp	Cd44	Cxcl2
	Mpa2L	Nek6	Cpne8	Hpgd	Timp1	Iigp1	Ifi202B
	Gfap	Vim	Serpina3N	Usp18	Cd14	Ggta1	Slc10A6
	S100A10	Cdkn1A	Gbp3	Oasl2	S1Pr3	Procr	Chil1
	Hspb6	Spp1	Tagln2	Lrg1	Cxcl10	Thbs2	Synpo
	Gap43	Sphkap	Aspg	Slc39A14	A2M	Osmr	Tgm1
	Ifitm3	Ier3	Cela1	Ptx3	Bcl3	Nt5E	
Expanded A1 Panel	C1S	Irgm1	Srgn	Il1R1	Tspo	Xaf1	Crispld2
	Fbl5	Kctd1	Dcn	Parp14	Sorbs1	Endou	Slc43A3
	Hsp1	Acsl5	Tgm2	Plin4	Gsr	Tapbpl	Slc1A5
	Il13Ra	Gpx3	Angpt1	Ifi44	H2-D1	H2-T23	C1Ra
	Pmsb8	Sulf2	Gbp2	Tgtp1	Tapbp	Amigo2	Tlr2
	Olfm1	Nfasc	Sema4C	H2-Q6	H2-K1	Fkbp5	Trim30A
	B2M	Igtp	Zc3Hav1	Saa3	Tnfaip2	Psmb9	H2-T10
	Ly6E	Slc22A4	Map3K6	Ugt1A1	Irgm1	C4B	C1Rb
Expanded A2 Panel	Agpat9	Gpx1	Fscn1	S100A11	Arpc1B	Anxa2	Nop58
	Cdbpd	Mrps6	Odc1	Gadd45A	Ctps	Tnfrsf12A	Plp2
	Chl4	S100A6	Klf6	Hmox1	Bcat1	Sphk1	Cav1
	Eii2	Asns	Txnrd1	Vgf	Tubb6	Fam129B	Dpysl3
	Hmga	Nhp2	Lmna	Eif1A	Anxa3	Prss23	Klhdc8A
	Jub	Esd	Ociad2	Gadd45B	Chac1	Ctgf	Tm4Sf1
	Lass6	Nupr1	Syt4	Lrrfip1	Col6A1	Msn	Klf5
	Odz2	Lgals1	Anxa7	Rnf19B	Hspb1	Mthfd2	Sbno2
	Tuba1A	Srxn1	Pcbp3	Camk2D	Ccnd1	Bdnf	Rnf125
	Zwint	Lrrc59	Mcl1	Litaf	Mest	Actn1	Gcnt2
	Uck2	Lgals3	Il13Ra1	Tlr4	Tgfbi	Vcan	Adam12
	Lonrf1	Slc7A1	Akap12	Pvr	Fosl1	Il6Ra	H19
	Tgif1	Adamts4	Ahr	Cdt1	Bdkrb2	Cdk6	Stx11
	Ecm1	Igfbp3	Adamts5	Sulf1	Spata13	Met	Clcf1
	Neto2	Akr1B8	Tmem74	Cacng5	Slc44A3	Gdf15	Flnc
	Anxa1	Socs3	Fosl2	Slc5A3	Col12A1	B3Gnt5	Hmga2
	Btg3	Flna	Gch1	Cyp1B1	Shisa6	Thbs1	Ifi203
	Nav2	Thbd	Nes	Pla2G4A	Emp1	Steap1	Pappa
	Grb10	Cd24A	Ahnak	Pde3B	Ahnak2	Fgl2	Eda2R
	Col6A2	Olfml3	Ptgs2	Lif	Ch25H	Il6	Ccl2
	Serpine1						

I used the above gene-panels to investigate how the reactivity profile of astrocytes change in response to P301S induced tauopathy. Pan-reactive markers are significantly upregulated in P301S cortex and spinal cord at 20 weeks **(Figure 5.6A)**. I found that in P301S spinal cord there is a significant increase in both A1 and A2 transcriptional signatures. In P301S cortex, the changes are much less marked. In the cortex, there is a significant increase in A2 markers but A1 markers but do not achieve significance as a group **(Figure 5.6 B, C)**.

One of the key pathways considered to form part of the neuroprotective A2 response is the upregulation of astrocyte antioxidant capacity. Indeed two key Nrf2-target antioxidant genes *Hmox1* and *Srxn2* are part of the expanded panel of A2 genes. Utilising a panel of Nrf2 activator genes that have been identified to be Nrf2 responsive (work in the Hardingham lab utilising Nrf2 KO mice), I found a marked Nrf2 activation signature in the P301S mouse **(Figure 5.6D)**.

Taken together, these data demonstrate that astrocytes in the P301S model undergo transcriptional changes consistent with reactivity. They demonstrate upregulation of both neurotoxic and neuroprotective transcriptional signatures, including evidence for upregulation of the Nrf2 responsive antioxidant gene-response.

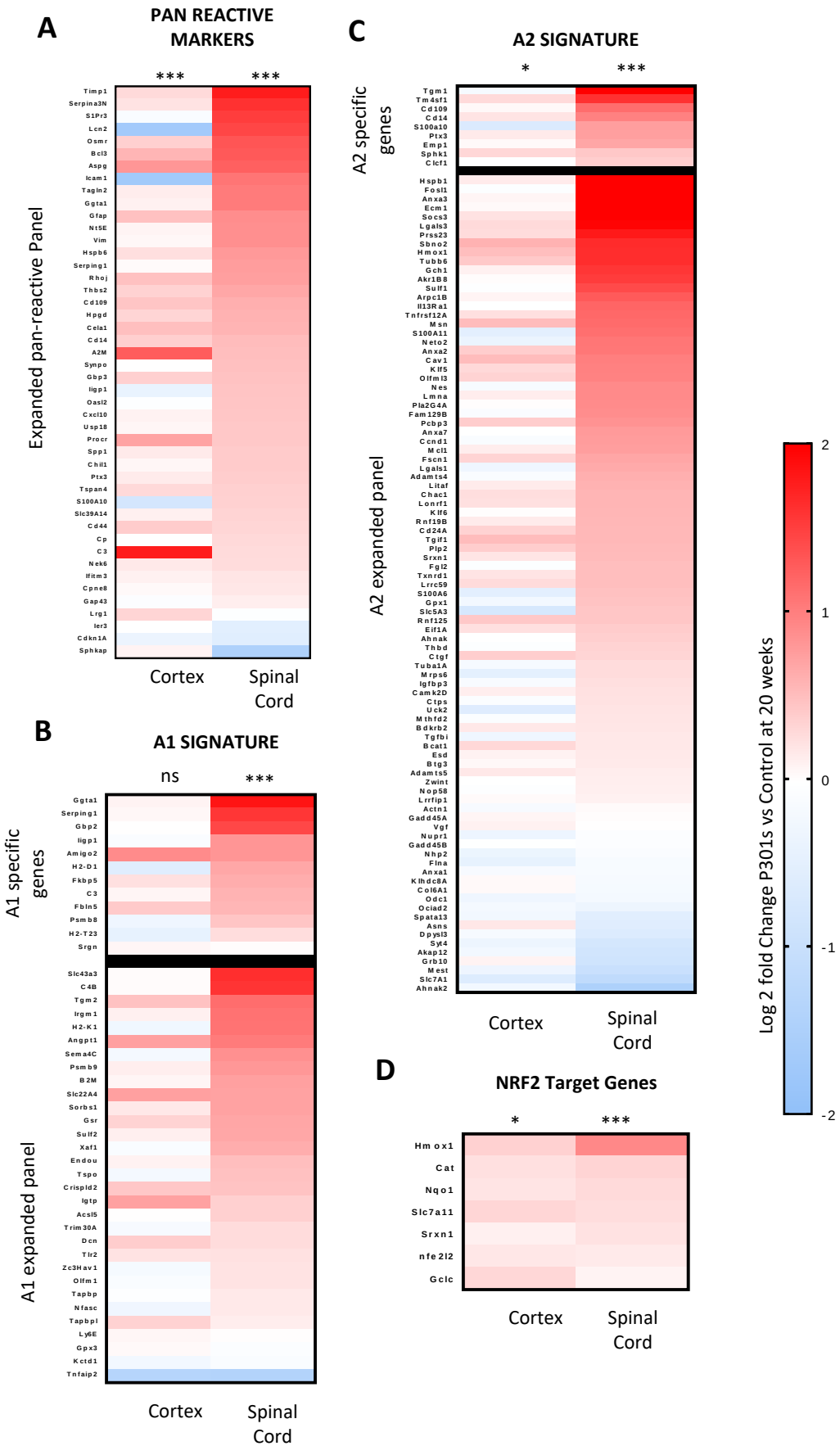
A
PAN REACTIVE MARKERS
***
***
Expanded pan-reactive Panel
Timp1
Serpina3N
S1Pr3
Lcn2
Osmr
Bcl3
Aspg
Icam1
Tagln2
Ggta1
Gfap
Nt5E
Vim
Hspb6
Serping1
Rhoj
Thbs2
Cd109
Hpgd
Cela1
Cd14
A2M
Sympo
Gbp3
Iigp1
Oasl2
Cxcl10
Usp18
Procr
Spp1
Chil1
Ptx3
Tspan4
S100A10
Slc39A14
Cd44
Cp
C3
Nek6
Ifitm3
Cpne8
Gap43
Lrg1
Ier3
Cdkn1A
Sphkap
Cortex
Spinal Cord
B
A1 SIGNATURE
ns
***
A1 specific genes
Ggta1
Serping1
Gbp2
Iigp1
Amigo2
H2-D1
Fkbp5
C3
Fbln5
Psmb8
H2-T23
Srgn
A1 expanded panel
Slc43a3
C4B
Tgm2
Irgm1
H2-K1
Angpt1
Sema4C
Psmb9
B2M
Slc22A4
Sorbs1
Gsr
Sulf2
Xaf1
Endou
Tspo
Crispld2
Igtp
Acsl5
Trim30A
Dcn
Tlr2
Zc3Hav1
Olfm1
Tapbp
Nfasc
Tapbpl
Ly6E
Gpx3
Kctd1
Tnfaip2
Cortex
Spinal Cord
C
A2 SIGNATURE
*
***
A2 specific genes
Tgm1
Tm4sf1
Cd109
Cd14
S100a10
Ptx3
Emp1
Sphk1
Clcf1
A2 expanded panel
Hspb1
Fosl1
Anxa3
Ecm1
Socs3
Lgals3
Prss23
Sbno2
Hmox1
Tubb6
Gch1
Akr1B8
Sulf1
Arpc1B
Il13Ra1
Tnfrsf12A
Msn
S100A11
Neto2
Anxa2
Cav1
Klf5
Olfml3
Nes
Lmna
Pla2G4A
Fam129B
Pcbp3
Anxa7
Ccnd1
Mcl1
Fscn1
Lgals1
Adamts4
Litaf
Chac1
Lonrf1
Klf6
Rnf19B
Cd24A
Tgif1
Plp2
Srxn1
Fgl2
Txnrd1
Lrrc59
S100A6
Gpx1
Slc5A3
Rnf125
Eif1A
Ahnak
Thbd
Ctgf
Tuba1A
Mrps6
Igfbp3
Camk2D
Ctps
Uck2
Mthfd2
Bdkrb2
Tgfbi
Bcat1
Esd
Btg3
Adamts5
Zwint
Nop58
Lrrfip1
Actn1
Gadd45A
Vgf
Nupr1
Gadd45B
Nhp2
Flna
Anxa1
Klhdc8A
Col6A1
Odc1
Ociad2
Spata13
Asns
Dpysl3
Syt4
Akap12
Grb10
Mest
Slc7A1
Ahnak2
Cortex
Spinal Cord
D
NRF2 Target Genes
*
***
Hmox1
Cat
Nqo1
Slc7a11
Srxn1
nfe2l2
Gclc
Cortex
Spinal Cord
Log 2 fold Change P301s vs Control at 20 weeks
2
1
0
-1
-2

Figure 5.6 - P301S tauopathy induces a pan-reactive astrocyte signature, consisting of both A1 neurotoxic and A2 neuroprotective responses. A. Spinal cord and cortex from P301S mouse demonstrates upregulation of pan-reactive astrocyte markers. (***p<0.001, 2-way ANOVA) **B.** Astrocytes from p301S spinal cord demonstrate significant upregulation of A1-specific genes as well as an expanded A1 panel. Cortex is tending towards upregulation but does not achieve significance. (Ctx: p = 0.37, *** p <0.001, 2-way ANOVA). **C.** Both cortex and spinal cord astrocytes from p301S mice demonstrate significant upregulation in A2 transcriptional signatures (*p = 0.04, *** p < 0.001, 2-way ANOVA). **D.** P301S tauopathy boosts Nrf2 target genes in both cortex and spinal cord (*p = 0.012, *** p < 0.001, 2 way ANOVA).

5.2.6. Transcriptional and synaptic changes in the P301S mouse precede functional loss.

The transcriptional changes described above represent the end-stage of neurodegenerative disease. Work from our lab has demonstrated that synapse and neuronal loss precede motor-deficits in the P301S model and can be detected as early as 12 weeks.

Therefore I investigated whether the transcriptional changes were present at the earlier time point of 12 weeks and how these compared to those seen in later disease. This knowledge would be important with regards to timing interventions for reversing and influencing disease trajectories. RNA was extracted from motor cortex from P301S mice at 12 weeks of age and gene-expression analysed with RNA-sequencing. This revealed cortical transcriptional changes (total RNA) at 12 weeks, which precedes functional impairment(**Figure 5.7A)**. Cortex transcriptional changes at 12 weeks correlate well with transcriptional changes found in the cortex at 20 weeks (**Figure 5.7B)**.

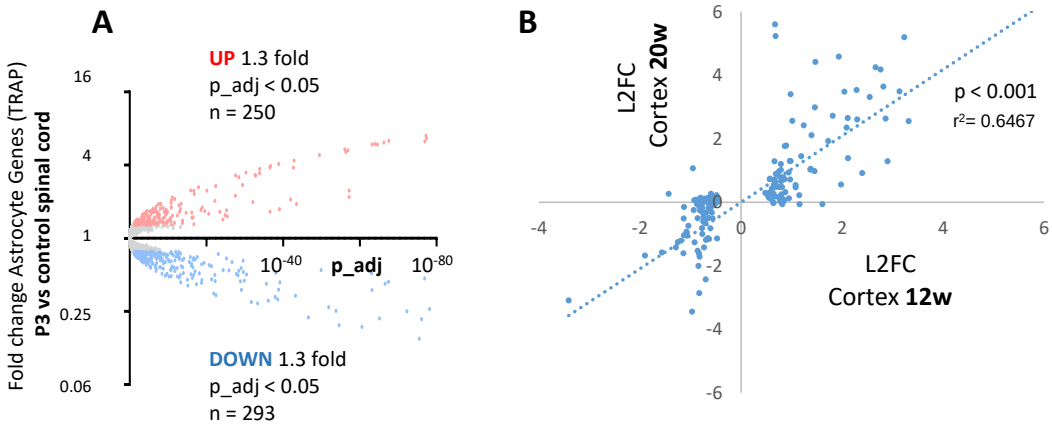

Figure 5.7 - Transcriptional changes observed in the P301S cortex at 12 weeks. A. RNA-sequencing reveals changes in multiple genes at 12 weeks in the cortex. **B.** Genes that are changed at 12 weeks correlate well with cortex genes that are found to be changed in the cortex at 20 weeks ($p<0.001$, Spearman's rank correlation. Cortex 20 weeks: N = 3 Control, N= 4 P301S, Cortex 12 weeks: N = 3 P301S, N = 6 Control).

5.2.7. Nrf2 over-expression reverses transcriptional and functional consequences of tauopathy.

A key element of the neuroprotective response upregulated in astrocytes in the P301S mouse was the increase in Nrf2 target gene-expression. These genes form part of the A2 neuroprotective response and are involved in increasing astrocyte antioxidant capacity – a key cyto-protective pathway in the brain.

We hypothesised that this response represented an adaptive-protective response by astrocytes, but that it was insufficient or too late to confer total neuroprotection. Subsequently progressive tau accumulation and inflammation in end-stage disease induces a switch towards a more neurotoxic A1 phenotype which worsens neurotoxic effects.

Therefore we set out to investigate whether boosting the adaptive-protective astrocyte Nrf2 response might confer neuroprotective benefit. This was achieved by crossing the P301S transgenic mouse with the GFAP-Nrf2 transgenic line. This line over-expresses Nrf2 specifically in astrocytes driven by the GFAP promoter. GFAP is a marker of astrocyte reactivity, ensuring that the Nrf2 response is focused on areas of neurodegeneration.

We confirmed successful upregulation of antioxidant gene expression in the cortices of P301S-Nrf2 mice **(Figure 5.8)**. Nrf2 over-expression does not change the levels of tau or total astrocyte numbers in P301S mice, but there is a reduced level of GFAP positive cells (**Appendix Figure 7.4A**).

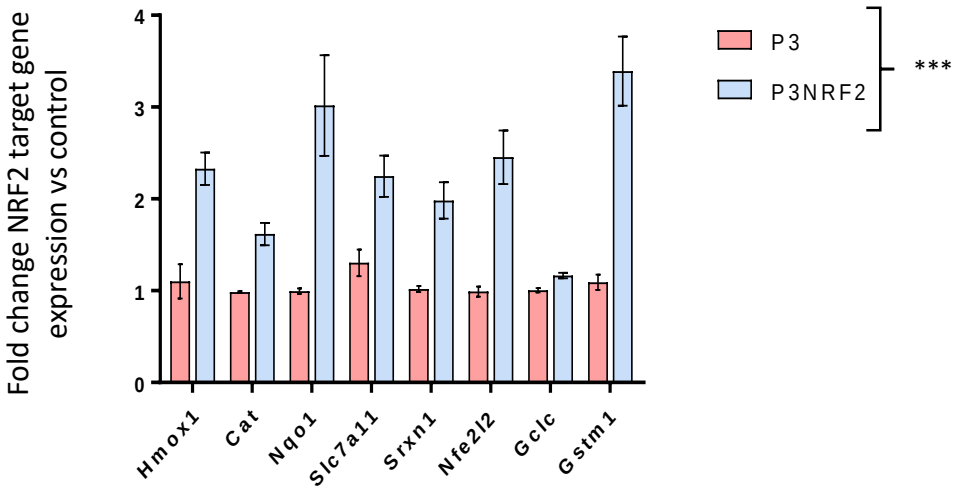

Figure 5.8 - P301S mice crossed with the GFAP-Nrf2 line upregulate expression of Nrf2 antioxidant target genes in the cortex. Levels of known Nrf2 target genes were measured in the cortex of P301s mice vs P301S-Nrf2 mice. As expected, there was a significant increase in antioxidant target gene expression (P301S: N=3, P301S-Nrf2: N=5 ***p<0.001 2-way ANOVA).

Strikingly, we found that over-expressing Nrf2 in astrocytes in P301S mice strongly reversed the transcriptomic changes seen vs WT mice (**Figure 5.9 A, B)**. Many genes that are upregulated or down-regulated by tauopathy-induced neurodegeneration in the CNS demonstrated a rescue in their expression in P301S mice crossed with GFAP-Nrf2. Selected genetic markers involved in neurogenesis and synaptogenesis, which are found to be down-regulated in P301S vs wt cortex, are restored **(Figure 5.9 C)**. Genes that are dyregulated and overlap between human FTD and P301S datasets are also restored by over-expression of Nrf2 **(Figure 5.10**).

Finally, we confirmed that the rescue of transcriptional changes translated into a functional rescue in P301S mice. Nrf2-expressing P301S mice had significantly reduced neuronal loss **(Appendix Figure 7.5A)** and Nrf2 over-expression led to a delay in the development of functional deficit, as assessed by grip-strength testing **(Appendix Figure 7.5B)**.

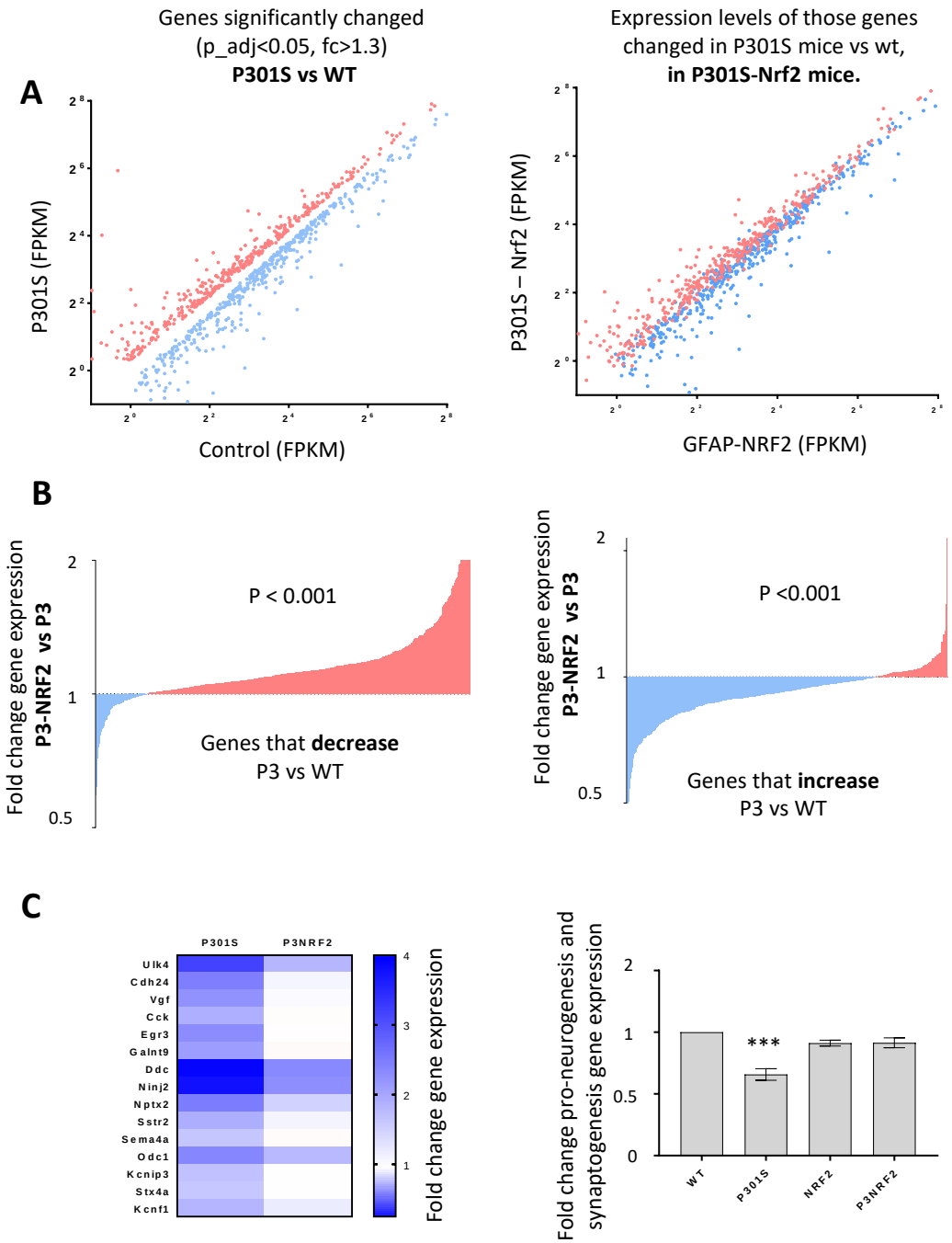
A
Genes significantly changed
(p_adj<0.05, fc>1.3)
P301S vs WT
P301S (FPKM)
Control (FPKM)
Expression levels of those genes
changed in P301S mice vs wt,
in P301S-Nrf2 mice.
P301S – Nrf2 (FPKM)
GFAP-NRF2 (FPKM)
B
Fold change gene expression
P3-NRF2 vs P3
P < 0.001
Genes that decrease
P3 vs WT
P <0.001
Genes that increase
P3 vs WT
C
P301S
P3NRF2
Ulk4
Cdh24
Vgf
Cck
Egr3
Galnt9
Ddc
Ninj2
Nptx2
Sstr2
Sema4a
Odc1
Kcnip3
Stx4a
Kcnf1
Fold change gene expression
Fold change pro-neurogenesis and
synaptogenesis gene expression
***
WT
P301S
NRF2
P3NRF2

Figure 5.9 - Over-expression of astrocyte-specific Nrf2 reverses transcriptional changes induced by p301S tauopathy. A Expression of genes that are significantly upregulated or downregulated (1.3 fold change, p_adj <0.05) in P301S vs WT are reversed in P301S-NRf2 mice. **B.** Nrf2 overexpression significantly reverses genes that are upregulated or down-regulated in P301S mice vs wild-type (***p<0.001 - 2-way ANOVA, control: N= 6, P301S: N = 3, P301S-Nrf2: N = 5). **C** Nrf2-overexpression boosts a large number of genes related to synaptogenesis and neurotrophic effects that are suppressed P301S vs WT (***p<0.001 2-way ANOVA with multiple comparisons).

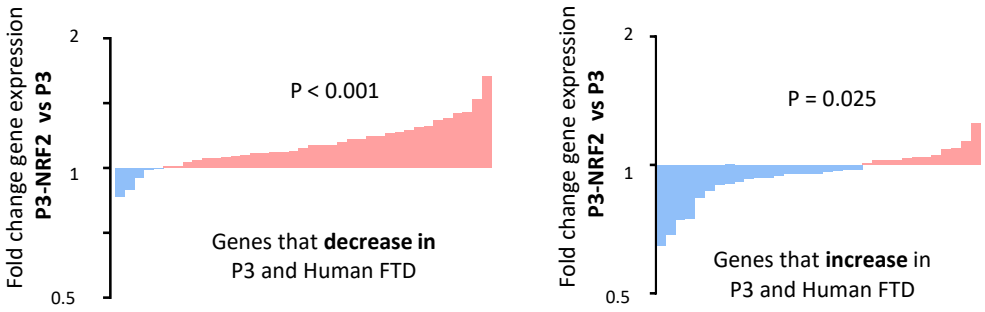

Figure 5.10 - Genes that are found to be changed in both human FTD samples and p301S mice are also genes that are found to be rescued by Nrf2 over-expression. The subset of genes that are upregulated (**A)** and downregulated **(B)** in both human FTD samples and P301S cortex at 12 weeks are significantly rescued by over-expression of astrocyte Nrf2 (P301S: N = 3, P301S-Nrf2 N=5: 2-way ANOVA).

5.3. Chapter Discussion

5.3.1. Tauopathy-induced neurodegeneration is associated with wide-spread CNS transcriptional changes.

In this chapter, I have described the transcriptional changes that occur in response to tauopathy-induced neurodegeneration, in both total CNS tissue and specifically in astrocytes.

In the P301S mouse model, by 20 weeks there is extensive neuronal cell death and neurodegeneration in the spinal cord and superficial frontal motor cortical areas. As expected, these pathological changes were associated with wide-spread transcriptional changes. The most marked signature was that associated with inflammation. Microglia-specific genes were the largest number changed and gene-ontology analysis revealed upregulation of several gene-sets associated with inflammatory pathways. This fits with current theories regarding the key role for inflammation and microglial activation at the end-stage of FTD (Zhang, 2015).

We also examined the changes that occur in human FTD samples taken post-mortem compared to non-affected samples. We found a strong correlation with transcriptional changes seen in the P301S model with changes found in post-mortem tissues. This strong transcriptional overlap gives confidence that the P301S transgenic mouse model recapitulates key pathological processes that occur in human tauopathy and FTD, and supports using it in the studies outlined in this chapter.

5.3.2. Neurodegeneration promotes a reactive astrocyte transcriptional signature consisting of both A1 and A2 responses.

The studies in this chapter also uncovered how neuronal tauopathy induces wide-spread astrocyte-specific transcriptional changes. A key finding was that many of the activity-dependent genes described in previous chapters are dysregulated following neurodegeneration. These gene sets are also found to be altered in old vs young mice. Activity-dependent astrocyte genes may become altered due to surrounding neuronal death and a possible reduction in the activity-mediated signals from neurons. It may also be that reactive astrocytes become less responsive to activity-dependent signals. As many of the activity-dependent genes found previously were shown to be important for CNS homeostatic processes, such as metabolism, it is likely that dysregulation of these pathways may impair the homeostatic processes in the CNS. This may in turn make the tissue more vulnerable and increase subsequent neuronal death.

Consistent with the current understanding of astrocytes becoming more reactive in disease, we found that astrocytes in the P301S model demonstrate an increase in a large number of reactivity-associated genes. We have extended this understanding and characterised the nature of this reactive response, demonstrating how the balance of neurotoxic A1 vs neuroprotective A2 responses is influenced during the course of the disease process.

Our studies reveal that neurodegeneration boosts both neurotoxic A1 and neuroprotective A2 reactive astrocyte responses. In the spinal cord, the area of greatest neurodegeneration, there is an upregulation of both A1 and A2 signatures. In the cortex, where there is less neurodegeneration, there is an upregulation of A2 but not A1 signatures. One explanation for this is that the cortex represents an earlier time-point of neurodegeneration vs the spinal cord. A2 responses may be enhanced first, conferring an element of neuroprotection in early disease. However, following increased cell-death and increased inflammation, astrocytes switch to an A1 response. This enhances neurotoxic effects and worsens end-stage neurodegeneration. An important caveat to the above finding is that the sample numbers for cortex are less than for spinal cord, and this may influence the total number of significant genes identified. We are currently obtaining further samples and performing further experiments to test the above hypothesis by looking at the A1 vs A2 signatures in cortex and spinal cord at earlier time-points.

5.3.3. Boosting Nrf2 activity in astrocytes confers neuroprotective effect.

We found that a key constituent of the A2 response in the P301S mouse was upregulation of the Nrf2 antioxidant response. Antioxidant capacity is a key protective role of astrocytes and dysregulation of antioxidant pathways is

thought to also play a key role in the end-stage processes of multiple neurodegenerative diseases.

We hypothesised that boosting the antioxidant aspect of the A2 protective response would confer neuroprotection. We therefore crossed the P301S line with the GFAP-Nrf2 transgenic mouse line. By coupling Nrf2 activation to the GFAP promoter, we achieved both astrocyte-specificity as well as ensuring that the greatest Nrf2 action occurs in reactive astrocytes at the site of neurodegeneration. Over-expressing Nrf2 in this manner led to reduced reactive changes in the CNS, and reversed not only many of the transcriptional changes seen in P301S mice, but also protected against neuronal loss and achieved functional improvement. Mice exhibited a significant delay in functional performance deterioration as measured by horizontal bar testing between 18-20 weeks.

Therefore, we have demonstrated that boosting astrocyte-specific Nrf2 offers neuroprotective benefits in this model of FTD. This is particularly interesting given that in this model tau is expressed in a neuron-specific manner, and demonstrates the importance of non-cell autonomous interactions in promoting neuronal resilience.

5.3.4. Limitations

It is important to acknowledge the limitations of the P301S transgenic mouse as a model for FTD. Firstly, the model is based on the overexpression of a single mutant *tau* gene. Overexpression models lead to very severe and rapid disease,

which is different from the typically slower and insidious onset of real dementia. Furthermore in the P301S model, the area most affected is the spinal cord. This contrasts to human FTD where the main pathological brain region is the frontal cortex. However, it is becoming increasingly recognised that FTD overlaps with spinal cord diseases such as ALS. The difference in regional expression in our model arises from the expression of tauopathy being driven by the Thy1.2 promoter, which induces this in all neurons throughout the CNS, with disease coming on earlier in the spinal cord. This contrasts to FTD which exhibits frontal-cortex specific onset of tau-accumulation.

However, despite these weaknesses, the P301S mouse is a powerful model in that it provides a model of region-specific, progressive neurodegeneration. The correlation found in transcriptomic changes with actual human post-mortem FTD samples gives confidence in utilising this model to answer the specific questions that I have set out to address in this chapter.

5.3.5. Chapter Conclusion

In this chapter, I have used the P301S transgenic mouse model of human tauopathy to describe how neurodegeneration drives wide-spread changes in astrocyte transcription. These changes include dysregulation of synaptic-activity regulated genes, and upregulation of both neurotoxic A1 and neuroprotective A2 reactive responses. Finally I have described how enhancing a key aspect of the A2 response – upregulation of astrocyte Nrf2-mediated cytoprotective antioxidant function – confers neuroprotection and delays disease progression.

Chapter 6

General Discussion

6.1. Overview of aims accomplished

The aim of the work described in this thesis was to understand how astrocyte transcription and function are controlled by neuronal interactions in both normal physiology and following neurodegenerative disease.

I first described how synaptic activity induces wide-spread transcriptomic changes in astrocytes and demonstrated that these lead to an increase in the ability of astrocytes to utilise glucose to produce lactate, which can be used as a fuel for neurons. This couples astrocyte glycolytic ability to neuronal metabolic demands and uncovers a novel pathway by which neurons are able to tune astrocytes to regulate metabolic homeostasis in the neuroglial unit.

I then described the capacity of synaptic activity to regulate astrocyte transcription *in vivo* and investigated how anaesthesia (a potent suppressor of neuronal activity) leads to widespread dysregulation of neuronal and astrocyte transcription. Transcriptional changes during anaesthesia induce a pro-vulnerability signature, which may contribute towards neuronal vulnerability in the perioperative period.

Subsequently I investigated the consequences of neurodegeneration on astrocyte transcription and phenotype. Using a transgenic mouse model of human tauopathy, I described how neurodegeneration alters astrocyte transcriptional phenotype. I found that the transcriptional response of astrocytes to neurodegenerative disease is complex and heterogeneous, with

upregulation of both neurotoxic and neuroprotective responses. Finally, I demonstrated that boosting a key aspect of the neuroprotective response (activation of the Nrf2 cytoprotective antioxidant pathway) in astrocytes enabled transcriptional and functional rescue in this neurodegeneration model.

6.2. Contribution to existing knowledge

The studies outlined in this thesis add to the growing understanding of the role of glia and non-cell autonomous signalling in the CNS in regulating homeostasis in health, and describe how these pathways are dysregulated in disease. This includes contributing towards published work which was the first complete description of how synaptic activity influences astrocyte transcription (Hasel *et al.*, 2017). A recently study published (Hrvatin *et al.*, 2018), utilising single-cell sequencing of activity-dependent responses of all neural cell-types in the visual cortex, has described a limited number of astrocyte genes changing in response to light- stimulus. The *in vivo* studies in this thesis complement this dataset and are the first studies *specifically* investigating how astrocytes alter transcriptional pathways in response to neuronal stimuli. Our methodology has revealed many more transcriptional targets in astrocytes that are altered by synaptic activity (1333 in our study vs total of 24 in Hrvatin *et al.*, 2018).

We have also established a detailed profile of transcriptional changes that occur within the CNS and specifically in astrocytes in response to end-stage neurodegeneration. The concept of astrocytes being both neurotoxic and

neuroprotective is an emerging idea (Liddelow and Barres, 2017). Here, we demonstrate that the astrocyte response to disease is complex with upregulation of both neurotoxic and neuroprotective responses. We have also described the novel finding that promoting elements of the astrocyte A2 protective response are able to confer neuroprotective benefit in FTD – a finding that complements studies that have found boosting Nrf2 (in astrocytes or total CNS) enhances neuroprotection in other different neurodegenerative disease models, including multiple sclerosis (Bomprezzi, 2015), amyotrophic lateral sclerosis (Vargas *et al.*, 2008) and Parkinson's disease (Jakel *et al.*, 2007).

6.3. Implications for future therapeutic benefit

The ultimate purpose of the studies in this thesis is to contribute towards our understanding of how homeostatic and resilience pathways in the brain are disrupted in dementia, with a hope that this understanding may contribute towards the development of future therapies. The studies in this thesis have highlighted some key putative pathways that form attractive therapeutic targets.

The astrocyte CREB pathway appears to regulate astrocyte activity-dependent responses. The studies in this thesis have described how these activity-dependent pathways are dysregulated with ageing and in neurodegeneration. Therefore targeting this transcriptional pathway may maintain and boost homeostatic pathways in the brain and enhance resilience during disease.

The CREB pathway can be enhanced by drugs that target the cAMP pathway, including forskolin and phosphodiesterase inhibitors. In fact, targets of cAMP pathway have already been studied in clinical trials for a range of CNS diseases. Rolipram (a selective type-4 PDE) was developed as an antidepressant but failed phase 3 trials due to severe nausea and gastrointestinal side-effects (Fleischhacker *et al.*, 1992). Cilostazol (a PDE3 inhibitor) is currently being tested as part of the LACI-2 clinical trial for SVD induced dementia (http://www.isrctn.com/ISRCTN14911850). Within this study, the rational for using this drug is for cerebral vasculature modulation. PDE-3A is actually expressed highest in astrocytes and given the findings in this thesis, it may be that any benefit conferred may be via enhancement of astrocyte pathways.

In this thesis, I have also described preliminary studies utilising non-invasive transcranial electrical stimulation (NTES) to boost CNS activity and to reverse transcriptional changes seen during anaesthesia. NTES has already been utilised in a number of clinical studies investigating whether it confers benefit in depression, schizophrenia and Parkinson's disease (Bennabi *et al.*, 2014). Therefore it would be interesting to investigate if this methodology could offer clinical benefit to boost CNS resilience pathways acutely in vulnerable patients undergoing sedative anaesthesia, and longer-term in neurodegenerative disease.

Finally, I described how enhancing astrocyte Nrf2 expression confers neuroprotection in the P301S model of tauopathy. Whilst these findings will

need to be confirmed in other models, they highlight Nrf2 as a putative target that could alter disease trajectory in FTD.

Targeting the astrocyte-specific Nrf2 pathway has been shown to confer protection in other neurodegenerative diseases including the SOD1 model of ALS (Vargas *et al.*, 2008) and in a - 6-hydroxydopamine injection model of Parkinsonism (Jakel *et al.*, 2007). Targeting Nrf2 in the clinical context has been difficult. Many activators are electrophilic compounds and hence extremely toxic, and have poor permeability of the blood brain barrier. However, more recent classes of drugs have been developed (for example triterpenoid-based compounds such as 2-cyano-3,12-dioxooleana-1,9-dien-28-oic acid (CDDO)) which have less toxic effects. Examples of current Nrf2 based therapeutics or those undergoing clinical trials include: Dimethylfumerate(DMF) for multiple sclerosis (Bomprezzi, 2015), omaveloxolone for Fredreich's ataxia (Trial number: NCT02255435) and Cu^{II}(atsm) for Parkinsons disease (Trial number: NCT03204929). The studies in this thesis are the first to highlight the utility of targeting astrocyte antioxidant pathways as way of conferring neuroprotection in dementia.

6.4. Limitations of studies and proposed future work

One of the key limitations of the studies outlined in this thesis, is that they consider transcriptomic changes in astrocytes pooled from a large number of cells. Therefore, this approach treats all astrocytes as exhibiting the same

response to a specific injury or insult. Therefore this approach has not allowed me to determine the number, arrangement and organisation of any distinct astrocyte populations within our experiments.

This can be resolved using a number of methodologies. Single-cell sequencing will reveal whether there are distinct astrocyte populations in the disease models used, and spatial transcriptomic approaches will allow probing of the anatomical distribution of these cells. Finally using fluorescence in-situ hybridisation (FISH) and RNAscope will allow specific cell-populations of astrocytes to be identified. We are currently carrying out these investigations to address this gap in our understanding.

Finally, this thesis has focused on neuron-astrocyte interactions. However, it is important to consider that astrocytes have interactions with all CNS cell-types, including microglia, oligodendrocytes, pericytes and brain endothelial cells. It is likely that there are yet-unstudied interactions between all these cell-types that regulate CNS homeostasis, and have a role to play in CNS dysfunction in disease. These complex interactions will only be understood through novel methodologies exploiting a combination of approaches. Example methods include TRAP-reporter mice driven by specific promoters for the above cell-types, as well as novel cell-type sequencing and proteomic approaches. Understanding the total cell-autonomous and non-cell autonomous interactions between the different cell-types in the brain and how these are disrupted in disease is a complex and challenging task. However, it would be

hoped that a more complete understanding of these signals would reveal key pathways that could be targeted to protect the brain and improve outcomes for patients with dementia.

6.5. Thesis conclusion

In this thesis, I have described studies demonstrating how astrocyte transcription is controlled by neuronal signals to regulate CNS metabolic homeostasis in health, and how astrocyte transcription is altered in a model of dementia. These involve transcriptional changes to both neuroprotective and neurotoxic astrocyte pathways and I have demonstrated that boosting beneficial astrocyte-functions confers neuroprotective benefit.

Dementia research has traditionally focused on neuronal pathology. Taken together, the studies in this thesis support emerging interest in also targeting non-neuronal cells for therapeutic benefit in neurodegenerative disease.

Chapter 7 Appendix

7.1. Supplementary Figures

7.1.1. Electrophysiological confirmation of enhanced neuronal firing achieved with pharmacological paradigm.

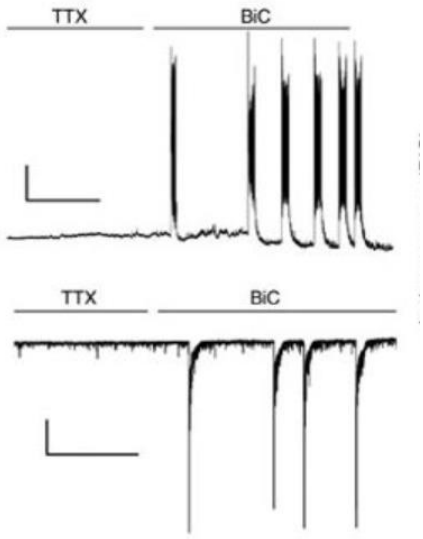

Figure 7.1 (Appendix) - Data collected by Sean Mackay. Figure from Hasel *et al.*, 2017. Sample trace showing effects of TTX and bicuculline (BiC) stimulation on neuronal firing. Cocultured cells were incubated overnight in tetrodotoxin (TTX), to block neuronal firing. Cells were then washed in the presence BiC. Whole-cell current-clamp (upper) and voltage-clamp (lower) recording of neurons exposed to this paradigm confirms resultant increase in burst activity. Scale bar, 15 mV, 30 s (upper); 50 pA, 30 s (lower)

7.1.2. Transcriptomic changes between GFAP-NRF2 and WT mice.

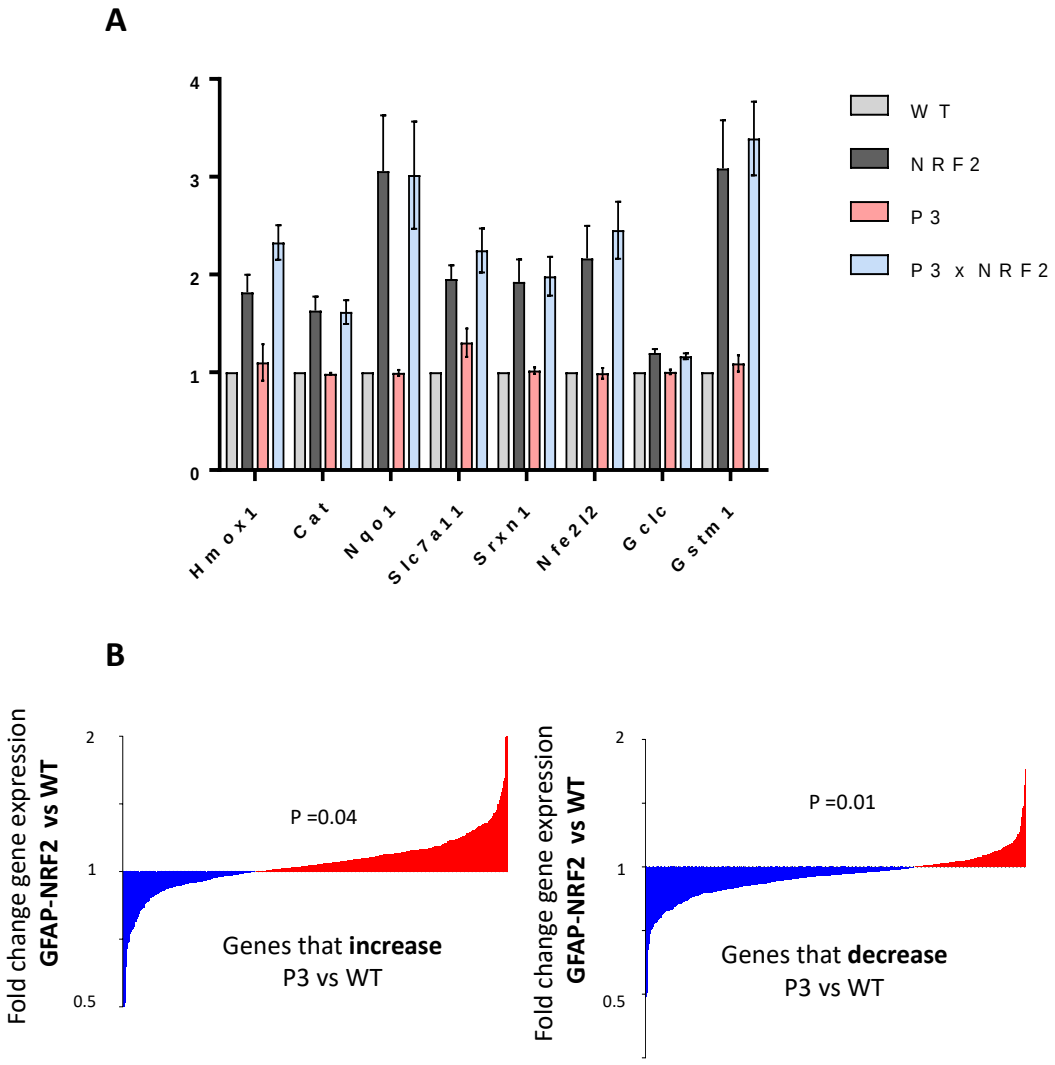

Figure 7.2 (Appendix) - Transcriptional Changes between GFAP-Nrf2 and WT controls. A. P301SxGFAP-Nrf2 mice demonstrate similar upregulation of Nrf2 target genes as GFAP-Nrf2 mice. **B.** GFAP-Nrf2 vs WT expression of genes changed in P301S vs WT mice. This confirms that the rescue of genes seen in the P301S mouse is not simply due to upregulation or downregulation of genes due to Nrf2 expression, but represents a rescue from the P301S effects. In fact, expression of Nrf2 alone changes genes that are found to be disrupted in P301S vs wt in the same direction (WT N=6; GFAP-Nrf2 N = 5; 2-way ANOVA).

7.1.3. Time-course of synapse and neuronal loss in the P301S model

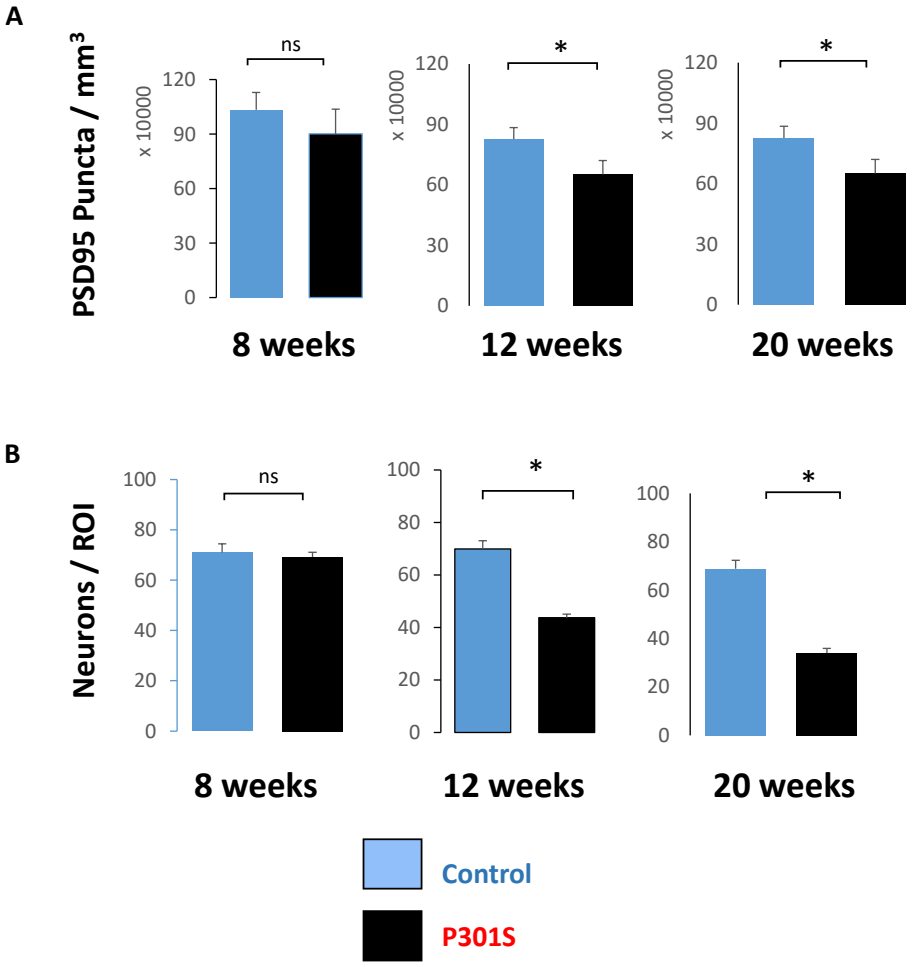

Figure 7.3 (Appendix) - Time-course of synapse and neuronal loss in the P301S human tauopathy model. Data collected by Sachin Tiwari. A. P301S transgenic mouse exhibits synapse loss at 12 weeks before functional changes. P301S mice were crossed with GFP-PSD95 transgenic line and PSD95 puncta counted. **B.** Neuronal loss begins at 12 weeks - assessed by NeuN staining and counting of neurons (* $p<0.05$, unpaired t-test).

7.1.4. Changes to tau-levels and astrocyte numbers with Nrf2-over-expression in the P301S model.

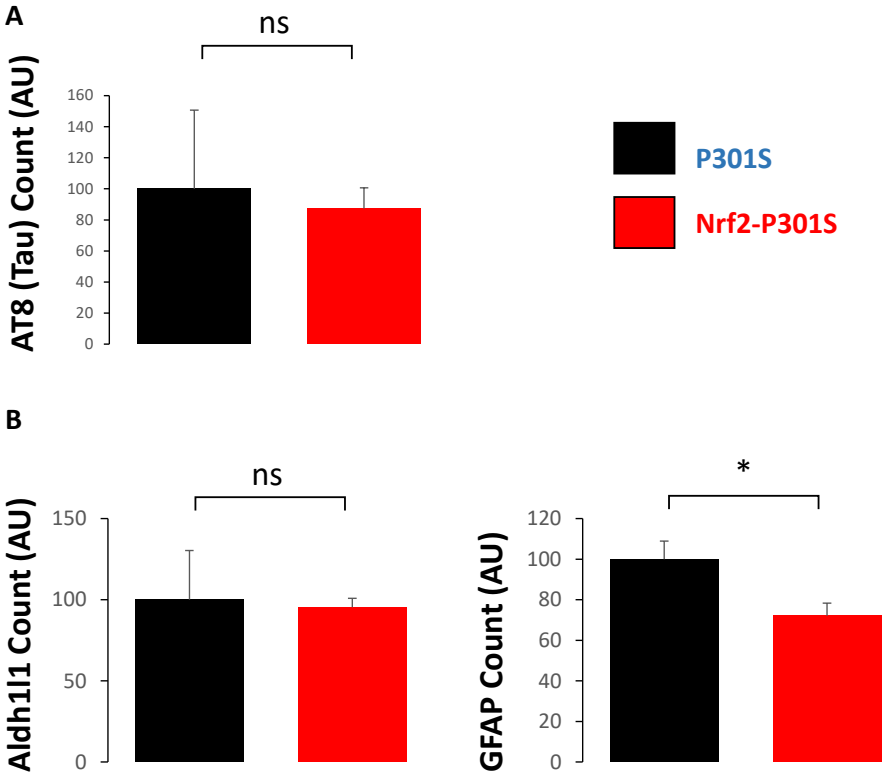

Figure 7.4 (Appendix) - Effects of Nrf2 over-expression on tau expression and astrocyte cell-numbers at 12 weeks in the P301S model. Data collected by Sachin Tiwari. Over-expression of Nrf2 does not change total tau staining (assessed by AT8 antibody staining) or total astrocyte numbers (assessed by staining with anti-Aldh1l1 staining). Total number of reactive astrocytes (using GFAP staining) are reduced (*$p<0.05$, unpaired t-test).

7.1.5. Rescue of neuronal and functional loss by Nrf2 over-expression in the P301S model.

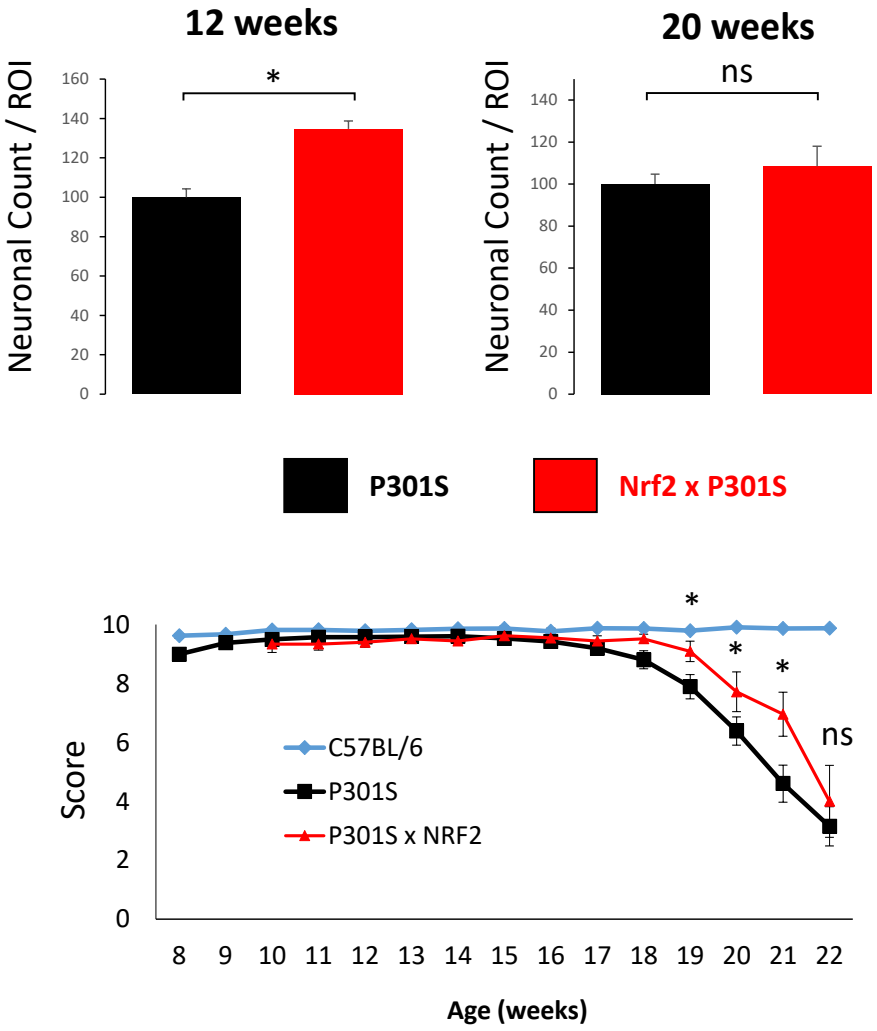

Figure 7.5 (Appendix) - Nrf2 over-expression rescues neuronal and functional loss in the P301S transgenic model. Data collected by Sachin Tiwari and Megan Torvell. A. Neuron number assessed by NeuN staining and counting. P301S mice demonstrate significantly greater neuronal numbers at 12 weeks with astroctye-Nrf2 over-expression. Differences are the same at 20 weeks. **B.** Astrocyte-Nrf2 over-expression rescues functional deficits in the P301S mouse at 18-21 weeks as assessed by horizontal bar strength-testing (*p<0.05).

Bibliography

Abbott, N. J. (2002) 'Astrocyte-endothelial interactions and blood-brain barrier permeability.', *Journal of anatomy*, 200(6), pp. 629–38.

Agulhon, C., Fiacco, T. A. and McCarthy, K. D. (2010) 'Hippocampal short- and long-term plasticity are not modulated by astrocyte Ca2+ signaling', *Science*, 327(5970), pp. 1250–1254.

Akiyama, H. *et al.* (2000) 'Cell mediators of inflammation in the Alzheimer disease brain.', *Alzheimer disease and associated disorders*, 14 Suppl 1, pp. S47-53.

Allen, B. *et al.* (2002) 'Abundant tau filaments and nonapoptotic neurodegeneration in transgenic mice expressing human P301S tau protein.', *The Journal of neuroscience : the official journal of the Society for Neuroscience*, 22(21), pp. 9340–51.

Allen, N. J. *et al.* (2012) 'Astrocyte glypicans 4 and 6 promote formation of excitatory synapses via GluA1 AMPA receptors.', *Nature*, 486(7403), pp. 410–4.

Allen, N. J. and Barres, B. A. (2009) 'Neuroscience: Glia — more than just brain glue', *Nature*, 457(7230), pp. 675–677.

Allen, N. J. and Eroglu, C. (2017) 'Cell Biology of Astrocyte-Synapse Interactions', *Neuron*, 96(3), pp. 697–708.

Anderson, C. M. and Swanson, R. A. (2000) 'Astrocyte glutamate transport: review of properties, regulation, and physiological functions.', *Glia*, 32(1), pp. 1–14.

Anderson, M. A. *et al.* (2016) 'Astrocyte scar formation aids central nervous system axon regeneration', *Nature*, 532(7598), pp. 195–200.

Ataman, B. *et al.* (2016) 'Evolution of Osteocrin as an activity-regulated factor

in the primate brain', *Nature*, 539(7628), pp. 242–247.

Attwell, D. and Laughlin, S. B. (2001) 'An energy budget for signaling in the grey matter of the brain.', *Journal of cerebral blood flow and metabolism : official journal of the International Society of Cerebral Blood Flow and Metabolism*, 21(10), pp. 1133–45.

Bading, H. and Greenberg, M. E. (1991) 'Stimulation of protein tyrosine phosphorylation by NMDA receptor activation.', *Science*, 253(5022), pp. 912–4.

Bal-Price, A., Moneer, Z. and Brown, G. C. (2002) 'Nitric oxide induces rapid, calcium-dependent release of vesicular glutamate and ATP from cultured rat astrocytes', *GLIA*, 40(3), pp. 312–323.

Barros, L. F. *et al.* (2013) 'Small is fast: astrocytic glucose and lactate metabolism at cellular resolution.', *Frontiers in cellular neuroscience*, 7(March), p. 27.

von Bartheld, C. S., Bahney, J. and Herculano-Houzel, S. (2016) 'The search for true numbers of neurons and glial cells in the human brain: A review of 150 years of cell counting', *Journal of Comparative Neurology*, 524(18), pp. 3865–3895.

Baxter, P. S. *et al.* (2015) 'Synaptic NMDA receptor activity is coupled to the transcriptional control of the glutathione system', *Nature Communications*, 6, p. 6761.

Baxter, P. S. and Hardingham, G. E. (2016) 'Adaptive regulation of the brain's antioxidant defences by neurons and astrocytes', *Free Radical Biology and Medicine*, 100, pp. 147–152.

Bayraktar, O. A. *et al.* (2018) 'Single-cell in situ transcriptomic map of astrocyte cortical layer diversity', *bioRxiv*, p. 432104.

Beart, P. M. and O'Shea, R. D. (2009) 'Transporters for L-glutamate: An update on their molecular pharmacology and pathological involvement',

British Journal of Pharmacology, 150(1), pp. 5–17.

Bélanger, M., Allaman, I. and Magistretti, P. J. (2011) 'Brain energy metabolism: focus on astrocyte-neuron metabolic cooperation.', *Cell metabolism*, 14(6), pp. 724–38.

Bell, K. F. S. *et al.* (2011) 'Activation of Nrf2-regulated glutathione pathway genes by ischemic preconditioning.', *Oxidative medicine and cellular longevity*, 2011, p. 689524.

Bell, K. F. S. *et al.* (2015) 'Neuronal development is promoted by weakened intrinsic antioxidant defences due to epigenetic repression of Nrf2', *Nature Communications*, 6(1), p. 7066.

Bell, K. F. S. and Hardingham, Giles E (2011) 'CNS peroxiredoxins and their regulation in health and disease.', *Antioxidants & redox signaling*, 14(8), pp. 1467–1477.

Bell, K. F. S. and Hardingham, Giles E. (2011) 'The influence of synaptic activity on neuronal health', *Current Opinion in Neurobiology*, 21(2), pp. 299–305.

Bellesi, M. *et al.* (2015) 'Effects of sleep and wake on astrocytes: clues from molecular and ultrastructural studies.', *BMC biology*, 13, p. 66.

Benito, E. *et al.* (2010) 'CREB's control of intrinsic and synaptic plasticity: implications for CREB-dependent memory models.', *Trends in neurosciences*, 33(5), pp. 230–40.

Bennabi, D. *et al.* (2014) 'Transcranial direct current stimulation for memory enhancement: from clinical research to animal models.', *Frontiers in systems neuroscience*, 8, p. 159.

Bernardinelli, Y. *et al.* (2014) 'Activity-Dependent Structural Plasticity of Perisynaptic Astrocytic Domains Promotes Excitatory Synapse Stability', *Current Biology*, 24(15), pp. 1679–1688.

Bialas, A. R. and Stevens, B. (2013) 'TGF-β signaling regulates neuronal C1q expression and developmental synaptic refinement', *Nature Neuroscience*, 16(12), pp. 1773–1782.

Bindocci, E. *et al.* (2017) 'Three-dimensional Ca $^{2+}$ imaging advances understanding of astrocyte biology', *Science*.

Boisvert, M. M. *et al.* (2018) 'The Aging Astrocyte Transcriptome from Multiple Regions of the Mouse Brain.', *Cell reports*, 22(1), pp. 269–285.

Bomprezzi, R. (2015) 'Dimethyl fumarate in the treatment of relapsing-remitting multiple sclerosis: an overview.', *Therapeutic advances in neurological disorders*, 8(1), pp. 20–30.

Bradley, S. J. and Challiss, R. A. J. A. J. (2012) *G protein-coupled receptor signalling in astrocytes in health and disease: A focus on metabotropic glutamate receptors*, *Biochemical Pharmacology*.

Brancaccio, M. *et al.* (2017) 'Astrocytes Control Circadian Timekeeping in the Suprachiasmatic Nucleus via Glutamatergic Signaling.', *Neuron*, 93(6), pp. 1420-1435.e5.

Bratzke, L. C. *et al.* (2018) 'Cognitive decline in the middle-aged after surgery and anaesthesia: results from the Wisconsin Registry for Alzheimer's Prevention cohort', *Anaesthesia*, 73(5), pp. 549–555.

Brown, A. M. and Ransom, B. R. (2007) 'Astrocyte glycogen and brain energy metabolism', *Glia*, 55(12), pp. 1263–1271.

Bushong, E. A. *et al.* (2002) 'Protoplasmic astrocytes in CA1 stratum radiatum occupy separate anatomical domains.', *The Journal of neuroscience : the official journal of the Society for Neuroscience*, 22(1), pp. 183–92.

Bussian, T. J. *et al.* (2018) *Clearance of senescent glial cells prevents tau-dependent pathology and cognitive decline*, *Nature*.

Cabezas, R. *et al.* (2014) 'Astrocytic modulation of blood brain barrier:

perspectives on Parkinson's disease.', *Frontiers in cellular neuroscience*, 8, p. 211.

Cahoy, J. D. *et al.* (2008) 'A transcriptome database for astrocytes, neurons, and oligodendrocytes: a new resource for understanding brain development and function.', *The Journal of neuroscience : the official journal of the Society for Neuroscience*, 28(1), pp. 264–78.

Cai, H. *et al.* (2012) 'Metabolic Dysfunction in Alzheimers Disease and Related Neurodegenerative Disorders', *Current Alzheimer Research*, 9(1), pp. 5–17.

Cajal, R. y (1909) *Histologie du système nerveux de l'homme & des vertébrésitle*.

Cao, G. and Ko, C.-P. (2007) 'Schwann cell-derived factors modulate synaptic activities at developing neuromuscular synapses.', *The Journal of neuroscience : the official journal of the Society for Neuroscience*, 27(25), pp. 6712–22.

Chai, H. *et al.* (2017) 'Neural Circuit-Specialized Astrocytes : NeuroResource Neural Circuit-Specialized Astrocytes ':, *Neuron*, pp. 1–19.

Christopherson, K. S. *et al.* (2005) 'Thrombospondins are astrocyte-secreted proteins that promote CNS synaptogenesis.', *Cell*, 120(3), pp. 421–33.

Chun, H. and Lee, C. J. (2018) 'Reactive astrocytes in Alzheimer's disease: A double-edged sword', *Neuroscience Research*, 126, pp. 44–52.

Chung, W.-S. *et al.* (2013) 'Astrocytes mediate synapse elimination through MEGF10 and MERTK pathways.', *Nature*, 504(7480), pp. 394–400.

Chuquet, J. *et al.* (2010) 'Predominant enhancement of glucose uptake in astrocytes versus neurons during activation of the somatosensory cortex.', *The Journal of neuroscience : the official journal of the Society for Neuroscience*, 30(45), pp. 15298–303.

Clarke, L. E. *et al.* (2018) 'Normal aging induces A1-like astrocyte reactivity', *Proceedings of the National Academy of Sciences*, 115(8), pp. E1896–E1905.

Colonnese, M. T., Shen, J. and Murata, Y. (2017) 'Uncorrelated Neural Firing in Mouse Visual Cortex during Spontaneous Retinal Waves', *Frontiers in Cellular Neuroscience*, 11, p. 289.

Cornell-Bell, A. H. *et al.* (1990) 'Glutamate induces calcium waves in cultured astrocytes: Long-range glial signaling', *Science*, 247(4941), pp. 470–473.

Culley, D. J. *et al.* (2004) 'Long-term Impairment of Acquisition of a Spatial Memory Task following Isoflurane-Nitrous Oxide Anesthesia in Rats', *Anesthesiology*, 100(2), pp. 309–314.

Dabir, D. V. (2006) 'Impaired Glutamate Transport in a Mouse Model of Tau Pathology in Astrocytes', *Journal of Neuroscience*.

Deighton, R. F. *et al.* (2014) 'Nrf2 target genes can be controlled by neuronal activity in the absence of Nrf2 and astrocytes.', *Proceedings of the National Academy of Sciences of the United States of America*, 111(18), pp. E1818-20.

Demetrius, L. A., Magistretti, P. J. and Pellerin, L. (2015) 'Alzheimer's disease: the amyloid hypothesis and the Inverse Warburg effect', *Frontiers in Physiology*, 5, p. 522.

Diniz, L. P. *et al.* (2012) 'Astrocyte-induced synaptogenesis is mediated by transforming growth factor β signaling through modulation of D-serine levels in cerebral cortex neurons.', *The Journal of biological chemistry*, 287(49), pp. 41432–45.

DiNuzzo, M. (2016) 'Astrocyte-Neuron Interactions during Learning May Occur by Lactate Signaling Rather than Metabolism.', *Frontiers in integrative neuroscience*, 10, p. 2.

Dong, X. X., Wang, Y. and Qin, Z. H. (2009) 'Molecular mechanisms of excitotoxicity and their relevance to pathogenesis of neurodegenerative diseases', *Acta Pharmacologica Sinica*, pp. 379–387.

Doody, R. S. *et al.* (2013) 'A Phase 3 Trial of Semagacestat for Treatment of

Alzheimer's Disease', *New England Journal of Medicine*, 369(4), pp. 341–350.

Doody, R. S. *et al.* (2014) 'Phase 3 Trials of Solanezumab for Mild-to-Moderate Alzheimer's Disease', *New England Journal of Medicine*, 370(4), pp. 311–321.

Dringen, R., Gutterer, J. M. and Hirrlinger, J. (2000) 'Glutathione metabolism in brain: Metabolic interaction between astrocytes and neurons in the defense against reactive oxygen species', *European Journal of Biochemistry*, pp. 4912–4916.

Dutton, R. C. *et al.* (2002) 'Isoflurane causes anterograde but not retrograde amnesia for pavlovian fear conditioning.', *Anesthesiology*, 96(5), pp. 1223–9.

Elmariah, S. B. *et al.* (2005) 'Astrocytes regulate inhibitory synapse formation via Trk-mediated modulation of postsynaptic GABAA receptors.', *The Journal of neuroscience : the official journal of the Society for Neuroscience*, 25(14), pp. 3638–50.

Farmer, W. T. and Murai, K. (2017) 'Resolving Astrocyte Heterogeneity in the CNS.', *Frontiers in cellular neuroscience*, 11, p. 300.

Fernandez-Fernandez, S. *et al.* (2012) 'Antioxidant and bioenergetic coupling between neurons and astrocytes', *Biochem. J*, 443, pp. 3–12.

Flavell, S. W. and Greenberg, M. E. (2008) 'Signaling Mechanisms Linking Neuronal Activity to Gene Expression and Plasticity of the Nervous System', *Annual Review of Neuroscience*, 31(1), pp. 563–590.

Fleischhacker, W. W. *et al.* (1992) 'A multicenter double-blind study of three different doses of the new cAMP-phosphodiesterase inhibitor rolipram in patients with major depressive disorder.', *Neuropsychobiology*, 26(1–2), pp. 59–64.

Foo, L. C. and Dougherty, J. D. (2013) 'Aldh1L1 is expressed by postnatal neural stem cells in vivo.', *Glia*, 61(9), pp. 1533–41.

Franks, N. P. and Lieb, W. R. (1994) 'Molecular and cellular mechanisms of general anaesthesia', *Nature*, 367(6464), pp. 607–614.

Furman, J. L. *et al.* (2012) 'Targeting astrocytes ameliorates neurologic changes in a mouse model of Alzheimer's disease.', *The Journal of neuroscience : the official journal of the Society for Neuroscience*, 32(46), pp. 16129–40.

Greber, B. J. and Ban, N. (2016) 'Structure and Function of the Mitochondrial Ribosome', *Annual Review of Biochemistry*, 85(1), pp. 103–132.

Greenberg, M. E., Ziff, E. B. and Greene, L. A. (1986) 'Stimulation of neuronal acetylcholine receptors induces rapid gene transcription.', *Science (New York, N.Y.)*, 234(4772), pp. 80–83.

Grossman, N. *et al.* (2017) 'Noninvasive Deep Brain Stimulation via Temporally Interfering Electric Fields', *Cell*, 169(6), pp. 1029-1041.e16.

Habas, A. *et al.* (2013) 'Neuronal activity regulates astrocytic Nrf2 signaling.', *Proceedings of the National Academy of Sciences of the United States of America*, 110(45), pp. 18291–6.

Hallmann, A.-L. *et al.* (2017) 'Astrocyte pathology in a human neural stem cell model of frontotemporal dementia caused by mutant TAU protein', *Scientific Reports*, 7(1), p. 42991.

Hampton, D. W. *et al.* (2010) 'Cell-Mediated Neuroprotection in a Mouse Model of Human Tauopathy', *Journal of Neuroscience*, 30(30), pp. 9973–9983.

Han, X. *et al.* (2013) 'Forebrain engraftment by human glial progenitor cells enhances synaptic plasticity and learning in adult mice.', *Cell stem cell*, 12(3), pp. 342–53.

Hardingham, G. E. *et al.* (2018) 'Lineage divergence of activity-driven transcription and evolution of cognitive ability', *Nature Reviews Neuroscience*, 19(1), pp. 9–15.

Hardingham, G. E. and Bading, H. (2003) 'The Yin and Yang of NMDA receptor signalling', *Trends in Neurosciences*, pp. 81–89.

Hasel, P. *et al.* (2017) 'Neurons and neuronal activity control gene expression in astrocytes to regulate their development and metabolism', *Nat. Commun.*, 8(May), p. 15132.

Hayakawa, K. *et al.* (2014) 'Reactive astrocytes promote adhesive interactions between brain endothelium and endothelial progenitor cells via HMGB1 and beta-2 integrin signaling', *Stem Cell Research*, 12(2), pp. 531–538.

Heiman, M. *et al.* (2008) 'A Translational Profiling Approach for the Molecular Characterization of CNS Cell Types', *Cell*, 135(4), pp. 738–748.

Heiman, M. *et al.* (2014) 'Cell type–specific mRNA purification by translating ribosome affinity purification (TRAP)', *Nature Protocols*, 9(6), pp. 1282–1291.

Henley, J. and Poo, M. M. (2004) 'Guiding neuronal growth cones using Ca2+ signals', *Trends in Cell Biology*, pp. 320–330.

Henneberger, C. *et al.* (2010) 'Long-term potentiation depends on release of d-serine from astrocytes', *Nature*, 463(7278), pp. 232–236.

Herrero-Mendez, A. *et al.* (2009) 'The bioenergetic and antioxidant status of neurons is controlled by continuous degradation of a key glycolytic enzyme by APC/C-Cdh1.', *Nature cell biology*, 11(6), pp. 747–52.

Hertz, L. and Chen, Y. (2016) 'Importance of astrocytes for potassium ion (K+) homeostasis in brain and glial effects of K+ and its transporters on learning', *Neuroscience & Biobehavioral Reviews*, 71, pp. 484–505.

Houghton, C. A., Fassett, R. G. and Coombes, J. S. (2016) 'Sulforaphane and Other Nutrigenomic Nrf2 Activators: Can the Clinician's Expectation Be Matched by the Reality?', *Oxidative Medicine and Cellular Longevity*, 2016, pp. 1–17.

Houlgatte, R. *et al.* (1989) 'Secretion of nerve growth factor in cultures of

glial cells and neurons derived from different regions of the mouse brain', *Journal of Neuroscience Research*, 24(2), pp. 143–152.

Howarth, C. (2014) 'The contribution of astrocytes to the regulation of cerebral blood flow.', *Frontiers in neuroscience*, 8, p. 103.

Hrvatin, S. *et al.* (2018) 'Single-cell analysis of experience-dependent transcriptomic states in the mouse visual cortex', *Nature Neuroscience*, 21(1), pp. 120–129.

Huber, C. M. *et al.* (2018) 'Cognitive Decline in Preclinical Alzheimer's Disease: Amyloid-Beta versus Tauopathy.', *Journal of Alzheimer's disease : JAD*, 61(1), pp. 265–281.

Hutton, M. *et al.* (1998) 'Association of missense and 5′-splice-site mutations in tau with the inherited dementia FTDP-17', *Nature*, 393(6686), pp. 702–705.

Iliff, J. J. *et al.* (2012) 'A paravascular pathway facilitates CSF flow through the brain parenchyma and the clearance of interstitial solutes, including amyloid β.', *Science translational medicine*, 4(147), p. 111.

Inada, A. *et al.* (2004) 'Overexpression of inducible cyclic AMP early repressor inhibits transactivation of genes and cell proliferation in pancreatic beta cells.', *Molecular and cellular biology*, 24(7), pp. 2831–41.

Itoh, N. *et al.* (2018) 'Cell-specific and region-specific transcriptomics in the multiple sclerosis model: Focus on astrocytes', *Proceedings of the National Academy of Sciences*, 115(2), pp. E302–E309.

Itoh, Y. *et al.* (2003) 'Dichloroacetate effects on glucose and lactate oxidation by neurons and astroglia in vitro and on glucose utilization by brain in vivo.', *Proceedings of the National Academy of Sciences of the United States of America*, 100(8), pp. 4879–84.

Jackson, J. G. *et al.* (2014) 'Neuronal Activity and Glutamate Uptake Decrease Mitochondrial Mobility in Astrocytes and Position Mitochondria Near

Glutamate Transporters', *Journal of Neuroscience*, 34(5), pp. 1613–1624.

Jakel, R. J. *et al.* (2007) 'Nrf2-mediated protection against 6-hydroxydopamine.', *Brain research*, 1144, pp. 192–201.

Jaworski, J. *et al.* (2018) 'Inducible cAMP early repressor, an endogenous antagonist of cAMP responsive element-binding protein, evokes neuronal apoptosis in vitro.', *The Journal of Neuroscience*.

Kametani, F. and Hasegawa, M. (2018) 'Reconsideration of Amyloid Hypothesis and Tau Hypothesis in Alzheimer's Disease.', *Frontiers in neuroscience*, 12, p. 25.

Kansanen, E. *et al.* (2013) 'The Keap1-Nrf2 pathway: Mechanisms of activation and dysregulation in cancer', *Redox Biology*, 1(1), pp. 45–49.

Khakh, B. S. and McCarthy, K. D. (2015) 'Astrocyte calcium signaling: From observations to functions and the challenges therein', *Cold Spring Harbor Perspectives in Biology*, 7(4).

Klemm, D. J. *et al.* (2001) 'Insulin-induced Adipocyte Differentiation', *Journal of Biological Chemistry*, 276(30), pp. 28430–28435.

Kržan, M. *et al.* (2018) 'Calcium-Dependent Exocytosis of Atrial Natriuretic Peptide from Astrocytes', *The Journal of Neuroscience*, 23(5), pp. 1580–1583.

Kucukdereli, H. *et al.* (2011) 'Control of excitatory CNS synaptogenesis by astrocyte-secreted proteins Hevin and SPARC.', *Proceedings of the National Academy of Sciences of the United States of America*, 108(32), pp. E440-9.

Lanjakornsiripan, D. *et al.* (2018) 'Layer-specific morphological and molecular differences in neocortical astrocytes and their dependence on neuronal layers', *Nature Communications*, 9(1).

Lau, L. T. and Yu, A. C.-H. (2001) 'Astrocytes Produce and Release Interleukin-1, Interleukin-6, Tumor Necrosis Factor Alpha and Interferon-Gamma Following Traumatic and Metabolic Injury', *Journal of Neurotrauma*,

18(3), pp. 351–359.

Lee, H. S. *et al.* (2014) 'Astrocytes contribute to gamma oscillations and recognition memory', *Proceedings of the National Academy of Sciences*, 111(32), pp. E3343–E3352.

Lee, L., Kosuri, P. and Arancio, O. (2014) 'Picomolar amyloid-β peptides enhance spontaneous astrocyte calcium transients.', *Journal of Alzheimer's disease : JAD*, 38(1), pp. 49–62.

Leslie, M. (2017) 'Will surgery sap your brain power?', *Science*.

Léveillé, F. *et al.* (2010) 'Suppression of the intrinsic apoptosis pathway by synaptic activity.', *The Journal of neuroscience : the official journal of the Society for Neuroscience*, 30(7), pp. 2623–35.

Licher, S. *et al.* (2018) 'Lifetime risk of common neurological diseases in the elderly population.', *Journal of neurology, neurosurgery, and psychiatry*, p. jnnp-2018-318650.

Liddelow, S. A. *et al.* (2017) 'Neurotoxic reactive astrocytes are induced by activated microglia', *Nature*, 541(7638), pp. 481–487.

Liddelow, S. A. and Barres, B. A. (2017) 'Reactive Astrocytes: Production, Function, and Therapeutic Potential.', *Immunity*, 46(6), pp. 957–967.

Lippens, G. *et al.* (2007) 'Tau aggregation in Alzheimer's disease: what role for phosphorylation?', *Prion*, 1(1), pp. 21–5.

Liu, C.-C. *et al.* (2017) 'Astrocytic LRP1 Mediates Brain Aβ Clearance and Impacts Amyloid Deposition', *The Journal of Neuroscience*, 37(15), pp. 4023–4031.

Liu, W., Morgan, K. M. and Pine, S. R. (2014) 'Activation of the Notch1 Stem Cell Signaling Pathway during Routine Cell Line Subculture.', *Frontiers in oncology*, 4, p. 211.

Lonze, B. E. and Ginty, D. D. (2002) 'Function and regulation of CREB family transcription factors in the nervous system', *Neuron*, pp. 605–623.

Lukatch, H. S., Kiddoo, C. E. and MacIver, M. B. (2005) 'Anesthetic-induced Burst Suppression EEG Activity Requires Glutamate-mediated Excitatory Synaptic Transmission', *Cerebral Cortex*, 15(9), pp. 1322–1331.

Macaluso, E., Frith, C. D. and Driver, J. (2000) 'Modulation of human visual cortex by crossmodal spatial attention.', *Science (New York, N.Y.)*, 289(5482), pp. 1206–8.

Magistretti, P. J. *et al.* (1999) 'Energy on demand.', *Science (New York, N.Y.)*, 283(5401), pp. 496–7.

Majdan, M. and Shatz, C. J. (2006) 'Effects of visual experience on activity-dependent gene regulation in cortex', *Nature Neuroscience*, 9(5), pp. 650–659.

Mathiisen, T. M. *et al.* (2010) 'The perivascular astroglial sheath provides a complete covering of the brain microvessels: An electron microscopic 3D reconstruction', *Glia*, 58(9), pp. 1094–1103.

Matsumoto, H. and Ugawa, Y. (2017) 'Adverse events of tDCS and tACS: A review', *Clinical Neurophysiology Practice*, 2, pp. 19–25.

Mauch, D. H. *et al.* (2001) 'CNS synaptogenesis promoted by glia-derived cholesterol.', *Science (New York, N.Y.)*, 294(5545), pp. 1354–7.

Miller, R. H. and Raff, M. C. (1984) 'Fibrous and protoplasmic astrocytes are biochemically and developmentally distinct.', *The Journal of neuroscience : the official journal of the Society for Neuroscience*, 4(2), pp. 585–92.

Mishra, A. *et al.* (2016) 'Astrocytes mediate neurovascular signaling to capillary pericytes but not to arterioles.', *Nature neuroscience*, 19(12), pp. 1619–1627.

Morte, B. and Bernal, J. (2014) 'Thyroid hormone action: Astrocyte-neuron communication', *Frontiers in Endocrinology*, pp. 88–89.

Mulligan, S. J. and MacVicar, B. A. (2004) 'Calcium transients in astrocyte endfeet cause cerebrovascular constrictions', *Nature*, 431(7005), pp. 195–199.

Murase, S., Lantz, C. L. and Quinlan, E. M. (2017) 'Light reintroduction after dark exposure reactivates plasticity in adults via perisynaptic activation of MMP-9.', *eLife*, 6.

Murphy-Royal, C. *et al.* (2015) 'Surface diffusion of astrocytic glutamate transporters shapes synaptic transmission', *Nature Neuroscience*, 18(2), pp. 219–226.

Nagai, M. *et al.* (2007) 'Astrocytes expressing ALS-linked mutated SOD1 release factors selectively toxic to motor neurons.', *Nature neuroscience*, 10(5), pp. 615–622.

Nagelhus, E. A. and Ottersen, O. P. (2013) 'Physiological roles of aquaporin-4 in brain.', *Physiological reviews*, 93(4), pp. 1543–62.

Nedergaard, M. (1994) 'Direct signaling from astrocytes to neurons in cultures of mammalian brain cells', *Science*, 263(5154), pp. 1768–1771.

Nippert, A. R., Biesecker, K. R. and Newman, E. A. (2018) 'Mechanisms Mediating Functional Hyperemia in the Brain', *Neuroscientist*, pp. 73–83.

O'Brien, R. J. and Wong, P. C. (2011) 'Amyloid Precursor Protein Processing and Alzheimer's Disease', *Annual Review of Neuroscience*, 34(1), pp. 185–204.

Oberheim, N. A. *et al.* (2009) 'Uniquely hominid features of adult human astrocytes.', *The Journal of neuroscience : the official journal of the Society for Neuroscience*, 29(10), pp. 3276–87.

Orr, A. G. *et al.* (2015) 'Astrocytic adenosine receptor A2A and Gs-coupled signaling regulate memory', *Nature Neuroscience*, 18(3), pp. 423–439.

Padmanabhan, J. *et al.* (2006) 'Alpha1-antichymotrypsin, an inflammatory protein overexpressed in Alzheimer's disease brain, induces tau phosphorylation in neurons', *Brain*, 129(11), pp. 3020–3034.

Panatier, A. *et al.* (2011) 'Astrocytes are endogenous regulators of basal transmission at central synapses.', *Cell*, 146(5), pp. 785–98.

Pardo, L. *et al.* (2016) 'Targeted activation of CREB in reactive astrocytes is neuroprotective in focal acute cortical injury', *Glia*, 64(5), pp. 853–874.

Pardo, L. *et al.* (2017) 'CREB Regulates Distinct Adaptive Transcriptional Programs in Astrocytes and Neurons', *Scientific Reports*, 7(1), p. 6390.

Parpura, V. *et al.* (1994) 'Glutamate-Mediated Astrocyte Neuron Signaling', *Nature*, 369(6483), pp. 744–747.

Pellerin, L. and Magistretti, P. J. (1994a) 'Glutamate uptake into astrocytes stimulates aerobic glycolysis: a mechanism coupling neuronal activity to glucose utilization.', *Proceedings of the National Academy of Sciences of the United States of America*, 91(22), pp. 10625–9.

Pellerin, L. and Magistretti, P. J. (1994b) 'Glutamate uptake into astrocytes stimulates aerobic glycolysis: a mechanism coupling neuronal activity to glucose utilization.', *Proceedings of the National Academy of Sciences of the United States of America*, 91(22), pp. 10625–9.

Perry, V. H. and Holmes, C. (2014) 'Microglial priming in neurodegenerative disease.', *Nature reviews. Neurology*, 10(4), pp. 217–24.

Pfrieger, F. W. (1997) 'Synaptic Efficacy Enhanced by Glial Cells in Vitro', *Science*, 277(5332), pp. 1684–1687.

Phatnani, H. *et al.* (2015) 'Astrocytes in Neurodegenerative Disease.', *Cold Spring Harbor perspectives in biology*, 7(a020628).

Pîrşcoveanu, D. F. V. *et al.* (2017) 'Tau protein in neurodegenerative diseases - a review.', *Romanian journal of morphology and embryology = Revue roumaine de morphologie et embryologie*, 58(4), pp. 1141–1150.

Porter, J. T. and McCarthy, K. D. (1997) 'Astrocytic neurotransmitter receptors in situ and in vivo.', *Progress in neurobiology*, 51(4), pp. 439–55.

Potokar, M., Jorgačevski, J. and Zorec, R. (2016) 'Astrocyte Aquaporin Dynamics in Health and Disease.', *International journal of molecular sciences*, 17(7).

Qiu, J. *et al.* (2018) 'Mixed-species RNA-seq for elucidation of non-cell-autonomous control of gene transcription', *Nature Protocols*, 13(10), pp. 2176–2199.

Radford, R. A. *et al.* (2015) 'The established and emerging roles of astrocytes and microglia in amyotrophic lateral sclerosis and frontotemporal dementia.', *Frontiers in cellular neuroscience*, 9, p. 414.

Ramos, M. *et al.* (2003) 'Developmental changes in the Ca2+-regulated mitochondrial aspartate–glutamate carrier araları in brain and prominent expression in the spinal cord', *Developmental Brain Research*, 143(1), pp. 33–46.

Rao, K. V. R. *et al.* (2005) 'Astrocytes Protect Neurons from Ammonia Toxicity', *Neurochemical Research*, 30(10), pp. 1311–1318.

Rappold, P. M. and Tieu, K. (2010) 'Astrocytes and therapeutics for Parkinson's disease.', *Neurotherapeutics : the journal of the American Society for Experimental NeuroTherapeutics*, 7(4), pp. 413–23.

Redmond, L. and Ghosh, A. (2005) 'Regulation of dendritic development by calcium signaling', *Cell Calcium*, pp. 411–416.

Reitz, C. (2012) 'Alzheimer's disease and the amyloid cascade hypothesis: a critical review.', *International journal of Alzheimer's disease*, 2012, p. 369808.

Ries, C. R. and Puil, E. (1993) 'Isoflurane prevents transitions to tonic and burst firing modes in thalamic neurons.', *Neuroscience letters*, 159(1–2), pp. 91–4.

Roche, N., Geiger, M. and Bussel, B. (2015) 'Mechanisms underlying transcranial direct current stimulation in rehabilitation', *Annals of Physical and Rehabilitation Medicine*, 58(4), pp. 214–219.

Salloway, S. *et al.* (2014) 'Two phase 3 trials of bapineuzumab in mild-to-moderate Alzheimer's disease.', *The New England journal of medicine*, 370(4), pp. 322–33.

San Martín, A. *et al.* (2014) 'Imaging Mitochondrial Flux in Single Cells with a FRET Sensor for Pyruvate', *PLoS ONE*. Edited by K.-W. Koch, 9(1), p. e85780.

Scemes, E. and Giaume, C. (2006) 'Astrocyte calcium waves: What they are and what they do', *Glia*, pp. 716–725.

Schell, M. J., Molliver, M. E. and Snyder, S. H. (1995) 'D-serine, an endogenous synaptic modulator: localization to astrocytes and glutamate-stimulated release.', *Proceedings of the National Academy of Sciences*, 92(9), pp. 3948–3952.

Schwanhäusser, B. *et al.* (2011) 'Global quantification of mammalian gene expression control', *Nature*, 473(7347), pp. 337–342.

Serio, A. *et al.* (2013) 'Astrocyte pathology and the absence of non-cell autonomy in an induced pluripotent stem cell model of TDP-43 proteinopathy.', *Proceedings of the National Academy of Sciences of the United States of America*, 110(12), pp. 4697–702.

Shaywitz, A. J. and Greenberg, M. E. (1999) 'CREB: A Stimulus-Induced Transcription Factor Activated by A Diverse Array of Extracellular Signals', *Annual Review of Biochemistry*, 68(1), pp. 821–861.

Shipton, O. A. *et al.* (2011) 'Tau Protein Is Required for Amyloid -Induced Impairment of Hippocampal Long-Term Potentiation', *Journal of Neuroscience*, 31(5), pp. 1688–1692.

Slusarski, D. C. and Pelegri, F. (2007) 'Calcium signaling in vertebrate embryonic patterning and morphogenesis.', *Developmental biology*, 307(1), pp. 1–13.

Sperfeld, A. D. *et al.* (1999) 'FTDP-17: an early-onset phenotype with

parkinsonism and epileptic seizures caused by a novel mutation.', *Annals of neurology*, 46(5), pp. 708–15.

Srinivasan, R. *et al.* (2016) 'New Transgenic Mouse Lines for Selectively Targeting Astrocytes and Studying Calcium Signals in Astrocyte Processes In Situ and In Vivo', *Neuron*, 0(0), pp. 439–463.

Stogsdill, J. A. *et al.* (2017) 'Astrocytic neuroligins control astrocyte morphogenesis and synaptogenesis', *Nature*, 551(7679), pp. 192–197.

De Strooper, B. and Karran, E. (2016) 'The Cellular Phase of Alzheimer's Disease', *Cell*, 164(4), pp. 603–615.

Suzuki, A. *et al.* (2011) 'Astrocyte-neuron lactate transport is required for long-term memory formation.', *Cell*, 144(5), pp. 810–23.

Takanaga, H., Chaudhuri, B. and Frommer, W. B. (2008) 'GLUT1 and GLUT9 as major contributors to glucose influx in HepG2 cells identified by a high sensitivity intramolecular FRET glucose sensor', *Biochimica et Biophysica Acta - Biomembranes*, 1778(4), pp. 1091–1099.

Tong, X. *et al.* (2014) 'Astrocyte Kir4.1 ion channel deficits contribute to neuronal dysfunction in Huntington's disease model mice.', *Nature neuroscience*, 17(5), pp. 694–703.

Ullian, E. M. *et al.* (2001) 'Control of synapse number by glia.', *Science (New York, N.Y.)*, 291(5504), pp. 657–61.

Vanzulli, I. and Butt, A. M. (2015) 'mGluR5 protect astrocytes from ischemic damage in postnatal CNS white matter.', *Cell calcium*, 58(5), pp. 423–30.

Vargas, M. R. *et al.* (2008) 'Nrf2 activation in astrocytes protects against neurodegeneration in mouse models of familial amyotrophic lateral sclerosis.', *The Journal of neuroscience : the official journal of the Society for Neuroscience*, 28(50), pp. 13574–81.

Virchow, R. (1855) 'Ein Fall von progressiver Muskelatrophie', *Archiv f. pathol.*

Anat. (1855) 8: 537., 8, p. 537.

Virchow, R. (1858) *Cellular pathology: as based upon physiological and pathological histology. Twenty lectures delivered in the pathological institute of Berlin during the months of February, March and April, [in German].*

Volkenhoff, A. *et al.* (2015) 'Glial glycolysis is essential for neuronal survival in drosophila', *Cell Metabolism*, 22(3), pp. 437–447.

Wang, H. *et al.* (2018) 'cAMP Response Element-Binding Protein (CREB): A Possible Signaling Molecule Link in the Pathophysiology of Schizophrenia', *Frontiers in Molecular Neuroscience*, 11, p. 255.

Weber, B. and Barros, L. F. (2015) 'The Astrocyte: Powerhouse and Recycling Center.', *Cold Spring Harbor perspectives in biology*, pp. 1–16.

West, A. E. and Greenberg, M. E. (2011) 'Neuronal Activity-Regulated Gene Transcription in Synapse Development and Cognitive Function', *Cold Spring Harbor Perspectives in Biology*, 3(6), pp. a005744–a005744.

Wiese, S., Karus, M. and Faissner, A. (2012) 'Astrocytes as a source for extracellular matrix molecules and cytokines.', *Frontiers in pharmacology*, 3, p. 120.

Wolfe, M. S. (2009) 'Tau Mutations in Neurodegenerative Diseases', *Journal of Biological Chemistry*, 284(10), pp. 6021–6025.

Yang, Y. *et al.* (2009) 'Presynaptic regulation of astroglial excitatory neurotransmitter transporter GLT1.', *Neuron*, 61(6), pp. 880–94.

Yiu, G. and He, Z. (2006) 'Glial inhibition of CNS axon regeneration', *Nature Reviews Neuroscience*, pp. 617–627.

Zamanian, J. L. *et al.* (2012) 'Genomic Analysis of Reactive Astrogliosis', *Journal of Neuroscience*, 32(18), pp. 6391–6410.

Zhang, J. (2015) 'Mapping neuroinflammation in frontotemporal dementia

with molecular PET imaging', *Journal of Neuroinflammation*, 12(1), p. 108.

Zhang, Y., Sloan, S. A., Clarke, L. E., Caneda, C., Plaza, C. A., Blumenthal, P. D., Vogel, H., Steinberg, G. K., Edwards, M. S. B., *et al.* (2016) 'Purification and Characterization of Pregenitor and Mature Human Astrocytes Reveals Transcriptonal and Functional Differences With Mouse', *Neuron*, 89(1), pp. 37–53.

Zimmer, E. R. *et al.* (2017) '[18F]FDG PET signal is driven by astroglial glutamate transport', *Nature neuroscience*, 20(3), pp. 393–395.

Lauda Finem